ISSN 2220-3249 (online)

World Journal of *Virology*

World J Virol 2016 February 12; 5(1): 1-37

Published by Baishideng Publishing Group Inc

World Journal of Virology

A peer-reviewed, online, open-access journal of virology

Editorial Board

2016-2019

The *World Journal of Virology* Editorial Board consists of 370 members, representing a team of worldwide experts in virology. They are from 59 countries, including Argentina (4), Australia (8), Austria (4), Barbados (1), Belgium (1), Brazil (7), Bulgaria (1), Cameroon (1), Canada (12), Chile (2), China (55), Croatia (2), Cuba (1), Czech Republic (1), Denmark (1), Egypt (3), Ethiopia (1), Finland (5), France (10), Gambia(1), Germany (11), Ghana (1), Greece (2), Hungary (1), India (13), Indonesia (1), Iran (2), Ireland (3), Israel (4), Italy (23), Japan (16), Kazakhstan (1), Kenya (1), Kosovo (1), Mexico (2), Netherlands (5), New Zealand (1), Nigeria (1), Pakistan (1), Palestine (1), Poland (1), Portugal (1), Romania (1), Russia (2), Saudi Arabia (1), Singapore (2), Slovakia (2), Slovenia (2), South Africa (2), South Korea (6), Spain (19), Sweden (4), Thailand (8), Tunisia (1), Turkey (4), United Arab Emirates (1), United Kingdom (8), United States (92), and Uruguay (1).

China

Kun-Long Ben, *Kunming*
Guang-Wen Cao, *Shanghai*
Paul KS Chan, *Hongkong*
Yuan-Ding Chen, *Kunming*
An-Chun Cheng, *Ya'an*
Shang-Jin Cui, *Harbin*
Xiao-Ping Dong, *Beijing*
Zai-Feng Fan, *Beijing*
Jean-Michel Garcia, *Hong Kong*
Guan-Zhu Han, *Nanjing*
Yu-Xian He, *Beijing*
Xiu-Guo Hua, *Shanghai*
Wen-Lin Huang, *Guangzhou*
Margaret Ip, *Hong Kong*
Dao-Hong Jiang, *Wuhan*
Jian-Qi Lian, *Xi'an*
Xiao-Yang Mo, *Hunan*
Beatrice Nal, *HongKong*
Cheng-Feng Qin, *Beijing*
Hua-Ji Qiu, *Harbin*
Xiao-feng Ren, *Harbin*
Hong Tang, *Chengdu*
Jian-Wei Wang, *Beijing*
You-Chun Wang, *Beijing*
Ning Wang, *Beijing*
Mary Miu Yee Waye, *Hong Kong*
Patrick CY Woo, *Hong Kong*
Yu-Zhang Wu, *Chongqing*
Jian-Qing Wu, *Nanjing*
Rui Wu, *Luoyang*
Xin-Yong Liu, *Jinan*
Xu-Qing Zhang, *Chongqing*
Guo-Zhong Zhang, *Beijing*
Chuang-Xi Zhang, *Hangzhou*
Ping Zhao, *Shanghai*
Shi-Jun Zheng, *Beijing*

Croatia

Snjezana Z Lepej, *Zagreb*
Pero Lucin, *Rijeka*

Cuba

Maria G Guzman, *Havana*

Czech Republic

Daniel Ruzek, *Ceske Budejovice*

Denmark

Havard Jenssen, *Roskilde*

Egypt

Mona El SH El-Raziky, *Cairo*
Samia A Kamal, *Cairo*
Abdel-Rahman N Zekri, *Cairo*

Ethiopia

Woldaregay E Abegaz, *Addis Ababa*

Finland

Jussi Hepojoki, *Helsinki*
Anne Jaaskelainen, *Helsinki*
Irmeli Lautenschlager, *Helsinki*
Pamela Osterlund, *Helsinki*
Antti Vaheri, *Helsinki*

France

Christian A Devaux, *Montpellier*
Jean Dubuisson, *Lille*
Duverlie Gilles, *Amiens*
Bedouelle Hugues, *Paris*
Eric J Kremer, *Montpellier*
Belec Laurent, *Paris*
Denis Rasschaert, *Tours*
Dominique Salmon-Céron, *Paris*
Christian Trépo, *Lyon*
Eric Wattel, *Lyon*

Gambia

Assan Jaye, *Banjul*

Germany

Claus-Thomas Bock, *Berlin*
Elke Bogner, *Berlin*
Andreas Dotzauer, *Bremen*
Ingo Drexler, *Düsseldorf*
Christoph Eisenbach, *Heidelberg*
Thomas Iftner, *Erlangen*
Florian Lang, *Tuebingen*
Jochen Mattner, *Erlangen*
Michael Nevels, *Regensburg*
Andreas MH Sauerbrei, *Jena*
Frank Tacke, *Aachen*

Ghana

Kwamena W Sagoe, *Accra*

Greece

Apostolos I Beloukas, *Athens*
George V Papatheodoridis, *Athens*

Hungary

Krisztián Bányai, *Budapest*

India

Akhil C Banerjea, *New Delhi*
Jayanta Bhattacharya, *Pune*
Runu Chakravarty, *Kolkatta*
Sibnarayan Datta, *Tezpur*
Kumar Jitendra, *Punjab*
Himansu Kesari Pradhan, *New Delhi*
Sachin Kumar, *Assam*
Sunil K Lal, *New Delhi*
Sunil K Mukherjee, *New Delhi*
Ramesh S Paranjape, *Pune*
Sharma Pradeep, *Karnal*
Shamala D Sekaran, *New Delhi*
Rasappa Viswanathan, *Coimbatore*

Indonesia

Andi Utama, *Tangerang*

Iran

Seyed M Ghiasi, *Tehran*
Farzin Roohvand, *Tehran*

Ireland

Carlo Bidoia, *Dublin*
Liam J Fanning, *Cork*
Weifeng Shi, *Dublin*

Israel

Irit Davidson, *Bet Dagan*
Yedidya Gafni, *Bet Dagan*
Murad Ghanim, *Bet Dagan*
Ilan Sela, *Rehovot*

Italy

Alberto Alberti, *Sassari*
Giorgio Barbarini, *Voghera*
Massimiliano Berretta, *Aviano*
Franco M Buonaguro, *Naples*
Maria R Capobianchi, *Naples*
Arnaldo Caruso, *Brescia*
Daniel O Cicero, *Rome*
Marco Ciotti, *Rome*
Cristina Costa, *Torino*
Piergiuseppe De Berardinis, *Naples*
Federico De Marco, *Rome*
Massimo EA De Paschale, *Legnano*
Maurizia Debiaggi, *Pavia*
Paolo Fabris, *Vicenza*
Daniele Focosi, *Pisa*
Simone Giannecchini, *Florence*
Fabrizio Maggi, *Pisa*
Roberto Manfredi, *Bologna*
Vito Martella, *Valenzano*
Giuseppe Portella, *Napoli*
Nicola Principi, *Milan*
Giovanni Rezza, *Roma*
Diego Ripamonti, *Bergamo*

Japan

Masanori Daibata, *Nankoku*
Bin Gotoh, *Otsu*
Shoji Ikuo, *Kobe*
Takashi Irie, *Hiroshima*
Hiroki Isomura, *Maebashi*
Hideya Kawasaki, *Hamamatsu*

Eiichi N Kodama, *Sendai*
Emoto Masashi, *Gunma*
Hiromitsu Moriyama, *Tokyo*
Kenji Okuda, *Yokohama*
Nobuhiro Suzuki, *Okayama*
Takashi Suzuki, *Shizuoka*
Tetsuro Suzuki, *Hamamatsu*
Yoshiyuki Suzuki, *Nagoya-shi*
Akifumi Takaori-Kondo, *Kyoto*
Tetsuya Toyoda, *Toyohashi*

Kazakhstan

Vladimir E Berezin, *Almaty*

Kenya

George G Maina, *Nairobi*

Kosovo

Lul Raka, *Prishtina*

Mexico

Juan E Ludert, *Mexico City*
Julio Reyes-Leyva, *Mexico*

Netherlands

Kimberley SM Benschop, *Amsterdam*
Benjamin Berkhout, *Amsterdam*
Byron EE Martina, *Rotterdam*
Willem JG Melchers, *Nijmegen*
Monique Nijhuis, *Utrecht*

New Zealand

Olga S Garkavenko, *Auckland*

Nigeria

Olajide A Owolodun, *Plateau State*

Pakistan

Muhammad I Qadir, *Faisalabad*

Palestine

Ahmad Y Amro, *Jerusalem*

Poland

Brygida Knysz, *Wroclaw*

Portugal

Celso Cunha, *Lisbon*

Romania

Anda Baicus, *Bucharest*

Russia

Anton Buzdin, *Moscow*
Elena V Gavrilova, *Novosibirsk*

Saudi Arabia

Ahmed S Abdel-Moneim, *Al-Taif*

Singapore

Sophie Bellanger, *Singapore*
Ding X Liu, *Singapore*

Slovakia

Gabriela Bukovska, *Bratislava*
Julius Rajcani, *Bratislava*

Slovenia

Uros Krapez, *Ljubljana*
Andrej Steyer, *Ljubljana*

South Africa

Janusz T Paweska, *Sandringham*
Dirk Stephan, *Matieland*

South Korea

Sang Hoon Ahn, *Seoul*
Tae-Jin Choi, *Busan*
Young-Ki Choi, *Cheongju*
Kee-Jong Hong, *Cheongwon*
Bum-Joon Kim, *Seoul*
Junsoo Park, *Wonju*

Spain

Alí Alejo, *Valdeolmos*
Alfredo Berzal-Herranz, *Granada*
Rafael Blasco, *Madrid*
Julio Collazos, *Usánsolo-Galdácano*
Juan M Hernández, *Madrid*
Gómez L Jaime, *Córdoba*
Josep M Llibre, *Badalona*
Cecilio López-Galíndez, *Madrid*
F. Xavier López-Labrador, *Valencia*
JoséA Melero, *Madrid*
Luis Menéndez-Arias, *Madrid*
Andrés Moya, *València*
David R Pereda, *Sevilla*
Pilar Perez-Romero, *Sevilla*
Josep Quer, *Barcelona*
Daniel López Rodríguez, *Majadahonda*
Juan-Carlos Saiz, *Madrid*
Noemi Sevilla, *Madrid*
Natalia Soriano-Sarabia, *Madrid*

Sweden

Goran PL Bucht, *Umea*
Ali Mirazimi, *Solna*
Muhammad Munir, *Uppdala*
Bo F Oberg, *Huddinge*

Thailand

Prasert Auewarakul, *Bangkok*
Parin Chaivisuthangkura, *Bangkok*
Wasin Charerntantanakul, *Chiang Mai*
Wansika Kiatpathomchai, *Bangkok*
Sasisopin Kiertiburanakul, *Bangkok*
Winyou Mitarnun, *Chiang Mai*
Yong Poovorawan, *Bangkok*
Viroj Wiwanitkit, *Bangkok*

Tunisia

Olfa Bahri, *Tunis*

Turkey

Omer Coskun, *Ankara*
Iftihar Koksal, *Trabzon*
Aykut Ozdarendeli, *Kayseri*
Ayca A Sayiner, *Izmir*

United Arab Emirates

Tahir A Rizvi, *Al Ain*

United Kingdom

Shiu-Wan Chan, *Manchester*
Simon R Clegg, *Preston*
Chiriva I Maurizio, *Nottingham*
Iain M Morgan, *Glasgow*
Mark R Nelson, *London*
Adrian W Philbey, *Glasgow*
James P Stewart, *Liverpool*
Gavin WG Wilkinson, *Cardiff*

United States

Nafees Ahmad, *Tucson*
Ashok Aiyar, *Los Angeles*
Hizi Amnon, *Bethesda*
Judith M Ball, *Texas*
Igor M Belyakov, *Frederick*
Bradford K Berges, *Provo*
Preeti Bharaj, *Orlando*
Jay C Brown, *Charlottesville*
Victor E Buckwold, *Walkersville*
Alexander A Bukreyev, *Galveston*
Joseph J Carter, *Seattle*
Maria G Castro, *Los Angeles*
Yan-Ping Chen, *Beltsville*

World Journal of Virology

Contents

Quarterly Volume 5 Number 1 February 12, 2016

World Journal of Virology
Volume 5 Number 1 February 12, 2016

Contents

NAME OF JOURNAL
World Journal of Virology

ISSN
ISSN 2220-3249 (online)

LAUNCH DATE
February 12, 2012

FREQUENCY
Quarterly

World Journal of Virology
Room 903, Building D, Ocean International Center,
No. 62 Dongsihuan Zhonglu, Chaoyang District,
Beijing 100025, China
Telephone: +86-10-85381891
Fax: +86-10-85381893
E-mail: editorialoffice@wjgnet.com
Help Desk: http://www.wjgnet.com/esps/helpdesk.aspx
http://www.wjgnet.com

PUBLISHER
Baishideng Publishing Group Inc
8226 Regency Drive,
Pleasanton, CA 94588, USA
Telephone: +1-925-223-8242
Fax: +1-925-223-8243
E-mail: bpgoffice@wjgnet.com
Help Desk: http://www.wjgnet.com/esps/helpdesk.aspx
http://www.wjgnet.com

PUBLICATION DATE
February 12, 2016

INSTRUCTIONS TO AUTHORS
Full instructions are available online at http://www.wjgnet.com/bpg/g_info_20160116143427.htm

ONLINE SUBMISSION
http://www.wjgnet.com/esps/

World Journal of Virology

Submit a Manuscript: http://www.wjgnet.com/esps/
Help Desk: http://www.wjgnet.com/esps/helpdesk.aspx
DOI: 10.5501/wjv.v5.i1.1

World J Virol 2016 February 12; 5(1): 1-13
ISSN 2220-3249 (online)

REVIEW

Infected cell protein 0 functional domains and their coordination in herpes simplex virus replication

Haidong Gu

Haidong Gu, Department of Biological Sciences, Wayne State University, Detroit, MI 48202, United States

Author contributions: Gu H wrote the paper.

Supported by National Institute of Allergy and Infectious Diseases, No. 1R01AI118992.

Conflict-of-interest statement: None.

Correspondence to: Haidong Gu, PhD, Assistant Professor, Department of Biological Sciences, Wayne State University, 5047 Gullen Mall, Detroit, MI 48202, United States. haidong.gu@wayne.edu
Telephone: +1-313-5776402

Received: August 29, 2015
Peer-review started: September 7, 2015
First decision: October 8, 2015
Revised: October 28, 2015
Accepted: December 4, 2015
Article in press: December 8, 2015
Published online: February 12, 2016

Abstract

Herpes simplex virus 1 (HSV-1) is a ubiquitous human pathogen that establishes latent infection in ganglia neurons. Its unique life cycle requires a balanced "conquer and compromise" strategy to deal with the host anti-viral defenses. One of HSV-1 α (immediate early) gene products, infected cell protein 0 (ICP0), is a multifunctional protein that interacts with and modulates a wide range of cellular defensive pathways. These pathways may locate in different cell compartments, which then migrate or exchange factors upon stimulation, for the purpose of a concerted and effective defense. ICP0 is able to simultaneously attack multiple host pathways by either degrading key restrictive factors or modifying repressive complexes. This is a viral protein that contains an E3 ubiquitin ligase, translocates among different cell compartments and interacts with major defensive complexes. The multiple functional domains of ICP0 can work independently and at the same time coordinate with each other. Dissecting the functional domains of ICP0 and delineating the coordination of these domains will help us understand HSV-1 pathogenicity as well as host defense mechanisms. This article focuses on describing individual ICP0 domains, their biochemical properties and their implication in HSV-1 infection. By putting individual domain functions back into the picture of host anti-viral defense network, this review seeks to elaborate the complex interactions between HSV-1 and its host.

Key words: Subcellular translocation; Herpes simplex virus 1; Infected cell protein 0; E3 ubiquitin ligase; Protein modification; ND10 nuclear bodies; Chromatin repression

Core tip: Due to the genomic limitation, viruses often use multifunctional proteins to ensure viral replication. Coordination of the multiple viral functions is critical for a successful viral infection. Infected cell protein 0 (ICP0) is notoriously multi-functional in terms of simultaneously targeting many host machineries located in different cellular compartments. Understanding the molecular basis of ICP0 multifunctionality is important for not only the elucidation of herpes simplex virus pathogenicity but also the delineation of host defense mechanisms.

Gu H. Infected cell protein 0 functional domains and their coordination in herpes simplex virus replication. *World J Virol* 2016; 5(1): 1-13 Available from: URL: http://www.wjgnet.com/2220-3249/full/v5/i1/1.htm DOI: http://dx.doi.org/10.5501/wjv.v5.i1.1

INTRODUCTION

Herpes simplex virus 1 (HSV-1) is a ubiquitous virus that infects over 70% of the world adult population. It causes a wide range of clinical manifestations, including cold sores, genital ulceration, keratitis, and herpes encephalitis. Once infected, HSV-1 establishes a lifelong latency in human trigeminal ganglia. Its sporadic reactivation nourishes a wide spread of the virus. It is one of the most prevalent opportunistic pathogens that can cause severe diseases in newborns or immunocompromised patients. Infected cell protein 0 (ICP0), an α (immediate early, IE) gene product of HSV-1, is a key regulator that activates viral gene expression in both lytic and latent infections[1]. This multifunctional protein plays a critical role in viral counteractions against the host anti-viral defenses.

In early studies, viral proteins expressed in HSV-1 infection were classified into two groups: Virion proteins and infected cell proteins (ICPs)[2]. Both groups were numbered in the order of their descending molecular weight, with number "1" representing the largest protein on high resolution polyacrylamide gels[2]. ICP0 was named outside of the natural numbers for two reasons. First, the protein level of ICP0 was significantly lower than other ICPs. ICP0 was not detected in the initial efforts of numbering the ICPs[2]. It was only discovered after a cycloheximide treatment, which augmented mRNA accumulation and boosted a sudden protein production following the cycloheximide withdrawal[3]. The second reason why ICP0 was named differently was its anomalous mobility in denaturing polyacrylamide gel electrophoresis. The relative position of ICP0 *vs* other ICPs was not consistent on gels with different acrylamide concentrations, which made it impossible to give ICP0 a fixed position in the descending order of molecular weight.

Later on ICP0 was found to be extensively post-translationally modified[4-8] and to undergo quick turnover at early infection[9,10]. The complex biochemical properties of ICP0 likely contribute to the aforementioned low abundancy and abnormal mobility. Three decades of studies have showed that ICP0 is an important viral multifunctional protein to counteract against host anti-viral defenses. It is essential for low multiplicity infection in cultured cells and for latency reactivation in animal models. However, the complexity of how ICP0 carries out those biological functions is not well understood. Understanding the biochemical foundations of ICP0 at different infection phases will help to elucidate the molecular basis of ICP0 functionality. Individual functions of ICP0 as E3 ubiquitin ligase or chromatin remodeler have been discussed elsewhere[11-16]. This review will focus on dissecting ICP0 biochemical properties and seek to understand the profound coordination in the multiple functions of ICP0.

THE TIMELINE OF REVEALING ICP0 ACTIVITIES, A BRIEF HISTORICAL OVERVIEW

Initially, ICP0 was found to transactivate HSV-1 promoters when co-transfected in mammalian cells, similar to many other IE viral proteins such as ICP4 of HSV[17,18], T antigen of SV40[19], and E1A of adenovirus[20]. However, it was quickly realized that the mechanism of ICP0 transactivation was quite different from that of other viral gene activators. For example, ICP4 is essential for viral replication. Deletion of ICP4 led to abnormal viral expression and defective DNA replication[21,22]. In the case of ICP0, gene deletion did not affect viral expression or DNA replication at high multiplicity of infection (MOI) but it had great impact on the viral yield when MOI was lower than 0.1[23]. In experimental animals, deletion of ICP0 mildly reduced the efficiency of latency establishment but completely abolished the latency reactivation[24], whereas ICP4 or ICP27 deletion rendered the mutant virus neither able to replicate in the eyes nor to establish latent infection[24]. Moreover, many viral IE proteins contain a DNA binding domain and they work in mechanisms similar to cognate transcription activators such as GAL4, but ICP0 did not bind to the DNAs it activated[25,26]. Extensive functional analysis showed that ICP0 can transactivate a wide range of cellular promoters or promoters from other DNA or RNA viruses, with no requirement of a specific *cis*-sequence[27-29]. Therefore, ICP0 is defined as a promiscuous transactivator.

The unique functionality of ICP0 energized a great amount of interests in the virology field. In early 1990s, a series of mutagenesis analyses identified a cysteine-rich region required for the ICP0 transactivation activity[30-32], which was later determined as a C3HC4 zinc binding really interesting new gene (*RING*) finger motif[33-35]. Conserved RING finger sequences were found in a large family of E3 ubiquitin ligases[36,37]. Later on, ICP0 was also proven to be an E3 ubiquitin ligase[38,39]. The discovery that various ICP0 substrates imposed restrictions on viral expression in the absence of ICP0[40-45] eventually led to a conclusion that one major function of ICP0 is to target host defensive molecules for ubiquitin-mediated proteasomal degradation. By degrading the restrictive host factors, ICP0 alleviates host defense and promotes viral gene expression.

Starting in the late 1990s, several labs made the efforts to identify ICP0 interacting proteins. From pull-down assays, yeast-2-hybrid screenings and coimmuno-

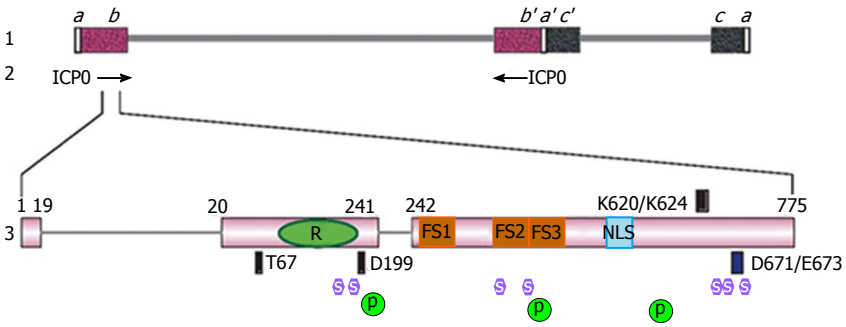

Figure 1 Schematic diagram of infected cell protein 0 gene structure and functional domains. Line 1: Genome structure of HSV-1; Line 2: Locations of the two inverted copies of ICP0 gene in the HSV-1 genome; Line 3: *ICP0* gene structure and domain properties. The amino acid numbers are labeled above the illustration of *ICP0* gene. RING finger domain, Proline-rich ND10-FSs and nuclear localization signal are represented by a green oval with "R", brown squares with "FS" and a blue rectangle with "NLS", respectively. The binding sites for RNF8 (T67), Cyclin D3 (D199), USP7 (K620/K624), and CoREST (D671/E673) are represented by the dark blue boxes above or beneath the *ICP0* gene. The positions of the seven SLSs are represented by lavender hexagons with "S" in the center. The positions of the three phosphorylation clusters are represented by dark green circles with "P" in the center. ICP0: Infected cell protein 0; HSV-1: Herpes simplex virus 1; RING: Really interesting new gene; ND10: Nuclear domains 10; NLS: Nuclear localization signal; USP7: Ubiquitin-specific protease 7; SLSs: SIM-like sequences.

precipitations, a wide range of cellular proteins were found to interact with ICP0[46-49]. Therefore ICP0 carries out viral counteractions by degrading restrictive factors and modulating repressive complexes, and consequently ICP0 enhances viral expression and replication. To better understand the coordination of ICP0 functional domains in counteracting host defenses, this review summarizes the current knowledge of ICP0 domains and ICP0 binding partners, and discusses their implications in HSV-1 infection.

ICP0 GENE STRUCTURE

The gene that encodes for ICP0 protein, also called *α0* gene, is located within the inverted sequences *ab* and *b′a′* that flank the unique long (U_L) region[50] (Figure 1). Therefore, the *ICP0* gene is one of the few HSV-1 genes that are diploid in the genome. The *ICP0* gene is also among the few HSV-1 genes that contain introns[51]. There are two introns of 765 and 136 nucleotides, respectively, intervening the three exons that encode for ICP0 amino acids 1-19, 20-241 and 242-775[51]. It is quite curious why the *ICP0* gene would evolve to bear introns because these introns do not seem to have significant functions in viral replication and alternative splicing of ICP0 has not been observed in infected cells. In one report, the ICP0 cDNA virus had a slight delay of gene expression depending on the cell-type used[52], whereas in another report differences between wild type virus and ICP0 cDNA viruses were not observed[53]. In animal models, recombinant viruses containing ICP0 deleted of introns showed no obvious defects in latency establishment and reactivation[54].

There is an in-frame stop codon located inside intron 2, which predicts a truncated form of ICP0 (ICP0R) if alternative splicing occurs. Overexpression of ICP0R inhibited the transactivation activity of the co-transfected wild type ICP0[55,56], suggesting ICP0R can work as a dominant negative to repress ICP0 activity. Although a band at the size of ICP0R was detected at low level in some cell lines[57], it remains unclear whether this is a product from alternative splicing or a product of proteolytic cleavage of ICP0. The function of ICP0R in the infection context is unknown.

One important fact about the *ICP0* gene is that the coding strand of ICP0 is anti-sense to the latency-associated transcript (LAT), the only transcript that is abundantly expressed in latently infected ganglia neurons[58,59]. The concept of LAT functioning as the anti-sense RNA to ICP0 mRNA has been explored and microRNAs identified in the LAT region have been shown to regulate ICP0 expression. Likely these actions fine-tune the basal level expression in latency maintenance and reactivation[60-62].

ICP0 PROTEIN: DOMAINS AND FUNCTIONS

RING finger domain and E3 ubiquitin ligase activity

The three exons of *ICP0* gene encodes for a 775-amino acid protein. It contains many functional domains and interacts with multiple binding partners (Table 1). The most important functional domain of ICP0 is the aforementioned C3HC4 zinc containing RING finger, which is located within exon 2 and spans through residues 116-156[63] (Figure 1). The promiscuous transactivator ability of ICP0 relies on a functional RING finger domain. Deletions or mutations of the consensus cysteine or histidine in the RING finger domain completely abolish the transactivation activity[63,64]. Recombinant viruses containing such deletions or mutations replicate at a rate similar to that of the ICP0-null virus[53,63,65]. This region is highly conserved among α-herpesviruses[34,63]. The structure of ICP0 RING finger has been solved by nuclear magnetic resonance (NMR)[35].

The RING finger domain of ICP0, like many RING superfamily members[36,66,67], works as an E3 ubiquitin ligase. Mediated by the E2 conjugating enzyme UbcH5a[68,69], ICP0 uses this domain to ubiquitinate its

Table 1 Infected cell protein 0 functional domains

Domain	Location	Function in HSV-1 replication	Section	Ref.
ICP0 cis-elements				
RING finger	aa 116-156	E3 ubiquitin ligase, degrading PML, Sp100, *etc.*	RING finger domain and E3 ubiquitin ligase activity	[63-65]
Proline-rich region	aa 241-553	Containing redundant ND10-fusion segments	Proline-rich region and ND10-fusion	[105]
NLS	aa 500-506	Nuclear localization	Nuclear localization domain and ICP0 nuclear/cytoplasmic translocation	[90]
Dimerization domain	aa 617-711	ICP0 self-dimerization, *in vivo* functions unclear	Dimerization	[115-117]
ND10-retention domain	aa 669-775	Retaining ICP0 at ND10	ND10-retention	[53]
SLSs			SUMO interaction motif and ICP0 substrate recognition	[113]
SLS-4	aa 361-367	Binding to SUMO-1/2/3, stimulating *in vitro* polyubiquitination		
SLS-5, SLS-7	aa 651-655, 681-685	Binding to SUMO-1, cooperating with SLS-4		
ICP0 binding partners				
RNF8	T67	Degrading RNF8 to regulate DNA damage responses	RNF8	[42,43]
Cyclin D3	D199	Involved in nuclear-to-cytoplasmic translocation of ICP0	Cyclin D3	[46,133-135]
BMAL1	aa 20-241	Activating viral transcription *via* BMAL1/CLOCK	BMAL1	[48,140]
EF-1δ	aa 543-768	Inhibiting translation *in vitro*, *in vivo* functions unclear	EF-1δ interaction	[96]
USP7	K620/K624	USP7 degradation, Cell-dependent ICP0 stabilization,	USP7 interaction	[47,85,88,123]
CoREST	D671/E673	Dislodging HDAC from REST/CoREST/HDAC repressor	CoREST interaction	[49,124]
WDR11	N/A	Regulating virion assembly and egress	WD repeat protein 11	[143]

ICP0: Infected cell protein 0; HSV-1: Herpes simplex virus 1; RING: Really interesting new gene; ND10: Nuclear domains 10; PML: Promyelocytic leukemia; Sp100: Speckled 100 kDa; NLS: Nuclear localization signal; SLS: SIM-like sequence; BMAL1: Brain and muscle ARNT-like protein 1; EF-1δ: Elongation factor 1δ; USP7: Ubiquitin-specific protease 7; SUMO: Small ubiquitin-like modifier; CLOCK: Circadian locomotor output cycles kaput.

substrate proteins and targets them for proteasomal degradation. The first two ICP0 substrates, promyelocytic leukemia (PML) and Sp100 (speckled 100 kDa) were identified by Chelbi-Alix and de Thé[40]. PML and Sp100 are the major organizer proteins for the dynamic nuclear bodies called nuclear domains 10 (ND10s) or PML nuclear bodies (for reviews, see references[70,71]). ND10s are nuclear structures that are composed of over 150 constituents[72]. They are involved in many cellular functions including gene regulation[73,74], cell cycle arrest[75], apoptosis[76], DNA repair[77] and anti-viral defense[78]. Degradation of PML and Sp100 by ICP0 leads to the dispersal of ND10 bodies[79]. In ICP0-null virus infection, depletion of PML and Sp100 was shown to compensate for the loss of ICP0 and to increase viral replication[41,80]. In $PML^{-/-}$ mouse embryotic fibroblasts (MEF), interferon (IFN) caused minimal effects on low multiplicity HSV-1 infection, whereas IFN treatment of $PML^{+/+}$ MEF reduced viral growth at least 1000 folds[81], suggesting that PML can mediate the IFN inhibition on viral replication. Taken together, PML is an important factor in host defense pathways and ICP0 targets PML, and maybe also Sp100, to alleviate anti-viral repressions.

Additional ICP0 substrates identified up to date include DNA-dependent protein kinase K (DNAPK)[82], centromeric proteins C and A (CENP-C and CENP-A)[83,84], ubiquitin-specific protease 7 (USP7)[85], RNF8[43], the 111-kDa isoform of poly (ADP-Ribose) glycohydrolase[86], interferon inducible protein 16 (IFI16)[44], and tripartite motif (TRIM) protein TRIM27[87]. Among these substrates, siRNA knock-down of RNF8 or IFI16 promoted the replication of ICP0-null virus[43,45], suggesting the involvement of these two proteins in host anti-viral defenses. However, depletion of TRIM27 reduced the viral yield in the absence of ICP0[87], and overexpression of USP7 accelerated gene expression in wild type HSV-1 infection[88]. These results indicate that not all ICP0 substrates place simple direct repressions on viral gene expression. Some of the substrate proteins may be degraded to regulate a more complicated cell network in order to benefit the overall viral outcome, especially the balanced actions in latent infection.

The E3 ubiquitin ligase activity of ICP0 RING finger is highly regulated by multiple factors, including its subcellular location, its phosphorylation status, and its other functional domains. For example, a failure of ICP0 to completely merge with ND10 bodies blocked substrate access and abolished PML degradation[53], and two amino acid substitutions in the C-terminal CoREST binding site (D671A/E673A) also negatively affected PML degradation[89]. The regulatory mechanisms of ICP0 E3 are not completely understood. Some of the known regulations will be discussed more in detail as we describe other important ICP0 properties in this review.

Nuclear localization domain and ICP0 nuclear/ cytoplasmic translocation

ICP0 contains a nuclear localization signal (NLS) mapped to the short stretch of basic amino acids VRPRKRR located at residues 500-506[90] (Figure 1). This arginine-rich NLS is sufficient and necessary for the nuclear localization of transiently transfected ICP0[90]. However, in infected cells, ICP0 is not an exclusively nuclear protein. Its subcellular distribution is regulated by many other factors in addition to the NLS.

First of all, ICP0 undergoes localization changes during the infection process. Early in infection, newly synthesized ICP0 is immediately transported into the nucleus in the presence of the NLS. Once inside the nucleus, ICP0 is immediately localized to the dynamic nuclear structure ND10[91]. This leads to the aforementioned degradation of ND10 organizers, PML and Sp100[40], and the subsequent disruption of ND10 nuclear bodies[79]. The dynamic interaction between ICP0 and ND10 is critical for the efficient access of ICP0 to its substrates, PML and Sp100, and their subsequent degradation[53], which will be discussed in depth in section "Proline-rich region and ND10-fusion".

After the dispersal of ND10 bodies, ICP0 diffuses throughout the nucleus. Once its nuclear functions are completed, ICP0 is translocated into the cytoplasm[92,93]. Many important ICP0 functions are carried out in the nucleus, where ICP0 degrades PML and interacts with REST/CoREST chromatin repressor (see section "CoREST interaction") early in infection. Pre-transfection of irrelevant DNA before infection can prolong ICP0 nuclear localization and delay the cytoplasmic translocation, especially in cell lines that poorly express transgenes[93]. These results suggest that ICP0 is kept within the nucleus until its nuclear functions are completed[93].

It is not yet clear how the NLS containing ICP0 protein is translocated into the cytoplasm at late infection. Either the NLS is modified late in infection so that newly translated ICP0 cannot enter the nucleus, or a nuclear export signal (NES) is unmasked late in infection so that nuclear ICP0 is exported. So far, a functional NES has not been identified.

Multiple viral factors have been found to participate in regulating the nuclear-to-cytoplasmic translocation of ICP0. For example, deletion of ICP4 caused ICP0 to lose its nuclear localization. Even at early infection, ICP0 expressed in the ICP4-null virus infected cell was solely found in the cytoplasm[94]. On the other hand, deletion of ICP27 retained ICP0 within nucleus throughout the infection and overexpression of ICP27 facilitated ICP0 export into the cytoplasm[94]. Since ICP27 is highly expressed in ICP4-null virus infected cells, ICP27 is likely the factor promoting ICP0 export. Another viral protein, VP22, has also been reported to play a role in the ICP0 cytoplasmic translocation. Deletion or mutation in VP22 restricted a series of viral proteins, including ICP0, inside the nucleus[95]. Whether or not VP22 affects a general nuclear export pathway and therefore indirectly delays ICP0 translocation remains unclear.

Functions of cytoplasmic ICP0 are not understood either. Kawaguchi *et al*[96] reported an interaction between ICP0 and translation elongation factor 1δ (EF-1δ) (also see in section "EF1δ interaction") and showed that ICP0 inhibited *in vitro* translation *via* this interaction. However, regulation of cellular translation by ICP0 is yet to be seen *in vivo*. Paladino *et al*[97] showed that ICP0 lacking NLS stayed in the cytoplasm and blocked IRF3 activation in infected cells. It remains unknown whether ICP0 directly interacts with IRF3 or secondary mediators are involved in this inhibition. Small amount of ICP0 has also been found in the tegument of purified virions[98,99]. Although the function of virion-associated ICP0 is not clear, it has been reported that ICP27 dependent cytoplasmic translocation of ICP0 is required for the incorporation of ICP0 into virions[100]. Delboy *et al*[101,102] also showed that an active ubiquitination was important for ICP0 to be incorporated into virions. Both RING finger mutation and proteasome inhibition precluded ICP0 from associating with virions. Since defective ubiquitination sequesters ICP0 within the ND10 bodies and prevents the cytoplasmic translocation of ICP0[89,92], Nicola's results are consistent with the observation that cytoplasmic localization of ICP0 in late infection is a prerequisite for the incorporation of ICP0 into virions. Since up to 49 cellular proteins have also been found in purified virions[99], the selection mechanism of low copy tegument proteins and their biological significance are not clear.

Proline-rich region and ND10-fusion

In the center of ICP0 protein, there is a long stretch of proline-rich region spanning residues 241 to 553. Initial deletion mapping found that serial deletions from the carboxyl-end of this region resulted in a progressive loss of the ICP0 transactivator activity[55], indicating the importance of this region in ICP0 functions. Multiple repeats of the PxxP motif in this region can interact with the Src homology 3 (SH3) domain in Cbl-interacting protein 85 kDa (CIN85), and a few other Src kinase family members[103,104]. Recently, Zheng *et al*[105] demonstrated that the proline-rich sequences were important to direct the fusion of ICP0 with ND10 nuclear bodies. As discussed above, ICP0 is localized to ND10 at early infection. This colocalization process is composed of three sequential dynamic steps: ND10-adhesion, ND10-fusion and ND10-retention[53]. Among these steps, a successful ICP0-ND10 fusion is essential for the ICP0 E3 ligase to access and degrade its substrate PML[53]. The proline-rich region of ICP0 is critical for the ND10-fusion step[105]. Zheng *et al*[105] showed that three proline-rich segments located at residues 242-291, 343-391, and 393-441, termed ND10-FS1, ND10-FS2 and ND10-FS3, respectively (Figure 1), redundantly facilitated the ND10-fusion of ICP0. Deletion of one or two ND10-FSs did not substantially affect the fusion process. However when all three ND10-FSs were deleted, ICP0 was blocked from entering the ND10 bodies[105]. Since most

of the cellular PML is located at ND10, the ICP0-ND10 fusion ensures a quick access of ICP0 to large amount of substrate and leads to an effective PML degradation. This likely increases the efficiency of ICP0 destroying the host restrictive factor PML and therefore enhances gene expression. The redundancy in proline-rich segments indicates the importance of ND10-fusion process in HSV-1 infection. Whether the redundant ND10-FSs synergistically improve the speed of ND10 fusion is a very important question waiting to be answered. It is also unknown whether ND10-FSs work *via* interacting with a SH3 domain or other proline-interacting motifs.

Small ubiquitin-like modifier interaction motif and ICP0 substrate recognition

Small ubiquitin-like modifier (SUMO) is a unique type of post-translational modification found on a variety of proteins. Protein SUMOylation functions in almost every aspect of a cell's life, including cell cycle, genome integrity, subcellular transport, and host immune defenses (for reviews, see references[15,106-108]). The SUMO moiety is recognized by hydrophobic sequences called the SUMO-interaction motif (SIM)[109,110]. RING-type E3 ubiquitin ligases that contain a SIM and specifically recognize SUMOylated substrates are classified as SUMO-targeted ubiquitin ligases (STUBL)[111,112]. Boutell *et al*[113] identified seven putative SIM-like sequences (SLSs) scattering throughout the ICP0 open reading frame (Figure 1). In yeast-2-hybrid assays, mutations in SLS-4 abolished the interaction between ICP0 and SUMO-2/3, whereas mutations in SLS-5 and SLS-7 did not affect such binding. SLS-4 was also found to be necessary for the *in vitro* ubiquitination of a SUMO-2 chain, indicating that ICP0 can work as a STUbL to preferentially recognize SUMOylated proteins for ubiquitination[113]. However, a recombinant virus containing mutant SLS-4 did not affect the degradation of endogenous PML in infected cells, while PML with all SUMOylation sites mutated were still degraded by ICP0[113], suggesting a more complex regulation on ICP0 substrate recognition in addition to the SUMO-SIM interaction. Moreover, although mutations in SLS-5 and SLS-7 did not interfere with the binding between ICP0 and SUMO-2/3, a recombinant virus carrying triple mutations in SLS-4/5/7 greatly demolished the ability of ICP0 to degrade PML[114]. This suggests there may be differences in the SLS affinities and multiple SLSs may work synergistically in PML degradation.

The C-terminus of ICP0 and a diverse array of functions

The C-terminus of ICP0, broadly defined for the region from downstream of NLS to the carboxyl-end, may be the most active but also the least understood region of ICP0. At least five major functions or interactions have been described in this region.

Dimerization: First, ICP0 is a protein known to aggregate and dimerize *in vitro* and *in vivo*[115-117]. In chromatography purification, ICP0 was fractionated at a much bigger molecular weight[117]. When wild type and mutant ICP0 were co-transfected into the same cell, the wild type ICP0 was able to correct the subcellular distribution of a mislocated mutant ICP0. The dimerization domain has been mapped to C-terminal residues 617-711[115]. The biological function of ICP0 dimerization is not yet clear.

ND10-retention: The second function of ICP0 C-terminus is related to the ND10 localization property of ICP0. Initial data showed that ICP0 lacking the C-terminus was evenly dispersed throughout the nucleus, compared to the full-length ICP0 that was colocalized to the ND10 bodies[117]. This led to an assumption that the C-terminus of ICP0 is responsible for ND10 localization[117,118]. However, recent results from Gu *et al*[53] showed that the C-terminus of ICP0 was not involved in the recruitment of ICP0 to ND10. In the absence of C-terminus, ICP0 did not aggregate at ND10 but had the ability to degrade PML. When a double mutant of both C-terminal truncation and RING finger mutation was introduced, ICP0 was found to localize at ND10. These results suggest that the C-truncated ICP0 undergoes adhesion and fusion steps to enter ND10, but it cycles in and out of ND10 in a more accelerated mode. Only when the inactive RING blocks the enzymatic reaction into a transition state, can the ICP0-ND10 colocalization be observed in a steady-state immunofluorescence staining. Therefore the C-terminus of ICP0 is responsible for the retention, but not the recruitment, of ICP0 to ND10.

USP7 interaction: The C-terminus of ICP0 also interacts with various proteins, such as USP7[47], CoREST[49] and EF-1δ[96], which are from proteasome pathway, chromatin repressor complex and translational machinery, respectively.

USP7 is the first ICP0 interacting protein identified *via* a GST pull-down/protein sequencing assay[47,119]. This is a deubiquitinase that regulates the ubiquitination status of many important cell check point proteins, such as p53[120], RE1-silencing transcription factor (REST)[121], and phosphatase and tensin homolog (PTEN)[122]. The minimum sequences required for the strong binding between the two are amino acids 615-633 of ICP0 and amino acids 535-889 of USP7[123]. The crystal structure of USP7 C-terminal ubiquitin-like domains bound with ICP0 peptide has been solved. Salt bridges between K620/K624 of ICP0 and D762/D764 of USP7 are critical for the interaction, while the peripheral residues form a binding pocket to support the strong ICP0-USP7 interaction[123]. Consistent structural data have also been obtained from NMR assays[124].

Initial *in vitro* ubiquitination assays showed that ICP0-USP7 interaction inhibited ICP0 autoubiquitination but promoted USP7 polyubiquitination[8,85]. Consistent with these observations, the ICP0-USP7 interaction was found essential for the degradation of USP7 by ICP0 in infected cells[85,88]. However, regarding to ICP0 autoubiquitination,

different groups have reported contradictory results[85,88]. Boutell *et al*[85] used HSV-1 (strain 17+) and reported that wild type ICP0 stayed at a steady level after cycloheximide treatment, whereas an R623L/K624I mutant virus, of which ICP0 was incapable of binding to USP7 and was quickly degraded in the presence of cycloheximide. On the other hand, Roizman and colleagues demonstrated that wild type ICP0 of HSV-1 (strain F) underwent rapid degradation at early infection and was only stabilized late in infection[9,10]. Furthermore, they found that a K620I mutant virus that abolished ICP0-USP7 interaction had enhanced, not reduced, viral gene expression but showed defects in plaque formation[88]. Therefore, ICP0-USP7 interaction may have profound biological significances, depending upon the virus strains and cell lines. Since both ICP0 and USP7 have a wide range of different substrates that are involved in critical cellular pathways, the interaction between ICP0 and USP7 may be more important in fine-tuning the ubiquitin status of these check point proteins than simply regulating ICP0 self-stability. A complex balance of these proteins may in return affect ICP0 stability in a cell type dependent manner.

CoREST interaction: CoREST binding to ICP0 was discovered by co-immunoprecipitation[125]. CoREST is the corepressor partner for REST[126]. REST/CoREST are the key components of a chromatin regulatory complex that determines neural cell fate during development[127]. The CoREST binding of ICP0 is mapped to the amino acids D671/E673[89]. Gu *et al*[125] showed that ICP0-CoREST interaction depended on the presence of viral kinases U_S3 and U_L13, and a prolonged infection resulted in less binding, suggesting that ICP0-CoREST interaction is a regulated transient process. This interaction was found essential for the dissociation of HDAC1 from REST/CoREST complex in HSV-1 infection[89,125]. A recombinant virus carrying a dominant negative CoREST incapable of HDAC1-binding showed a higher viral productivity in the absence of ICP0, which means the disruption of HDAC1-CoREST interaction is beneficial for viral replication[49]. Furthermore, on the molecular level, a recombinant virus containing D671A/E673A mutations had less acetylated histone H3 compared with the wild type virus or a mutant virus that kept the effective ICP0-CoREST interaction[128]. In contrast to these results, Everett showed that depletion of CoREST did not improve the yield of ICP0-null virus[129]. The seemingly contradictory results are reconciled from the fact that lysine-specific demethylase-1 (LSD1), another important component in the REST/CoREST complex, is required in HSV-1 replication[130]. Therefore the stoichiometry of REST/CoREST/LSD1/HDAC components[127] may play a role in determining the interaction to different viral proteins at different infection phases.

EF1δ interaction: Interaction between ICP0 and EF-1δ was identified through a yeast-2-hybrid screening[96]. The binding has been mapped to the C-terminal residues 543-768 and found to inhibit *in vitro* translation[96]. However, *in vivo* function of this interaction is not clear.

For all these different C-terminal functions it is not clear how these seemingly unrelated activities coordinate in this region. Are there different subsets of ICP0 distributed in distinct subcellular compartments? Or some of the components from different pathways converge at certain cellular hubs, such as ND10? Answers to these questions will be the key to understanding the complex functions of ICP0 in both lytic and latent infections.

Other ICP0 interaction partners

Cyclin D3: Cyclin D3 is identified as an ICP0-interacting protein by a yeast-2-hybrid screening[46]. D-type cyclins form complexes with cyclin-dependent kinases to regulate G1 to S phase transition[131,132], which can be manipulated by many DNA viruses for the purpose of promoting DNA synthesis in infected cells[133]. ICP0 interacts with Cyclin D3 through its amino acid D199 located in exon 2, downstream to the RING finger domain (Figure 1). The D199-Cyclin D3 interaction is important in the nuclear-to-cytoplasmic translocation of ICP0. Mutation in cyclin D3 binding site or treatment by CDK4 inhibitor during the infection prevented ICP0 from translocating to the cytoplasm[134,135], whereas insertion of cyclin D3 gene into the HSV-1 genome to overexpress cyclin D3 led to an accelerated cytoplasmic translocation[135,136]. The regulation of the cell cycle during HSV-1 infection is a profound event involving multiple factors. For example, HSV-1 ICP22 and U_L13 are found to participate in G2/M transition[137], and CDK inhibitor roscovitine inhibits HSV-1 gene transcription without affecting PML degradation[138,139]. Moreover, the D199 dependent nuclear-to-cytoplasmic translocation of ICP0 is a process that depends on viral DNA replication and the expression of a late protein(s)[92]. Therefore different cell cycle regulatory pathways are interwoven with ICP0 phosphorylation, translocation and possibly other infection events. The concerted efforts from both viral and cellular sides determine the ultimate productivity of an HSV-1 infection.

Brain and muscle ARNT-like protein 1: Brain and muscle ARNT-like protein 1 (BMAL1) interacting with ICP0 is also identified by a yeast-2-hybrid screening[48]. The interaction site to BMAL1 is located in the exon 2 of ICP0[48]. BMAL1 and circadian locomotor output cycles kaput (CLOCK), a histone acetyltransferase, forms a heterodimer to regulate mammalian circadian oscillation[140]. During HSV-1 infection, CLOCK is stabilized and recruited to ND10, which acts as a transcription activator to stimulate viral transcription and replication[141].

RNF8: The identification of ICP0-RNF8 interaction was based on the observation that RNF8 was degraded by ICP0 in HSV-1 infection[42,43]. RNF8 is an RING type E3 ubiquitin ligase that plays a key role in histone ubiquitination and chromatin remodeling upon DNA double-

stranded break (DBS) damage[142,143]. ICP0-RNF8 binding is mapped to the phosphorylated amino acid T67 of ICP0, and amino acid R42 of RNF8[43]. A recombinant virus carrying the T67A mutation did not degrade RNF8 but had no problems in degrading DNAPK or USP7, which means ICP0-RNF8 interaction is likely important for a specific RNF8 substrate recognition[43]. Interestingly, knock-down of RNF8 only mildly delayed *ICP27* gene transcription and had no effects on viral DNA replication, suggesting that the involvement of ICP0-RNF8 interaction in responding to DBS DNA damage is, again, a complex action.

WD repeat protein 11: WD repeat protein 11 (WDR11) is a newly reported ICP0 interacting protein identified by co-immunoprecipitation[144]. Taylor *et al*[144] showed that the trans-Golgi network localized WDR11 pulled down several viral proteins including gB, VP16 and VP5 in additional to ICP0, suggesting its possible role in virion assembly and egress.

POST-TRANSLATIONAL PROCESSING OF ICP0

Modification

ICP0 protein contains 775 amino acids, but the apparent molecular weight of ICP0 is about 110 kDa[3], suggesting the presence of post-translational modifications for ICP0. First of all, ICP0 is highly phosphorylated. On two-dimensional gel electrophoreses, ICP0 phosphorylation status changes along with the progression of infection[6]. The phosphorylation sites on ICP0 has been mapped to three phosphor-clusters by tandem mass spectrometry. Cluster 1 is at residues 222-250, cluster 2 is at residues 356-386, and duster 3 is at residues 505-528[145] (Figure 1). Davido and colleagues showed that serine/threonine mutations in these clusters demolished the transactivation activity of ICP0 and reduced the viral replication in mice[145,146]. Viral protein U_L13 was found important for ICP0 phosphorylation[147]. However, how ICP0 phosphorylation coordinates with ICP0 localizations or ICP0 protein-protein interactions to affect the infection is not yet known.

Other modifications of ICP0 are understudied. ICP0 is believed to be nucleotidylated because it can be radiolabeled in infected cells cultured with [α-^{32}P]GTP or [2-^{3}H]ATP containing medium[5]. ICP0 may also be ubiquitinated because it is found to autoubiquitinate itself in *in vitro* polyubiquitination assays[8].

Proteolytic cleavage and rapid turnover

At least in the infection of HSV-1 (strain F), ICP0 undergoes a rapid degradation at early infection in both proteasome dependent and proteasome independent manners. The protein is then stabilized at late infection[9]. The proteasome independent cleavage occurs in the central region of ICP0 and the rapid turnover depends on the *cis* presence of an active RING finger as well as the phosphorylation status of ICP0[9,10].

CONCLUSION

Like all herpesvirus family members, HSV-1 establishes latent infection. The peculiar life cycle of HSV-1 necessitates a close interaction and a delicate balance between the virus and its host. ICP0 of HSV-1, a unique multifunctional protein, plays a key regulatory role to enhance gene expression in lytic infection and to reactivate virion production from latent infection. This protein is tightly regulated on transcriptional, post-transcriptional and post-translational levels. Through its intrinsic functional domains and its ability to interact with a wide range of binding partners, ICP0 can target many cellular protein for proteasomal degradation and regulate various cell pathways *via* protein-protein interactions.

To achieve its multiple functions, ICP0 undergoes modification and subcellular translocation. Early in infection, ICP0 is immediately imported into the nucleus upon synthesis. Once inside the nucleus, it is recruited to adhere at and then fuse with ND10 to co-mingle with ND10 components. The ND10-fusion process ensures ICP0 to quickly access large amounts of PML and Sp100 for degradation and to extensively interact with many of the regulatory factors located within ND10. This early step in HSV-1 infection is vital for the outcome of a productive infection, not only by destroying and dispersing the repressive factors but also by capturing favorable factors that help establishing replication compartment. Upon viral DNA entering the nucleus, host cell attempt to silence the foreign intrusion by: (1) forming ND10 bodies near viral DNA[148]; (2) recruiting chromatin repressors[149]; and (3) stimulating IFN responses[45]. In a way, HSV-1 deploys ICP0 to approach ND10 is a "smart" move because ND10 serves as a molecular hub for many cellular pathways and it is able to recruit component factors upon specific stimulations[78]. Therefore, adopting factors recruited to ND10 during infection while destroying and repelling restrictive components is an effective strategy to boost viral replication. In fact, various cellular check point proteins such as USP7, CoREST, Cyclin D3, BMAL1 and CLOCK are all recruited to ND10 upon infection and they are found in HSV-1 replication compartments[47,135,141,149]. In fact, HSV-1 replication compartments are established at the sites where ND10 loci have been located before their dispersal[149]. ICP0 interacting with the molecular hub ND10 is a major adaptation to coordinate the multitasking of ICP0 functions. Likely the sequential steps of ICP0-ND10 interaction, ND10-adhesion, ND10-fusion, ND10-retention[53], play important roles in achieving the "destroy and then take over" strategy.

Once the replication compartments are set up in the infected cells, ICP0 may have additional functions in a diffused pattern in nucleus and then in the cytoplasm. Whether the trafficking of ICP0 is regulated by post-translational modification or proteolytic processing is currently unknown. Solving the road map of ICP0 being in the right place at the right time will be a continuous

interest in the near future for herpes virology field.

ICP0 is required for latency reactivation[24]. The subtle balance of ICP0 level in latent infection may be achieved by microRNA regulation. The rapid turnover of ICP0 on the protein level may also be essential for the maintenance and reactivation of latent infection. After all, one good way to achieve massive spreading is to keep the sporadic but not severe recurrent infections.

REFERENCES

1 **Roizman B**, Knipe DM., Whitley RJ. Herpes Simplex Viruses, in Fields Virology, 6 Edition, Lippincott Williams & Wilkins, 2013: 1823-1897

2 **Honess RW**, Roizman B. Proteins specified by herpes simplex virus. XI. Identification and relative molar rates of synthesis of structural and nonstructural herpes virus polypeptides in the infected cell. *J Virol* 1973; **12**: 1347-1365 [PMID: 4357511]

3 **Honess RW**, Roizman B. Regulation of herpesvirus macromolecular synthesis. I. Cascade regulation of the synthesis of three groups of viral proteins. *J Virol* 1974; **14**: 8-19 [PMID: 4365321]

4 **Ackermann M**, Braun DK, Pereira L, Roizman B. Characterization of herpes simplex virus 1 alpha proteins 0, 4, and 27 with monoclonal antibodies. *J Virol* 1984; **52**: 108-118 [PMID: 6090689]

5 **Blaho JA**, Mitchell C, Roizman B. Guanylylation and adenylylation of the alpha regulatory proteins of herpes simplex virus require a viral beta or gamma function. *J Virol* 1993; **67**: 3891-3900 [PMID: 8389911]

6 **Advani SJ**, Hagglund R, Weichselbaum RR, Roizman B. Post-translational processing of infected cell proteins 0 and 4 of herpes simplex virus 1 is sequential and reflects the subcellular compartment in which the proteins localize. *J Virol* 2001; **75**: 7904-7912 [PMID: 11483735 DOI: 10.1128/JVI.75.17.7904-7912.2001]

7 **Weber PC**, Spatz SJ, Nordby EC. Stable ubiquitination of the ICP0R protein of herpes simplex virus type 1 during productive infection. *Virology* 1999; **253**: 288-298 [PMID: 9918887 DOI: 10.1006/viro.1998.9502]

8 **Canning M**, Boutell C, Parkinson J, Everett RD. A RING finger ubiquitin ligase is protected from autocatalyzed ubiquitination and degradation by binding to ubiquitin-specific protease USP7. *J Biol Chem* 2004; **279**: 38160-38168 [PMID: 15247261 DOI: 10.1074/jbc.M402885200]

9 **Gu H**, Poon AP, Roizman B. During its nuclear phase the multifunctional regulatory protein ICP0 undergoes proteolytic cleavage characteristic of polyproteins. *Proc Natl Acad Sci USA* 2009; **106**: 19132-19137 [PMID: 19850872 DOI: 10.1073/pnas.0910920106]

10 **Zhu Z**, Du T, Zhou G, Roizman B. The stability of herpes simplex virus 1 ICP0 early after infection is defined by the RING finger and the UL13 protein kinase. *J Virol* 2014; **88**: 5437-5443 [PMID: 24574411 DOI: 10.1128/JVI.00542-14]

11 **Everett RD**. ICP0, a regulator of herpes simplex virus during lytic and latent infection. *Bioessays* 2000; **22**: 761-770 [PMID: 10918307 DOI: 10.1002/1521-1878(200008)22:8<761::AID-BIES10>3.0.CO;2-A]

12 **Hagglund R**, Roizman B. Role of ICP0 in the strategy of conquest of the host cell by herpes simplex virus 1. *J Virol* 2004; **78**: 2169-2178 [PMID: 14963113 DOI: 10.1128/JVI.78.5.2169-2178.2004]

13 **Roizman B**, Gu H, Mandel G. The first 30 minutes in the life of a virus: unREST in the nucleus. *Cell Cycle* 2005; **4**: 1019-1021 [PMID: 16082207 DOI: 10.4161/cc.4.8.1902]

14 **Boutell C**, Everett RD. Regulation of alphaherpesvirus infections by the ICP0 family of proteins. *J Gen Virol* 2013; **94**: 465-481 [PMID: 23239572 DOI: 10.1099/vir.0.048900-0]

15 **Everett RD**, Boutell C, Hale BG. Interplay between viruses and host sumoylation pathways. *Nat Rev Microbiol* 2013; **11**: 400-411 [PMID: 23624814 DOI: 10.1038/nrmicro3015]

16 **Zhou G**, Du T, Roizman B. The role of the CoREST/REST repressor complex in herpes simplex virus 1 productive infection and in latency. *Viruses* 2013; **5**: 1208-1218 [PMID: 23628827 DOI: 10.3390/v5051208]

17 **Gelman IH**, Silverstein S. Identification of immediate early genes from herpes simplex virus that transactivate the virus thymidine kinase gene. *Proc Natl Acad Sci USA* 1985; **82**: 5265-5269 [PMID: 2991915 DOI: 10.1073/pnas.82.16.5265]

18 **Quinlan MP**, Knipe DM. Stimulation of expression of a herpes simplex virus DNA-binding protein by two viral functions. *Mol Cell Biol* 1985; **5**: 957-963 [PMID: 2987684 DOI: 10.1128/MCB.5.5.957]

19 **Myers RM**, Rio DC, Robbins AK, Tjian R. SV40 gene expression is modulated by the cooperative binding of T antigen to DNA. *Cell* 1981; **25**: 373-384 [PMID: 6269743 DOI: 10.1016/0092-8674(81)90056-8]

20 **Nevins JR**. Mechanism of activation of early viral transcription by the adenovirus E1A gene product. *Cell* 1981; **26**: 213-220 [PMID: 7332929 DOI: 10.1016/0092-8674(81)90304-4]

21 **Dixon RA**, Schaffer PA. Fine-structure mapping and functional analysis of temperature-sensitive mutants in the gene encoding the herpes simplex virus type 1 immediate early protein VP175. *J Virol* 1980; **36**: 189-203 [PMID: 6255206]

22 **DeLuca NA**, McCarthy AM, Schaffer PA. Isolation and characterization of deletion mutants of herpes simplex virus type 1 in the gene encoding immediate-early regulatory protein ICP4. *J Virol* 1985; **56**: 558-570 [PMID: 2997476]

23 **Stow ND**, Stow EC. Isolation and characterization of a herpes simplex virus type 1 mutant containing a deletion within the gene encoding the immediate early polypeptide Vmw110. *J Gen Virol* 1986; **67** (Pt 12): 2571-2585 [PMID: 3025339 DOI: 10.1099/0022-1317-67-12-2571]

24 **Leib DA**, Coen DM, Bogard CL, Hicks KA, Yager DR, Knipe DM, Tyler KL, Schaffer PA. Immediate-early regulatory gene mutants define different stages in the establishment and reactivation of herpes simplex virus latency. *J Virol* 1989; **63**: 759-768 [PMID: 2536101]

25 **Purifoy DJ**, Powell KL. DNA-binding proteins induced by herpes simplex virus type 2 in HEp-2 cells. *J Virol* 1976; **19**: 717-731 [PMID: 183021]

26 **Wilcox KW**, Kohn A, Sklyanskaya E, Roizman B. Herpes simplex virus phosphoproteins. I. Phosphate cycles on and off some viral polypeptides and can alter their affinity for DNA. *J Virol* 1980; **33**: 167-182 [PMID: 6245226]

27 **Nabel GJ**, Rice SA, Knipe DM, Baltimore D. Alternative mechanisms for activation of human immunodeficiency virus enhancer in T cells. *Science* 1988; **239**: 1299-1302 [PMID: 2830675 DOI: 10.1126/science.2830675]

28 **Gius D**, Laimins LA. Activation of human papillomavirus type 18 gene expression by herpes simplex virus type 1 viral transactivators and a phorbol ester. *J Virol* 1989; **63**: 555-563 [PMID: 2536091]

29 **Kwun HJ**, Han HJ, Lee WJ, Kim HS, Jang KL. Transactivation of the human endogenous retrovirus K long terminal repeat by herpes simplex virus type 1 immediate early protein 0. *Virus Res* 2002; **86**: 93-100 [PMID: 12076833 DOI: 10.1016/S0168-1702(02)00058-8]

30 **Chen JX**, Zhu XX, Silverstein S. Mutational analysis of the sequence encoding ICP0 from herpes simplex virus type 1. *Virology* 1991; **180**: 207-220 [PMID: 1845823 DOI: 10.1016/0042-6822(91)90025-7]

31 **Everett RD**. A detailed mutational analysis of Vmw110, a trans-acting transcriptional activator encoded by herpes simplex virus type 1. *EMBO J* 1987; **6**: 2069-2076 [PMID: 2820720]

32 **Everett R**, O'Hare P, O'Rourke D, Barlow P, Orr A. Point mutations in the herpes simplex virus type 1 Vmw110 RING finger helix affect activation of gene expression, viral growth, and interaction with PML-containing nuclear structures. *J Virol* 1995; **69**: 7339-7344 [PMID: 7474166]

33 **Freemont PS**, Hanson IM, Trowsdale J. A novel cysteine-rich sequence motif. *Cell* 1991; **64**: 483-484 [PMID: 1991318]

34 **Everett RD**, Barlow P, Milner A, Luisi B, Orr A, Hope G, Lyon D. A novel arrangement of zinc-binding residues and secondary structure in the C3HC4 motif of an alpha herpes virus protein family. *J Mol Biol* 1993; **234**: 1038-1047 [PMID: 8263911 DOI:

10.1006/jmbi.1993.1657]
35 **Barlow PN**, Luisi B, Milner A, Elliott M, Everett R. Structure of the C3HC4 domain by 1H-nuclear magnetic resonance spectroscopy. A new structural class of zinc-finger. *J Mol Biol* 1994; **237**: 201-211 [PMID: 8126734 DOI: 10.1006/jmbi.1994.1222]
36 **Freemont PS**. RING for destruction? *Curr Biol* 2000; **10**: R84-R87 [PMID: 10662664]
37 **Metzger MB**, Pruneda JN, Klevit RE, Weissman AM. RING-type E3 ligases: master manipulators of E2 ubiquitin-conjugating enzymes and ubiquitination. *Biochim Biophys Acta* 2014; **1843**: 47-60 [PMID: 23747565 DOI: 10.1016/j.bbamcr.2013.05.026]
38 **Boutell C**, Sadis S, Everett RD. Herpes simplex virus type 1 immediate-early protein ICP0 and is isolated RING finger domain act as ubiquitin E3 ligases in vitro. *J Virol* 2002; **76**: 841-850 [PMID: 11752173 DOI: 10.1128/JVI.76.2.841-850.2002]
39 **Hagglund R**, Van Sant C, Lopez P, Roizman B. Herpes simplex virus 1-infected cell protein 0 contains two E3 ubiquitin ligase sites specific for different E2 ubiquitin-conjugating enzymes. *Proc Natl Acad Sci USA* 2002; **99**: 631-636 [PMID: 11805320 DOI: 10.1073/pnas.022531599]
40 **Chelbi-Alix MK**, de Thé H. Herpes virus induced proteasome-dependent degradation of the nuclear bodies-associated PML and Sp100 proteins. *Oncogene* 1999; **18**: 935-941 [PMID: 10023669 DOI: 10.1038/sj.onc.1202366]
41 **Everett RD**, Parada C, Gripon P, Sirma H, Orr A. Replication of ICP0-null mutant herpes simplex virus type 1 is restricted by both PML and Sp100. *J Virol* 2008; **82**: 2661-2672 [PMID: 18160441 DOI: 10.1128/JVI.02308-07]
42 **Lilley CE**, Chaurushiya MS, Boutell C, Landry S, Suh J, Panier S, Everett RD, Stewart GS, Durocher D, Weitzman MD. A viral E3 ligase targets RNF8 and RNF168 to control histone ubiquitination and DNA damage responses. *EMBO J* 2010; **29**: 943-955 [PMID: 20075863 DOI: 10.1038/emboj.2009.400]
43 **Chaurushiya MS**, Lilley CE, Aslanian A, Meisenhelder J, Scott DC, Landry S, Ticau S, Boutell C, Yates JR, Schulman BA, Hunter T, Weitzman MD. Viral E3 ubiquitin ligase-mediated degradation of a cellular E3: viral mimicry of a cellular phosphorylation mark targets the RNF8 FHA domain. *Mol Cell* 2012; **46**: 79-90 [PMID: 22405594 DOI: 10.1016/j.molcel.2012.02.004]
44 **Orzalli MH**, DeLuca NA, Knipe DM. Nuclear IFI16 induction of IRF-3 signaling during herpesviral infection and degradation of IFI16 by the viral ICP0 protein. *Proc Natl Acad Sci USA* 2012; **109**: E3008-E3017 [PMID: 23027953 DOI: 10.1073/pnas.1211302109]
45 **Orzalli MH**, Conwell SE, Berrios C, DeCaprio JA, Knipe DM. Nuclear interferon-inducible protein 16 promotes silencing of herpesviral and transfected DNA. *Proc Natl Acad Sci USA* 2013; **110**: E4492-E4501 [PMID: 24198334 DOI: 10.1073/pnas.1316194110]
46 **Kawaguchi Y**, Van Sant C, Roizman B. Herpes simplex virus 1 alpha regulatory protein ICP0 interacts with and stabilizes the cell cycle regulator cyclin D3. *J Virol* 1997; **71**: 7328-7336 [PMID: 9311810]
47 **Everett RD**, Meredith M, Orr A, Cross A, Kathoria M, Parkinson J. A novel ubiquitin-specific protease is dynamically associated with the PML nuclear domain and binds to a herpesvirus regulatory protein. *EMBO J* 1997; **16**: 1519-1530 [PMID: 9130697 DOI: 10.1093/emboj/16.7.1519]
48 **Kawaguchi Y**, Tanaka M, Yokoymama A, Matsuda G, Kato K, Kagawa H, Hirai K, Roizman B. Herpes simplex virus 1 alpha regulatory protein ICP0 functionally interacts with cellular transcription factor BMAL1. *Proc Natl Acad Sci USA* 2001; **98**: 1877-1882 [PMID: 11172044 DOI: 10.1073/pnas.041592598]
49 **Gu H**, Roizman B. Herpes simplex virus-infected cell protein 0 blocks the silencing of viral DNA by dissociating histone deacetylases from the CoREST-REST complex. *Proc Natl Acad Sci USA* 2007; **104**: 17134-17139 [PMID: 17939992 DOI: 10.1073/pnas.0707266104]
50 **Wadsworth S**, Jacob RJ, Roizman B. Anatomy of herpes simplex virus DNA. II. Size, composition, and arrangement of inverted terminal repetitions. *J Virol* 1975; **15**: 1487-1497 [PMID: 167196]
51 **Perry LJ**, Rixon FJ, Everett RD, Frame MC, McGeoch DJ. Characterization of the IE110 gene of herpes simplex virus type 1. *J Gen Virol* 1986; **67** (Pt 11): 2365-2380 [PMID: 3023529 DOI: 10.1099/0022-1317-67-11-2365]
52 **Poon AP**, Silverstein SJ, Roizman B. An early regulatory function required in a cell type-dependent manner is expressed by the genomic but not the cDNA copy of the herpes simplex virus 1 gene encoding infected cell protein 0. *J Virol* 2002; **76**: 9744-9755 [PMID: 12208953 DOI: 10.1128/JVI.76.19.9744-9755.2002]
53 **Gu H**, Zheng Y, Roizman B. Interaction of herpes simplex virus ICP0 with ND10 bodies: a sequential process of adhesion, fusion, and retention. *J Virol* 2013; **87**: 10244-10254 [PMID: 23864622 DOI: 10.1128/jvi.01487-13]
54 **Natarajan R**, Deshmane S, Valyi-Nagy T, Everett R, Fraser NW. A herpes simplex virus type 1 mutant lacking the ICP0 introns reactivates with normal efficiency. *J Virol* 1991; **65**: 5569-5573 [PMID: 1654452]
55 **Weber PC**, Wigdahl B. Identification of dominant-negative mutants of the herpes simplex virus type 1 immediate-early protein ICP0. *J Virol* 1992; **66**: 2261-2267 [PMID: 1312631]
56 **Weber PC**, Kenny JJ, Wigdahl B. Antiviral properties of a dominant negative mutant of the herpes simplex virus type 1 regulatory protein ICP0. *J Gen Virol* 1992; **73** (Pt 11): 2955-2961 [PMID: 1331297 DOI: 10.1099/0022-1317-73-11-2955]
57 **Everett RD**, Cross A, Orr A. A truncated form of herpes simplex virus type 1 immediate-early protein Vmw110 is expressed in a cell type dependent manner. *Virology* 1993; **197**: 751-756 [PMID: 7504367 DOI: 10.1006/viro.1993.1651]
58 **Stevens JG**, Wagner EK, Devi-Rao GB, Cook ML, Feldman LT. RNA complementary to a herpesvirus alpha gene mRNA is prominent in latently infected neurons. *Science* 1987; **235**: 1056-1059 [PMID: 2434993 DOI: 10.1126/science.2434993]
59 **Rock DL**, Nesburn AB, Ghiasi H, Ong J, Lewis TL, Lokensgard JR, Wechsler SL. Detection of latency-related viral RNAs in trigeminal ganglia of rabbits latently infected with herpes simplex virus type 1. *J Virol* 1987; **61**: 3820-3826 [PMID: 2824816]
60 **Cui C**, Griffiths A, Li G, Silva LM, Kramer MF, Gaasterland T, Wang XJ, Coen DM. Prediction and identification of herpes simplex virus 1-encoded microRNAs. *J Virol* 2006; **80**: 5499-5508 [PMID: 16699030 DOI: 10.1128/JVI.00200-06]
61 **Umbach JL**, Kramer MF, Jurak I, Karnowski HW, Coen DM, Cullen BR. MicroRNAs expressed by herpes simplex virus 1 during latent infection regulate viral mRNAs. *Nature* 2008; **454**: 780-783 [PMID: 18596690 DOI: 10.1038/nature07103]
62 **Jiang X**, Brown D, Osorio N, Hsiang C, Li L, Chan L, Ben–Mohamed L, Wechsler SL. A herpes simplex virus type 1 mutant disrupted for microRNA H2 with increased neurovirulence and rate of reactivation. *J Neurovirol* 2015; **21**: 199-209 [PMID: 25645379 DOI: 10.1007/s13365-015-0319-1]
63 **Lium EK**, Silverstein S. Mutational analysis of the herpes simplex virus type 1 ICP0 C3HC4 zinc ring finger reveals a requirement for ICP0 in the expression of the essential alpha27 gene. *J Virol* 1997; **71**: 8602-8614 [PMID: 9343218]
64 **Everett RD**. Analysis of the functional domains of herpes simplex virus type 1 immediate-early polypeptide Vmw110. *J Mol Biol* 1988; **202**: 87-96 [PMID: 2845096 DOI: 10.1016/0022-2836(88)90521-9]
65 **Everett RD**. Construction and characterization of herpes simplex virus type 1 mutants with defined lesions in immediate early gene 1. *J Gen Virol* 1989; **70** (Pt 5): 1185-1202 [PMID: 2543774 DOI: 10.1099/0022-1317-70-5-1185]
66 **Tyers M**, Willems AR. One ring to rule a superfamily of E3 ubiquitin ligases. *Science* 1999; **284**: 601, 603-604 [PMID: 10328744 DOI: 10.1126/science.284.5414.601]
67 **Joazeiro CA**, Weissman AM. RING finger proteins: mediators of ubiquitin ligase activity. *Cell* 2000; **102**: 549-552 [PMID: 11007473 DOI: 10.1016/S0092-8674(00)00077-5]
68 **Gu H**, Roizman B. The degradation of promyelocytic leukemia and Sp100 proteins by herpes simplex virus 1 is mediated by the ubiquitin-conjugating enzyme UbcH5a. *Proc Natl Acad Sci USA* 2003; **100**: 8963-8968 [PMID: 12855769 DOI: 10.1073/

pnas.1533420100]
69 **Vanni E**, Gatherer D, Tong L, Everett RD, Boutell C. Functional characterization of residues required for the herpes simplex virus 1 E3 ubiquitin ligase ICP0 to interact with the cellular E2 ubiquitin-conjugating enzyme UBE2D1 (UbcH5a). *J Virol* 2012; **86**: 6323-6333 [PMID: 22438555 DOI: 10.1128/JVI.07210-11]
70 **Maul GG**, Negorev D, Bell P, Ishov AM. Review: properties and assembly mechanisms of ND10, PML bodies, or PODs. *J Struct Biol* 2000; **129**: 278-287 [PMID: 10806078 DOI: 10.1006/jsbi.2000.4239]
71 **Everett RD**, Chelbi-Alix MK. PML and PML nuclear bodies: implications in antiviral defence. *Biochimie* 2007; **89**: 819-830 [PMID: 17343971 DOI: 10.1016/j.biochi.2007.01.004]
72 **Van Damme E**, Laukens K, Dang TH, Van Ostade X. A manually curated network of the PML nuclear body interactome reveals an important role for PML-NBs in SUMOylation dynamics. *Int J Biol Sci* 2010; **6**: 51-67 [PMID: 20087442 DOI: 10.7150/ijbs.6.51]
73 **Zhong S**, Salomoni P, Pandolfi PP. The transcriptional role of PML and the nuclear body. *Nat Cell Biol* 2000; **2**: E85-E90 [PMID: 10806494 DOI: 10.1038/35010583]
74 **Cohen N**, Sharma M, Kentsis A, Perez JM, Strudwick S, Borden KL. PML RING suppresses oncogenic transformation by reducing the affinity of eIF4E for mRNA. *EMBO J* 2001; **20**: 4547-4559 [PMID: 11500381 DOI: 10.1093/emboj/20.16.4547]
75 **Wang ZG**, Delva L, Gaboli M, Rivi R, Giorgio M, Cordon-Cardo C, Grosveld F, Pandolfi PP. Role of PML in cell growth and the retinoic acid pathway. *Science* 1998; **279**: 1547-1551 [PMID: 9488655 DOI: 10.1126/science.279.5356.1547]
76 **Bernardi R**, Pandolfi PP. Role of PML and the PML-nuclear body in the control of programmed cell death. *Oncogene* 2003; **22**: 9048-9057 [PMID: 14663483 DOI: 10.1038/sj.onc.1207106]
77 **Carbone R**, Pearson M, Minucci S, Pelicci PG. PML NBs associate with the hMre11 complex and p53 at sites of irradiation induced DNA damage. *Oncogene* 2002; **21**: 1633-1640 [PMID: 11896594 DOI: 10.1038/sj.onc.1205227]
78 **Geoffroy MC**, Chelbi-Alix MK. Role of promyelocytic leukemia protein in host antiviral defense. *J Interferon Cytokine Res* 2011; **31**: 145-158 [PMID: 21198351 DOI: 10.1089/jir.2010.0111]
79 **Everett RD**, Freemont P, Saitoh H, Dasso M, Orr A, Kathoria M, Parkinson J. The disruption of ND10 during herpes simplex virus infection correlates with the Vmw110- and proteasome-dependent loss of several PML isoforms. *J Virol* 1998; **72**: 6581-6591 [PMID: 9658103]
80 **Everett RD**, Rechter S, Papior P, Tavalai N, Stamminger T, Orr A. PML contributes to a cellular mechanism of repression of herpes simplex virus type 1 infection that is inactivated by ICP0. *J Virol* 2006; **80**: 7995-8005 [PMID: 16873256 DOI: 10.1128/JVI.00734-06]
81 **Chee AV**, Lopez P, Pandolfi PP, Roizman B. Promyelocytic leukemia protein mediates interferon-based anti-herpes simplex virus 1 effects. *J Virol* 2003; **77**: 7101-7105 [PMID: 12768029 DOI: 10.1128/JVI.77.12.7101-7105.2003]
82 **Parkinson J**, Lees-Miller SP, Everett RD. Herpes simplex virus type 1 immediate-early protein vmw110 induces the proteasome-dependent degradation of the catalytic subunit of DNA-dependent protein kinase. *J Virol* 1999; **73**: 650-657 [PMID: 9847370]
83 **Everett RD**, Earnshaw WC, Findlay J, Lomonte P. Specific destruction of kinetochore protein CENP-C and disruption of cell division by herpes simplex virus immediate-early protein Vmw110. *EMBO J* 1999; **18**: 1526-1538 [PMID: 10075924 DOI: 10.1093/emboj/18.6.1526]
84 **Lomonte P**, Sullivan KF, Everett RD. Degradation of nucleosome-associated centromeric histone H3-like protein CENP-A induced by herpes simplex virus type 1 protein ICP0. *J Biol Chem* 2001; **276**: 5829-5835 [PMID: 11053442 DOI: 10.1074/jbc.M008547200]
85 **Boutell C**, Canning M, Orr A, Everett RD. Reciprocal activities between herpes simplex virus type 1 regulatory protein ICP0, a ubiquitin E3 ligase, and ubiquitin-specific protease USP7. *J Virol* 2005; **79**: 12342-12354 [PMID: 16160161 DOI: 10.1128/JVI.79.19.12342-12354.2005]
86 **Grady SL**, Hwang J, Vastag L, Rabinowitz JD, Shenk T. Herpes simplex virus 1 infection activates poly(ADP-ribose) polymerase and triggers the degradation of poly(ADP-ribose) glycohydrolase. *J Virol* 2012; **86**: 8259-8268 [PMID: 22623791 DOI: 10.1128/JVI.00495-12]
87 **Conwell SE**, White AE, Harper JW, Knipe DM. Identification of TRIM27 as a novel degradation target of herpes simplex virus 1 ICP0. *J Virol* 2015; **89**: 220-229 [PMID: 25320289 DOI: 10.1128/JVI.02635-14]
88 **Kalamvoki M**, Gu H, Roizman B. Overexpression of the ubiquitin-specific protease 7 resulting from transfection or mutations in the ICP0 binding site accelerates rather than depresses herpes simplex virus 1 gene expression. *J Virol* 2012; **86**: 12871-12878 [PMID: 22993145 DOI: 10.1128/JVI.01981-12]
89 **Gu H**, Roizman B. The two functions of herpes simplex virus 1 ICP0, inhibition of silencing by the CoREST/REST/HDAC complex and degradation of PML, are executed in tandem. *J Virol* 2009; **83**: 181-187 [PMID: 18945770 DOI: 10.1128/JVI.01940-08]
90 **Mullen MA**, Ciufo DM, Hayward GS. Mapping of intracellular localization domains and evidence for colocalization interactions between the IE110 and IE175 nuclear transactivator proteins of herpes simplex virus. *J Virol* 1994; **68**: 3250-3266 [PMID: 8151787]
91 **Everett RD**, Maul GG. HSV-1 IE protein Vmw110 causes redistribution of PML. *EMBO J* 1994; **13**: 5062-5069 [PMID: 7957072]
92 **Lopez P**, Van Sant C, Roizman B. Requirements for the nuclear-cytoplasmic translocation of infected-cell protein 0 of herpes simplex virus 1. *J Virol* 2001; **75**: 3832-3840 [PMID: 11264372 DOI: 10.1128/JVI.75.8.3832-3840.2001]
93 **Kalamvoki M**, Roizman B. Role of herpes simplex virus ICP0 in the transactivation of genes introduced by infection or transfection: a reappraisal. *J Virol* 2010; **84**: 4222-4228 [PMID: 20164233 DOI: 10.1128/JVI.02585-09]
94 **Zhu Z**, Cai W, Schaffer PA. Cooperativity among herpes simplex virus type 1 immediate-early regulatory proteins: ICP4 and ICP27 affect the intracellular localization of ICP0. *J Virol* 1994; **68**: 3027-3040 [PMID: 8151771]
95 **Tanaka M**, Kato A, Satoh Y, Ide T, Sagou K, Kimura K, Hasegawa H, Kawaguchi Y. Herpes simplex virus 1 VP22 regulates translocation of multiple viral and cellular proteins and promotes neurovirulence. *J Virol* 2012; **86**: 5264-5277 [PMID: 22357273 DOI: 10.1128/JVI.06913-11]
96 **Kawaguchi Y**, Bruni R, Roizman B. Interaction of herpes simplex virus 1 alpha regulatory protein ICP0 with elongation factor 1delta: ICP0 affects translational machinery. *J Virol* 1997; **71**: 1019-1024 [PMID: 8995621]
97 **Paladino P**, Collins SE, Mossman KL. Cellular localization of the herpes simplex virus ICP0 protein dictates its ability to block IRF3-mediated innate immune responses. *PLoS One* 2010; **5**: e10428 [PMID: 20454685 DOI: 10.1371/journal.pone.0010428]
98 **Yao F**, Courtney RJ. Association of ICP0 but not ICP27 with purified virions of herpes simplex virus type 1. *J Virol* 1992; **66**: 2709-2716 [PMID: 1313896]
99 **Loret S**, Guay G, Lippé R. Comprehensive characterization of extracellular herpes simplex virus type 1 virions. *J Virol* 2008; **82**: 8605-8618 [PMID: 18596102 DOI: 10.1128/JVI.00904-08]
100 **Sedlackova L**, Rice SA. Herpes simplex virus type 1 immediate-early protein ICP27 is required for efficient incorporation of ICP0 and ICP4 into virions. *J Virol* 2008; **82**: 268-277 [PMID: 17959681 DOI: 10.1128/JVI.01588-07]
101 **Delboy MG**, Siekavizza-Robles CR, Nicola AV. Herpes simplex virus tegument ICP0 is capsid associated, and its E3 ubiquitin ligase domain is important for incorporation into virions. *J Virol* 2010; **84**: 1637-1640 [PMID: 19906912 DOI: 10.1128/JVI.02041-09]
102 **Delboy MG**, Nicola AV. A pre-immediate-early role for tegument ICP0 in the proteasome-dependent entry of herpes simplex virus. *J Virol* 2011; **85**: 5910-5918 [PMID: 21471243 DOI: 10.1128/JVI.00267-11]
103 **Liang Y**, Kurakin A, Roizman B. Herpes simplex virus 1 infected cell protein 0 forms a complex with CIN85 and Cbl and mediates the degradation of EGF receptor from cell surfaces. *Proc Natl Acad*

Sci USA 2005; **102**: 5838-5843 [PMID: 15824310 DOI: 10.1073/pnas.0501253102]
104 **Liang Y**, Roizman B. State and role of SRC family kinases in replication of herpes simplex virus 1. *J Virol* 2006; **80**: 3349-3359 [PMID: 16537602 DOI: 10.1128/JVI.80.7.3349-3359.2006]
105 **Zheng Y**, Gu H. Identification of three redundant segments responsible for herpes simplex virus 1 ICP0 to fuse with ND10 nuclear bodies. *J Virol* 2015; **89**: 4214-4226 [PMID: 25631093 DOI: 10.1128/JVI.03658-14]
106 **Hay RT**. SUMO: a history of modification. *Mol Cell* 2005; **18**: 1-12 [PMID: 15808504 DOI: 10.1016/j.molcel.2005.03.012]
107 **Geiss-Friedlander R**, Melchior F. Concepts in sumoylation: a decade on. *Nat Rev Mol Cell Biol* 2007; **8**: 947-956 [PMID: 18000527 DOI: 10.1038/nrm2293]
108 **Wimmer P**, Schreiner S, Dobner T. Human pathogens and the host cell SUMOylation system. *J Virol* 2012; **86**: 642-654 [PMID: 22072786 DOI: 10.1128/JVI.06227-11]
109 **Song J**, Durrin LK, Wilkinson TA, Krontiris TG, Chen Y. Identification of a SUMO-binding motif that recognizes SUMO-modified proteins. *Proc Natl Acad Sci USA* 2004; **101**: 14373-14378 [PMID: 15388847 DOI: 10.1073/pnas.0403498101]
110 **Hecker CM**, Rabiller M, Haglund K, Bayer P, Dikic I. Specification of SUMO1- and SUMO2-interacting motifs. *J Biol Chem* 2006; **281**: 16117-16127 [PMID: 16524884 DOI: 10.1074/jbc.M512757200]
111 **Sun H**, Leverson JD, Hunter T. Conserved function of RNF4 family proteins in eukaryotes: targeting a ubiquitin ligase to SUMOylated proteins. *EMBO J* 2007; **26**: 4102-4112 [PMID: 17762864 DOI: 10.1038/sj.emboj.7601839]
112 **Prudden J**, Pebernard S, Raffa G, Slavin DA, Perry JJ, Tainer JA, McGowan CH, Boddy MN. SUMO-targeted ubiquitin ligases in genome stability. *EMBO J* 2007; **26**: 4089-4101 [PMID: 17762865 DOI: 10.1038/sj.emboj.7601838]
113 **Boutell C**, Cuchet-Lourenço D, Vanni E, Orr A, Glass M, McFarlane S, Everett RD. A viral ubiquitin ligase has substrate preferential SUMO targeted ubiquitin ligase activity that counteracts intrinsic antiviral defence. *PLoS Pathog* 2011; **7**: e1002245 [PMID: 21949651 DOI: 10.1371/journal.ppat.1002245]
114 **Everett RD**, Boutell C, Pheasant K, Cuchet-Lourenço D, Orr A. Sequences related to SUMO interaction motifs in herpes simplex virus 1 protein ICP0 act cooperatively to stimulate virus infection. *J Virol* 2014; **88**: 2763-2774 [PMID: 24352468 DOI: 10.1128/JVI.03417-13]
115 **Ciufo DM**, Mullen MA, Hayward GS. Identification of a dimerization domain in the C-terminal segment of the IE110 transactivator protein from herpes simplex virus. *J Virol* 1994; **68**: 3267-3282 [PMID: 8151788]
116 **Lium EK**, Panagiotidis CA, Wen X, Silverstein SJ. The NH2 terminus of the herpes simplex virus type 1 regulatory protein ICP0 contains a promoter-specific transcription activation domain. *J Virol* 1998; **72**: 7785-7795 [PMID: 9733814]
117 **Meredith M**, Orr A, Elliott M, Everett R. Separation of sequence requirements for HSV-1 Vmw110 multimerisation and interaction with a 135-kDa cellular protein. *Virology* 1995; **209**: 174-187 [PMID: 7747467 DOI: 10.1006/viro.1995.1241]
118 **Perusina Lanfranca M**, Mostafa HH, Davido DJ. Two overlapping regions within the N-terminal half of the herpes simplex virus 1 E3 ubiquitin ligase ICP0 facilitate the degradation and dissociation of PML and dissociation of Sp100 from ND10. *J Virol* 2013; **87**: 13287-13296 [PMID: 24089549 DOI: 10.1128/JVI.02304-13]
119 **Meredith M**, Orr A, Everett R. Herpes simplex virus type 1 immediate-early protein Vmw110 binds strongly and specifically to a 135-kDa cellular protein. *Virology* 1994; **200**: 457-469 [PMID: 8178435 DOI: 10.1006/viro.1994.1209]
120 **Li M**, Chen D, Shiloh A, Luo J, Nikolaev AY, Qin J, Gu W. Deubiquitination of p53 by HAUSP is an important pathway for p53 stabilization. *Nature* 2002; **416**: 648-653 [PMID: 11923872 DOI: 10.1038/nature737]
121 **Huang Z**, Wu Q, Guryanova OA, Cheng L, Shou W, Rich JN, Bao S. Deubiquitylase HAUSP stabilizes REST and promotes maintenance of neural progenitor cells. *Nat Cell Biol* 2011; **13**: 142-152 [PMID: 21258371 DOI: 10.1038/ncb2153]
122 **Song MS**, Salmena L, Carracedo A, Egia A, Lo-Coco F, Teruya-Feldstein J, Pandolfi PP. The deubiquitinylation and localization of PTEN are regulated by a HAUSP-PML network. *Nature* 2008; **455**: 813-817 [PMID: 18716620 DOI: 10.1038/nature07290]
123 **Pfoh R**, Lacdao IK, Georges AA, Capar A, Zheng H, Frappier L, Saridakis V. Crystal Structure of USP7 Ubiquitin-like Domains with an ICP0 Peptide Reveals a Novel Mechanism Used by Viral and Cellular Proteins to Target USP7. *PLoS Pathog* 2015; **11**: e1004950 [PMID: 26046769 DOI: 10.1371/journal.ppat.1004950]
124 **Pozhidaeva AK**, Mohni KN, Dhe-Paganon S, Arrowsmith CH, Weller SK, Korzhnev DM, Bezsonova I. Structural Characterization of Interaction between Human Ubiquitin-specific Protease 7 and Immediate-Early Protein ICP0 of Herpes Simplex Virus-1. *J Biol Chem* 2015; **290**: 22907-22918 [PMID: 26224631 DOI: 10.1074/jbc.M115.664805]
125 **Gu H**, Liang Y, Mandel G, Roizman B. Components of the REST/CoREST/histone deacetylase repressor complex are disrupted, modified, and translocated in HSV-1-infected cells. *Proc Natl Acad Sci USA* 2005; **102**: 7571-7576 [PMID: 15897453 DOI: 10.1073/pnas.0502658102]
126 **Andrés ME**, Burger C, Peral-Rubio MJ, Battaglioli E, Anderson ME, Grimes J, Dallman J, Ballas N, Mandel G. CoREST: a functional corepressor required for regulation of neural-specific gene expression. *Proc Natl Acad Sci USA* 1999; **96**: 9873-9878 [PMID: 10449787 DOI: 10.1073/pnas.96.17.9873]
127 **Qureshi IA**, Gokhan S, Mehler MF. REST and CoREST are transcriptional and epigenetic regulators of seminal neural fate decisions. *Cell Cycle* 2010; **9**: 4477-4486 [PMID: 21088488 DOI: 10.4161/cc.9.22.13973]
128 **Ferenczy MW**, Ranayhossaini DJ, Deluca NA. Activities of ICP0 involved in the reversal of silencing of quiescent herpes simplex virus 1. *J Virol* 2011; **85**: 4993-5002 [PMID: 21411540 DOI: 10.1128/JVI.02265-10]
129 **Everett RD**. Depletion of CoREST does not improve the replication of ICP0 null mutant herpes simplex virus type 1. *J Virol* 2010; **84**: 3695-3698 [PMID: 20106915 DOI: 10.1128/JVI.00021-10]
130 **Liang Y**, Vogel JL, Narayanan A, Peng H, Kristie TM. Inhibition of the histone demethylase LSD1 blocks alpha-herpesvirus lytic replication and reactivation from latency. *Nat Med* 2009; **15**: 1312-1317 [PMID: 19855399 DOI: 10.1038/nm.2051]
131 **Sherr CJ**. D-type cyclins. *Trends Biochem Sci* 1995; **20**: 187-190 [PMID: 7610482]
132 **Malumbres M**, Barbacid M. Cell cycle, CDKs and cancer: a changing paradigm. *Nat Rev Cancer* 2009; **9**: 153-166 [PMID: 19238148 DOI: 10.1038/nrc2602]
133 **DeCaprio JA**. How the Rb tumor suppressor structure and function was revealed by the study of Adenovirus and SV40. *Virology* 2009; **384**: 274-284 [PMID: 19150725 DOI: 10.1016/j.virol.2008.12.010]
134 **Van Sant C**, Kawaguchi Y, Roizman B. A single amino acid substitution in the cyclin D binding domain of the infected cell protein no. 0 abrogates the neuroinvasiveness of herpes simplex virus without affecting its ability to replicate. *Proc Natl Acad Sci USA* 1999; **96**: 8184-8189 [PMID: 10393969]
135 **Kalamvoki M**, Roizman B. ICP0 enables and monitors the function of D cyclins in herpes simplex virus 1 infected cells. *Proc Natl Acad Sci USA* 2009; **106**: 14576-14580 [PMID: 19706544 DOI: 10.1073/pnas.0906905106]
136 **Van Sant C**, Lopez P, Advani SJ, Roizman B. Role of cyclin D3 in the biology of herpes simplex virus 1 ICPO. *J Virol* 2001; **75**: 1888-1898 [PMID: 11160688 DOI: 10.1128/JVI.75.4.1888-1898.2001]
137 **Advani SJ**, Brandimarti R, Weichselbaum RR, Roizman B. The disappearance of cyclins A and B and the increase in activity of the G(2)/M-phase cellular kinase cdc2 in herpes simplex virus 1-infected cells require expression of the alpha22/U(S)1.5 and U(L)13 viral genes. *J Virol* 2000; **74**: 8-15 [PMID: 10590085 DOI: 10.1128/JVI.74.1.8-15.2000]
138 **Schang LM**, Rosenberg A, Schaffer PA. Transcription of herpes simplex virus immediate-early and early genes is inhibited by

roscovitine, an inhibitor specific for cellular cyclin-dependent kinases. *J Virol* 1999; **73**: 2161-2172 [PMID: 9971799]

139 **Davido DJ**, Von Zagorski WF, Maul GG, Schaffer PA. The differential requirement for cyclin-dependent kinase activities distinguishes two functions of herpes simplex virus type 1 ICP0. *J Virol* 2003; **77**: 12603-12616 [PMID: 14610183 DOI: 10.1128/JVI.77.23.12603-12616.2003]

140 **Glossop NR**, Hardin PE. Central and peripheral circadian oscillator mechanisms in flies and mammals. *J Cell Sci* 2002; **115**: 3369-3377 [PMID: 12154068]

141 **Kalamvoki M**, Roizman B. Circadian CLOCK histone acetyl transferase localizes at ND10 nuclear bodies and enables herpes simplex virus gene expression. *Proc Natl Acad Sci USA* 2010; **107**: 17721-17726 [PMID: 20876123 DOI: 10.1073/pnas.1012991107]

142 **Panier S**, Durocher D. Regulatory ubiquitylation in response to DNA double-strand breaks. *DNA Repair* (Amst) 2009; **8**: 436-443 [PMID: 19230794 DOI: 10.1016/j.dnarep.2009.01.013]

143 **Luijsterburg MS**, van Attikum H. Close encounters of the RNF8th kind: when chromatin meets DNA repair. *Curr Opin Cell Biol* 2012; **24**: 439-447 [PMID: 22464734 DOI: 10.1016/j.ceb.2012.03.008]

144 **Taylor KE**, Mossman KL. Cellular Protein WDR11 Interacts with Specific Herpes Simplex Virus Proteins at the trans-Golgi Network To Promote Virus Replication. *J Virol* 2015; **89**: 9841-9852 [PMID: 26178983 DOI: 10.1128/JVI.01705-15]

145 **Davido DJ**, von Zagorski WF, Lane WS, Schaffer PA. Phosphorylation site mutations affect herpes simplex virus type 1 ICP0 function. *J Virol* 2005; **79**: 1232-1243 [PMID: 15613350 DOI: 10.1128/JVI.79.2.1232-1243.2005]

146 **Mostafa HH**, Thompson TW, Kushnir AS, Haenchen SD, Bayless AM, Hilliard JG, Link MA, Pitcher LA, Loveday E, Schaffer PA, Davido DJ. Herpes simplex virus 1 ICP0 phosphorylation site mutants are attenuated for viral replication and impaired for explant-induced reactivation. *J Virol* 2011; **85**: 12631-12637 [PMID: 21937654 DOI: 10.1128/JVI.05661-11]

147 **Ogle WO**, Ng TI, Carter KL, Roizman B. The UL13 protein kinase and the infected cell type are determinants of posttranslational modification of ICP0. *Virology* 1997; **235**: 406-413 [PMID: 9281521 DOI: 10.1006/viro.1997.8710]

148 **Maul GG**, Ishov AM, Everett RD. Nuclear domain 10 as preexisting potential replication start sites of herpes simplex virus type-1. *Virology* 1996; **217**: 67-75 [PMID: 8599237 DOI: 10.1006/viro.1996.0094]

149 **Gu H**, Roizman B. Engagement of the lysine-specific demethylase/HDAC1/CoREST/REST complex by herpes simplex virus 1. *J Virol* 2009; **83**: 4376-4385 [PMID: 19193804 DOI: 10.1128/JVI.02515-08]

P- Reviewer: Diefenbach R, Li QH, Rajcani J, Zheng CF
S- Editor: Kong JX **L- Editor**: A **E- Editor**: Li D

World Journal of Virology

Submit a Manuscript: http://www.wjgnet.com/esps/
Help Desk: http://www.wjgnet.com/esps/helpdesk.aspx
DOI: 10.5501/wjv.v5.i1.14

World J Virol 2016 February 12; 5(1): 14-22
ISSN 2220-3249 (online)

ORIGINAL ARTICLE

Basic Study

Modelling the prevalence of hepatitis C virus amongst blood donors in Libya: An investigation of providing a preventive strategy

Mohamed A Daw, Amira Shabash, Abdallah El-Bouzedi, Aghnya A Dau, Moktar Habas; Libyan Study Group of Hepatitis and HIV

Mohamed A Daw, Acting Physician of Internal Medicine, Scientific Coordinator of Libyan National Surveillance Studies of Viral hepatitis and HIV, Tripoli 82668, Libya

Mohamed A Daw, Amira Shabash, Department of Medical Microbiology, Faculty of Medicine, Tripoli 82668, Libya

Abdallah El-Bouzedi, Department of Laboratory Medicine, Faculty of Biotechnology, Tripoli 82668, Libya

Agnya A Dau, Department of Surgery, Faculty of Medicine, Tripoli Medical Center, Tripoli 82668, Libya

Moktar Habas, Department of Medicine, Faculty of Medicine, Tripoli Central Hospital, Tripoli 82668, Libya

Author contributions: Daw MA designed the study, extracted the data, and drafted and finalized the manuscript; Shabash A and El-Bouzedi A collected the data and contributed to the drafting of the manuscript; Dau AA drafted, analyzed, and corrected the manuscript; Habas M collected the data and reviewed the clinical status of all patients; all authors read and approved the final manuscript.

Institutional review board statement: The study was reviewed by the board of Faculty of Medicine Tripoli Libya and found that the utilization and analysis of microbial epidemiological data did not require oversight by Libyan National Ethics committee. Hence no ethical approval was needed for this study.

Institutional animal care and use committee statement: We declare that no animals or human volunteers were used in the study.

Conflict-of-interest statement: All authors declare that there is no potential conflict of interests regarding this article.

Data sharing statement: All data will be made freely available via the corresponding author (mohamedadaw@gmail.com). There are no security or licensing matters related to the study.

Correspondence to: Mohamed A Daw, FTCDA, MD, MPS, PhD, Professor of Clinical Microbiology and Microbial Epidemiology, Department of Medical Microbiology, Faculty of Medicine, Alfrnaj Road, Tripoli 82668, Libya. mohamedadaw@gmail.com
Telephone: +218-91-2144972
Fax: +218-21-3366218

Received: May 11, 2015
Peer-review started: May 18, 2015
First decision: July 26, 2015
Revised: August 24, 2015
Accepted: September 16, 2015
Article in press: September 18, 2015
Published online: February 12, 2016

Abstract

AIM: To determine hepatitis C virus (HCV) seroprevalence among the Libyan population using blood donors and applying the autoregressive integrated moving average (ARIMA) model to predict future trends and formulate plans to minimize the burden of HCV infection.

METHODS: HCV positive cases were collected from 1008214 healthy blood donors over a 6-year period from 2008 to 2013. Data were used to construct the ARIMA model to forecast HCV seroprevalence among blood donors. The validity of the model was assessed using the mean absolute percentage error between the observed and fitted seroprevalence. The fitted ARIMA model

was used to forecast the incidence of HCV beyond the observed period for the year 2014 and further to 2055.

RESULTS: The overall prevalence of HCV among blood donors was 1.8%, varying over the study period from 1.7% to 2.5%, though no significant variation was found within each calendar year. The ARIMA model showed a non-significant auto-correlation of the residuals, and the prevalence was steady within the last 3 years as expressed by the goodness-of-fit test. The forecast incidence showed an increase in HCV seropositivity in 2014, ranging from 500 to 700 per 10000 population, with an overall prevalence of 2.3%-2.7%. This may be extended to 2055 with minimal periodical variation within each 6-year period.

CONCLUSION: The applied model was found to be valuable in evaluating the seroprevalence of HCV among blood donors, and highlighted the growing burden of such infection on the Libyan health care system. The model may help in formulating national policies to prevent increases in HCV infection and plan future strategies that target the consequences of the infection.

Key words: Autoregressive integrated moving average model; Libya; Hepatitis C virus; Blood donors

Core tip: Hepatitis C virus (HCV) infection has major consequences and an overwhelming impact particularly among developing countries, hence prediction of its prevalence is important for future planning to mitigate its impact. This is an innovative study highlighting the importance of using a modified mathematical model to forecast and predict the future prevalence and consequence of HCV infection using data collected from blood donors. The results will allow strategists in health care services to plan immediate and long-term policies.

Daw MA, Shabash A, El-Bouzedi A, Dau AA, Habas M; Libyan Study Group of Hepatitis and HIV. Modeling the prevalence of hepatitis C virus amongst Libyan blood donors: Investigation of a preventive strategy. *World J Virol* 2016; 5(1): 14-22 Available from: URL: http://www.wjgnet.com/2220-3249/full/v5/i1/14.htm DOI: http://dx.doi.org/10.5501/wjv.v5.i1.14

INTRODUCTION

Hepatitis C virus (HCV) has been known to be one of the leading causes of chronic viral hepatitis with devastating consequences such as cirrhosis and hepatocellular carcinoma which are the major reasons for liver transplantation[1]. The geo-epidemiology of HCV infection varies greatly and is dynamic over time[2]. Indeed, 3% of the world's population are chronically infected with HCV and over 3 million new infection occur each year[3]. Africa and Asia represent the largest reservoir of chronic HCV infection[4,5], though prevalence varies from one country to another and among regions within each country[2,3]. The prevalence of HCV infection are highest in Africa, ranging from 1% to 26%, and Egypt, Senegal, and Cameroon have the highest rates worldwide[6].

Hepatitis C is well documented in Libya and different studies have shown the prevalence of HCV infection and genotypes among Libyans[7-9]. Recently a comprehensive study in over 1% of the Libyan population has shown that the prevalence of HCV infection is 1.2%, varying from 0.6% to 2.2% according to the region within the country[10]. The prevalence indicated an alarming increase in HCV among the younger generation, particularly within new emerging risk groups in Libyan society such as intravenous drug users (IVDUs)[10,11]. As age increases and disease progresses among infected individuals, there will be an increase in expected complications. This will place an increasing burden on the Libyan health care system which is still developing. Hence, studies should be directed to formulate policies to combat the effects of infection.

Early identification of epidemics of infectious diseases and prediction of their outcomes are an important step toward implementing effective intervention measurements and reducing mortality and morbidity[12]. Such goals are a challenge in health care surveillance studies. Mathematical dynamic modeling has contributed greatly in exploring such challenges. Surveillance data however, are usually necessary for these modeling purposes[13].

Different statistical models including linear regression and correlation coefficients have been used for prediction of viral hepatitis. Autoregressive integrated moving average (ARIMA) or Box-Jenkins has potential application in studies of disease dynamics[14]. Helfinstein was the first to show that the ARIMA model can be used successfully for forecasting and predicting the different relationships between viral infections and associated diseases[15]. Different studies applied such modeling to detect spikes, steps, and trends for hepatitis E, hepatitis B and hepatitis C infection[16,17]. A considerable effort has been undertaken to forecast the epidemiology of hepatitis C, and different models were used to estimate the burden and complications of the infection[18]. Recently, Corson *et al*[19] used a mathematical model to project the future of HCV among IVDUs and its impact on the future development of HCV-related morbidity and mortality.

Blood donors are generally considered to be a healthier cohort of any community and viral hepatitis seropositivity among them may mirror the seroprevalence in the general population[20]. In Libya, a study conducted between 1991 and 2001 indicated that the prevalence of HCV infection ranged from 1.2% to 1.6% among blood donors, similar to the prevalence among the general population reported in 2014 of 1.2%, though it was much higher (20.5%) among hospital personnel[7,10]. Therefore, modeling and forecasting using HCV data from blood donors may provide an opportunity for planning

Table 1 Number of blood donors included in the study, Tripoli, Libya, 2008-2013

Study period	No. of volunteers	No. HCV seropositive
2008	35859	937
2009	65330	1713
2010	254177	3958
2011	173873	3060
2012	260139	4480
2013	218836	3749
Total	1008214	17897

2011-2013 were post-revolution years where many Libyan were injured during the Libyan conflict (2011)[35]. HCV: Hepatitis C virus.

and intervention to control HCV infection. In this study, we aimed to forecast the prevalence of HCV trends among blood donors by analyzing HCV dynamics and highlighting the need for further intervention strategies.

MATERIALS AND METHODS

Ethical consideration

The study was reviewed by the Board of the Faculty of Medicine, Tripoli, Libya, who declared that the utilization and analysis of microbial epidemiological data did not require oversight by the Libyan National Ethics Committee. Hence, no ethical approval was needed for this study.

Study population

A total of 1008214 healthy individuals, aged 18 to 50 years, were recruited from three different main blood banks in Tripoli over 6 years from 2008-2013 (Table 1). These included Tripoli Central Hospital, Karda Teaching Hospital, and Tripoli Reference Laboratory. Each person was subjected to screening for known risk factors associated with blood donation according to the national and international standards applicable in all three hospitals. Those who failed to meet the criteria for blood donation were excluded from the study, such as those who had previous blood transfusion, jaundice, a history of illicit drug-taking, and other potential risk factors.

Laboratory diagnosis

The laboratory analysis was carried out using ELISA (Vitros EciQ, Orthodiagnostic-Switzerland), and samples were considered to be confirmed positive according to the manufacturer's instructions. HCV infection was defined as the presence of anti-HCV antibodies in the serum as detected by ELISA.

Modeling

The ARIMA model was developed to forecast the incidence of HCV infection among blood donors in Libya. This was applied using data for 72 mo between January 2008 and December 2013 to then forecast the incidence of HCV infection from January to December 2014 and predict the prevalence of HCV infection from 2008 to 2055 under nonexclusive expectation. The model was constructed using the Box-Jenkins method. The identification and selection steps for ARIMA were carried *via* autocorrelation and partial autocorrelation functions. The model parameters were determined by the maximum likelihood method. Goodness-of-fit among ARIMA models was compared using diagnostic checks such as residual analysis and other relevant information. The accuracy of the model was finally subjected to critical estimation and rigorous checking to fulfill the required criteria for the model. The details of the ARIMA model were recently described by Yu *et al*[21] in 2013 and used to analyze the epidemiology of HIV infection among the Korean population.

Table 2 Seroprevalence of hepatitis C virus among blood donors, Tripoli, Libya, 2008-2013

Yr	Prevalence (%)	OR	95%CI		Minimum	Maximum
			Lower	Upper		
2008	2.6	1.4	2.3	2.8	2.0	3.2
2009	2.6	1.4	1.7	3.4	1.1	4.1
2010	1.5	0.8	1.3	1.6	0.9	2.1
2011	1.7	0.7	1.3	2.0	0.8	2.8
2012	1.7	1.1	0.8	2.6	0.6	2.9
2013	1.7	1.1	0.9	2.5	0.7	2.7
Total	1.8	1.1	1.4	2.5	1.0	3.0

Statistical analysis

Data were analyzed using Microsoft Excel, Minitab version 15 (State College, PA, United States), and SPSS version 16 (SPSS Inc., Chicago, IL, United States). A *P*-value < 0.05 indicated a significant difference between HCV and HBV prevalence. The Excel 2007 forecast function was used to predict the number of infected people. The following equation was used to calculate the expected number of infected persons each year, 1-Y = 613.2X + 836.5, where Y = number of expected infected persons with HCV, and X = the serial number for the year calculated from 2008; for example for 2009 and 2010 the serial numbers were 2 and 3, respectively.

RESULTS

A total of 1008214 volunteer blood donors were screened for HCV over a 6-year period from 2008 till 2013. Of these, 17897 were found to be positive for anti-HCV antibodies, with an overall prevalence of 1.8%. There was no apparent monthly difference in HCV infection among individuals screened during the same year. Based on year-to-year analysis, a substantial variation in the seroprevalence of HCV was observed as shown in Table 2. The highest prevalence of HCV infection was reported in 2008 and 2009 as (2.6%) though it was 1.5% in 2010 and 1.7% in 2011-2013. In 2008, 35869 individuals were reviewed, of whom 937 (2.6%) were positive for anti-HCV antibodies. During 2009 the number of screened people doubled, and 1713 (2.6%) were positive for anti-HCV antibodies. In 2010, the number screened was 254177, a 7-fold increase compared with 2008, and 3958 (1.5%) were positive for HCV antibodies. In

2011, 3060 (1.7%) were HCV-positive. Although 260139 people were screened during 2012, the largest number over the 5-year period, the prevalence was the same (1.7%) as to that in 2011 and 2013, when a combined total of 218836 persons were screened (Table 1).

ARIMA modeling was applied to the data for identification, estimation, and then forecasting of HCV infection. The first stage was construction of an estimation model followed by forecasting and model evaluation. The data collected from 2008-2013 was used to construct the ARIMA model as depicted by Box *et al*[14]. Figure 1 shows the sample autocorrelation and partial autocorrelation functions [autocorrelation function (ACF) and partial ACF (PACF)] for the case structure which allowed identification of an appropriate ARIMA form to model the stationary series. A small variation was noted but it was not statistically different from zero which confirms the adequacy of the ARIMA model. The model forecast a steady increase for the following 6 years.

The sample ACF and PACF in Figure 2 showed a good fit which allowed us to determine the appropriate ARIMA model for HCV seroprevalence among blood donors. The adequacy of the model was evident as the residuals of autocorrelation had little variation with no significant difference ($P > 0.05$).

The plot of observed *vs* fitted values indicated that the model provided an excellent fit of the data as shown in Figure 3. The ARIMA model was used to forecast HCV prevalence for 72 mo over the 6-year period from January 2008 to December 2013 (Figure 3). Detailed analysis of observed *vs* forecast values of HCV prevalence over the study period showed a steady increase, with a maximum value at 1.8% to 2.01%, and an increasing tendency beyond the observed period in the short-term forecast (January-December 2014), reaching a maximum of 700 per 10000 population (2.3% to 2.7%). This was then used as a basis for estimating the prevalence of HCV infection among the Libyan population up to 2055, based on 6-year periods (Figure 4). According to our model, the prevalence of HCV infection will decrease and thus all sequelae of the infection will continue to decrease steadily in the future.

DISCUSSION

HCV infection has been known to be an important cause of chronic liver diseases though accurate representative epidemiological data are difficult to obtain, particularly in developing countries, as this infection has been considered to be endemic[2]. Statistical analysis of surveillance data on the prevalence of various infections was shown to be helpful in establishing a hypotheses to highlight and anticipate the dynamics of HCV infection and subsequently implement appropriate preventive measures and allocation of required resources[22]. The ARIMA model is one of the most widely used forecasting techniques due to its structured modeling base and acceptable forecasting performance[23].

In this study, we developed a calibrated ARIMA model for HCV infection with the aim of taking full advantage of available epidemiological information from registered blood donors in Libyan blood banks. The overall prevalence of HCV among the blood donors was found to be 1.8%, ranging from 2.5% in 2008 to 1.7% in 2013. This is consistent with a recent comprehensive study published by our group who reported that the prevalence of HCV among the Libyan population varied from 0.6% to 2.2%[10]. Comparing such results with regional published data, the prevalence of HCV infection was found to be similar to that in neighboring countries, with 1.6% in Tunis and 1.8% in Algeria, though it was higher in Egypt (22%)[24,25]. However, this was higher than the prevalence among developed countries such as the United States and Germany (< 1.5%)[26,27]. Hence, further studies are needed to elucidate the different factors associated with the higher prevalence of HCV among Libyan blood donors.

In our study, the applied model showed accuracy for the prevalence and dynamics of HCV infection among blood donors over a 6-year period and the forecast after that. This is in agreement with other studies who also declared that this model provides a better forecast than traditional methods for case notification of an infectious disease[28]. Although the prevalence of HCV was steady over the last 3 years (1.7% for 2011-2013), we predicted an increase for the year after. This was consistent with other studies from China and Latin America which showed that the prevalence of HCV was steady or increasing and that the number of infected individuals will increase[29,30]. This suggested that other risk factors are set to play a major role in continued new infection. Further studies are needed to clarify such an assumption.

Despite the increase in rates of HCV seropositivity in this study, we did not predict the burden of HCV infection over the next decades, nor did we calculated the estimated number of individual morbidities associated with HCV infection. However, different studies have shown that the prevalence of HCV-related cirrhosis is expected to increase by 24% within a decade, though decompensated cirrhosis cases and hepatocellular carcinoma will increase by 50% within the same period[31-33]. Hence, further studies are needed to elucidate such consequent complications of HCV infection among Libyan populations.

Modeling studies have projected a dismal future for HCV infection and related disease burden. In general, these models make forecasts based on current conditions of low rates of screening and treatment, and thus do not include a widespread program of identifying and treating the large proportion of undiagnosed HCV-infected individuals[34]. According to the results of our model, the incidence of the more serious outcomes of HCV infection will continue to rise, at least until 2055, unless modified. In our projections of HCV infection to 2055, we did not take into account the effective HCV prevention programs and the possible impact of the use of antiviral medications. Both these developments could have a considerable impact on our future projections, and thus the prevalence of HCV infection projected to 2055 may be less than that estimated by our model. Furthermore,

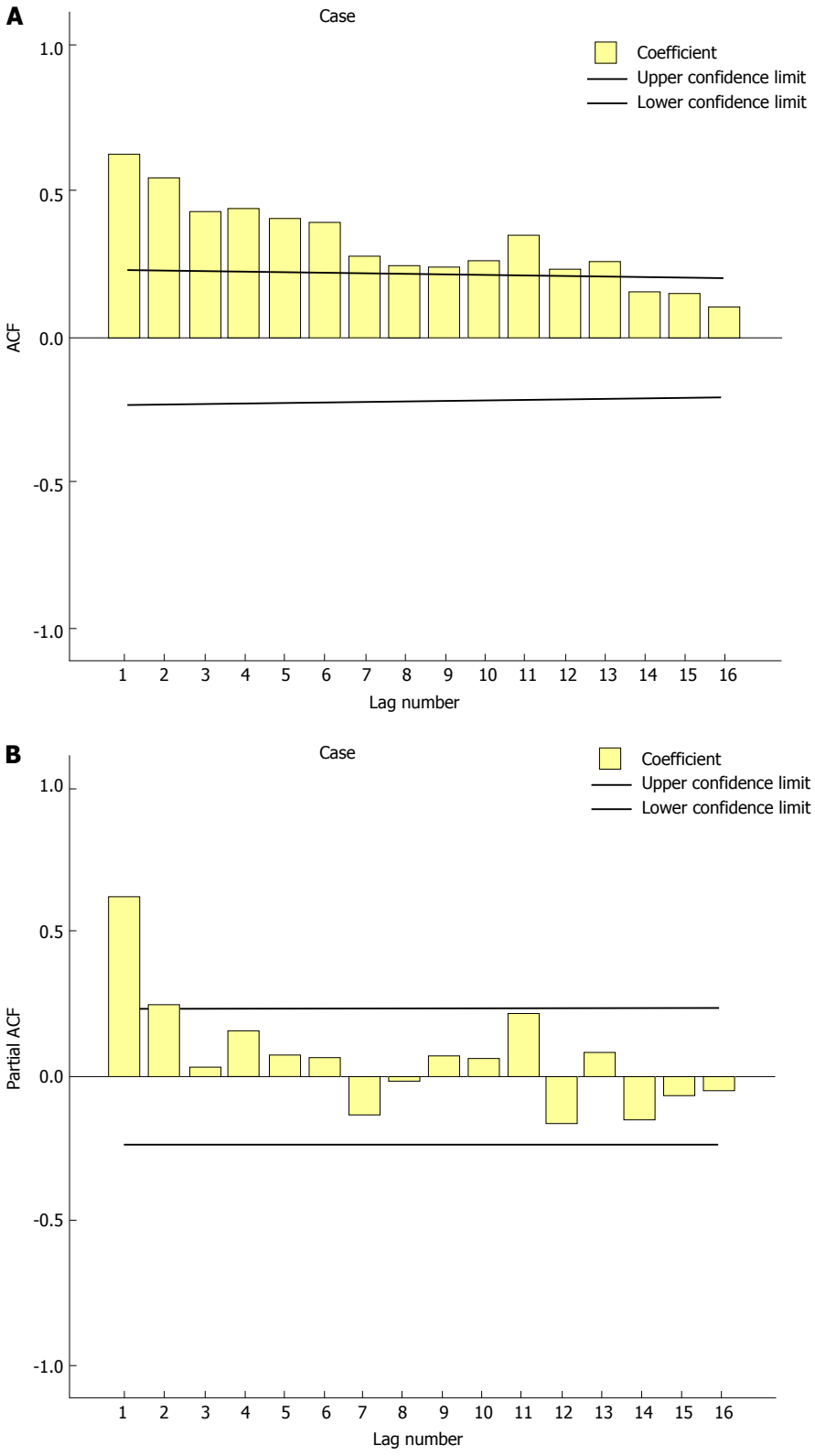

Figure 1 Correlogram and partial correlogram for a case structure control used for autoregressive integrated moving average model. A: ACF; B: Partial ACF. ACF: Autocorrelation function.

socioeconomic conditions in the country should be taken in consideration, particularly among developing countries; Libya is experiencing a major challenge regarding its geographical, political and social-ethnic identity[35,36]. Thus, future planning regarding infectious disease should be prioritized[37,38].

Monitoring HCV seropositivity among blood donors could be used to evaluate the effectiveness of the national efforts and guidelines to provide safe blood donation and good blood bank services[39]. In many

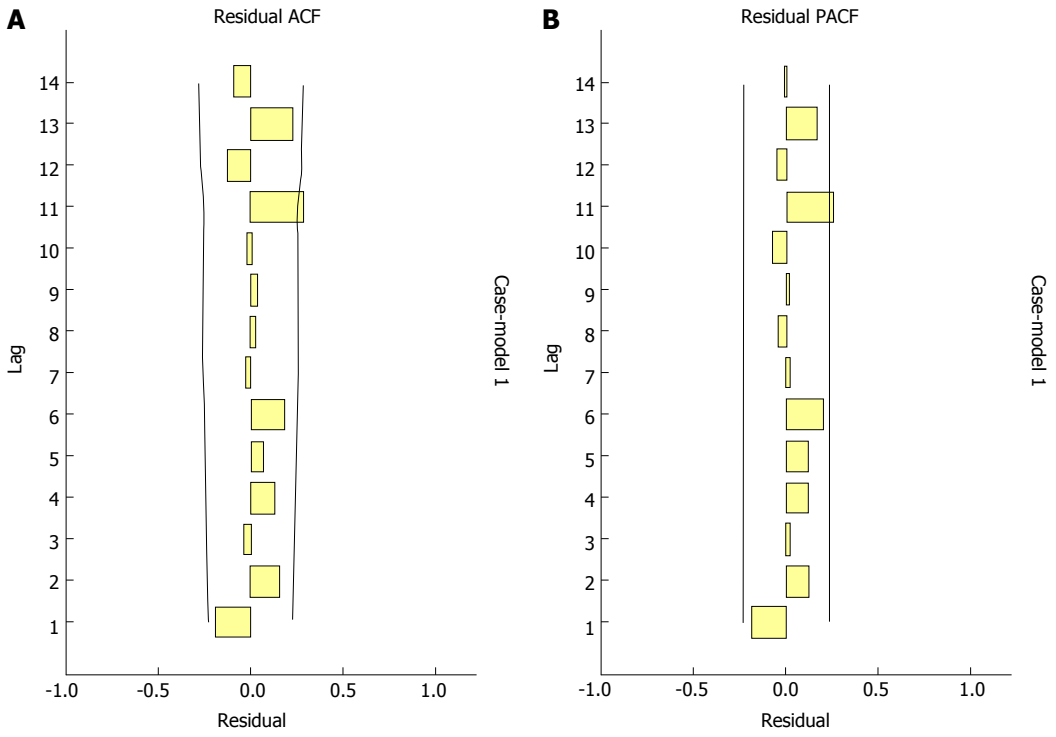

Figure 2 Residual plots for the final autoregressive integrated moving average (2, 1, 7) model of hepatitis C virus seroprevalence among volunteer blood donors in Libya, 2008-2013. A: ACF; B: Partial ACF. Lines indicate 95%CI. ACF: Autocorrelation function.

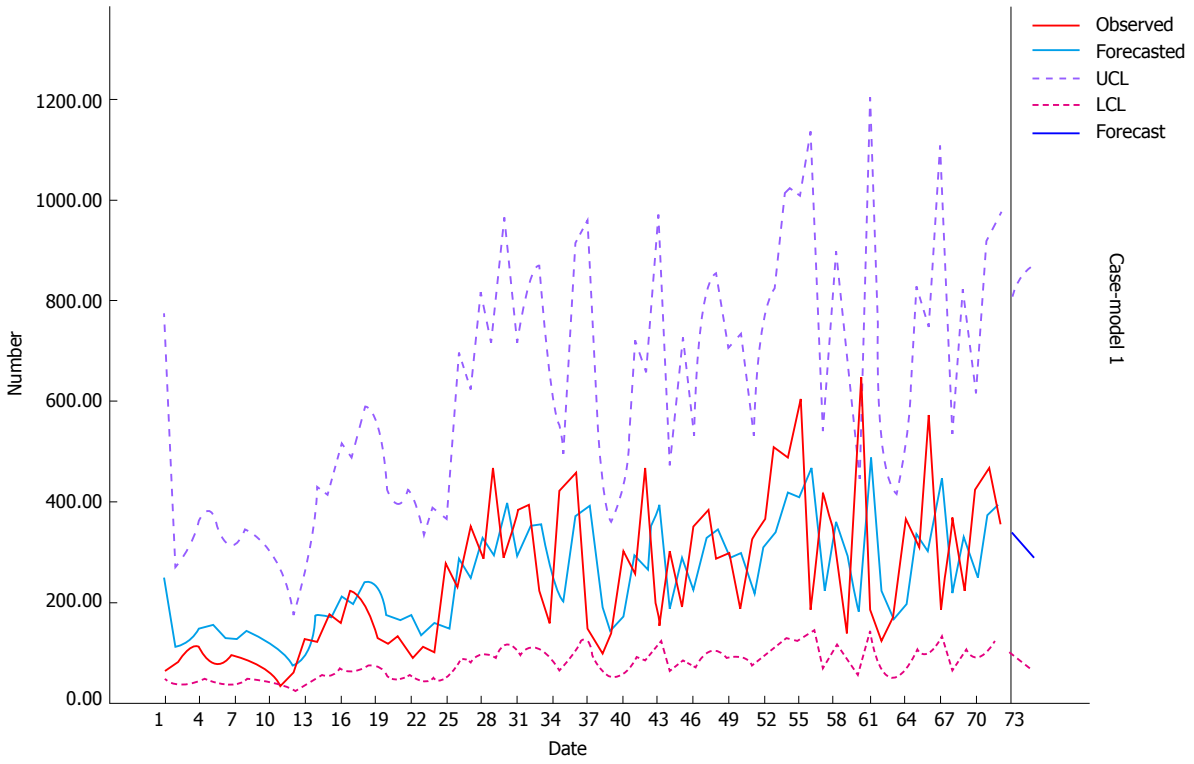

Figure 3 Number of observed and forecast hepatitis C virus seropositive volunteers among blood donors in Libya, 2008-2013. Date: Period of observation (months: 2008-2013); Number: Estimated number of HCV seropositive/month. UCL: Upper confidence limit; LCL: Lower confidence limit; HCV: Hepatitis C virus.

countries, HCV transmission rates decreased markedly with the introduction of blood screening[40]. Despite such a decline, mathematical models still predict a continuing rise in the prevalence of HCV infection within blood banks[41]. This was evident in our study where the increase in HCV seroprevalence may be attributed to the lack of quality assurance within the blood donation system. In Arab countries, blood transfusion is still a

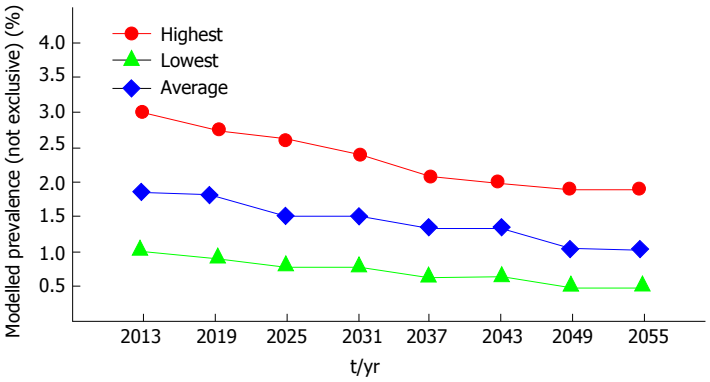

Figure 4 Modeled prevalence (not exclusive[1]) of hepatitis C virus infection by 6-year period, Libya, 2008-2055. [1]Estimates assume stable risk populations and HCV infection risks and do not adjust for treatment. HCV: Hepatitis C virus.

problem due to lack of an organized infrastructure and altruistic volunteers. The main sources of blood donation are usually relatives and friends who attend because of social pressure and in an emergency where questions regarding risk behaviors are rarely asked[2].

Many difficulties surround the determination of HCV prevalence using blood donors, since high risk groups including IVDUs are often excluded from blood donation, leading to underestimation of the true prevalence of HCV infection[42]. Nevertheless, our data do not necessarily represent the true HCV prevalence among the general population and thus are in need of further updating. The applicability and effectiveness of this monitoring system in its practical application as conducted here is able to detect the epidemic situation of HCV infection in Libya. However, such an infection is dynamic and evolves over time. Therefore, the model should be periodically reassessed and updated to maintain long-term sustainability and precision. This study highlights the need for preventive initiatives and strategies to be adapted by health care policy-makers to reduce HCV infection.

In conclusion, there is an important need for monitoring and predicting the prevalence of HCV infection to reduce the substantial consequences particularly in developing countries. The model applied was verified and could be used to monitor and predict the epidemiology of HCV infection. A better understanding of the epidemiology of HCV infection will allow health authorities to revise and plan new strategies within the health care system.

ACKNOWLEDGMENTS

The authors would like to acknowledge the help and assistance of blood banks in Tripoli, and the Libyan Reference Laboratory. Further thanks should go to Dr Reiad M Gaja, Department of Statistics, Faculty of Science-Tripoli University for his comments on the model applied.

COMMENTS

Background

Viral hepatitis, particularly hepatitis C virus (HCV) is known to be a serious problem particularly among developing countries. Hence, using a simple and reliable method for predicting the future course and consequences of this infection are a priority for researchers and health care planners. Reliable data regarding the prevalence of HCV infection among blood donors are available in all blood banks and this could be used to achieve such objectives.

Research frontiers

Studies on the prevalence of HCV infection utilizing blood bank data could be used as a basis for future planning. However, such studies are rare and few researchers have focused on using such data as a model for future planning.

Innovations and breakthroughs

This is a novel study which applied a mathematical model utilizing basic data from blood banks regarding the pathogen HCV. This is a rare study which modeled data to predict the prevalence of HCV infection among the general population over the next 50 years (2008-2055).

Applications

The practical approach of this study allows strategists and health care professionals to plan appropriate intervention and prevention methods not only to minimize the spread of HCV infection but also to reduce the associated consequences and complications, such as hepatocellular carcinoma and cirrhosis, and may be used further for other infections such as hepatitis B virus and human immunodeficiency virus.

Terminology

The ARIMA model is an autoregressive integrated moving average or Box-jenkins mathematical model which has a potential application in studying disease dynamics. The model can be used successfully for forecasting and predicting the relationships among viral infections and associated diseases.

Peer-review

This is a well conducted epidemiologic study carried out in a developing country.

REFERENCES

1 **Howell J**, Angus P, Gow P. Hepatitis C recurrence: the Achilles heel of liver transplantation. *Transpl Infect Dis* 2014; **16**: 1-16 [PMID: 24372756 DOI: 10.1111/tid.12173]
2 **Daw MA**, Dau AA. Hepatitis C virus in Arab world: a state of concern. *Sci World J* 2012; **2012**: 719494 [PMID: 22629189 DOI: 10.1100/2012/719494]
3 **Mohd Hanafiah K**, Groeger J, Flaxman AD, Wiersma ST. Global epidemiology of hepatitis C virus infection: new estimates of age-specific antibody to HCV seroprevalence. *Hepatology* 2013; **57**: 1333-1342 [PMID: 23172780 DOI: 10.1002/hep.26141]
4 **Karoney MJ**, Siika AM. Hepatitis C virus (HCV) infection in Africa: a review. *Pan Afr Med J* 2013; **14**: 44 [PMID: 23560127]

5 **Zidan A**, Scheuerlein H, Schüle S, Settmacher U, Rauchfuss F. Epidemiological pattern of hepatitis B and hepatitis C as etiological agents for hepatocellular carcinoma in iran and worldwide. *Hepat Mon* 2012; **12**: e6894 [PMID: 23233864 DOI: 10.5812/hepatmon.6894]

6 **Jobarteh M**, Malfroy M, Peterson I, Jeng A, Sarge-Njie R, Alabi A, Peterson K, Cotten M, Hall A, Rowland-Jones S, Whittle H, Tedder R, Jaye A, Mendy M. Seroprevalence of hepatitis B and C virus in HIV-1 and HIV-2 infected Gambians. *Virol J* 2010; **7**: 230 [PMID: 20843322 DOI: 10.1186/1743-422X-7-230]

7 **Daw MA**, Elkaber MA, Drah AM, Werfalli MM, Mihat AA, Siala IM. Prevalence of hepatitis C virus antibodies among different populations of relative and attributable risk. *Saudi Med J* 2002; **23**: 1356-1360 [PMID: 12506296]

8 **Elasifer HA**, Agnnyia YM, Al-Alagi BA, Daw MA. Epidemiological manifestations of hepatitis C virus genotypes and its association with potential risk factors among Libyan patients. *Virol J* 2010; **7**: 317 [PMID: 21073743 DOI: 10.1186/1743-422X-7-317]

9 **Alashek WA**, McIntyre CW, Taal MW. Hepatitis B and C infection in haemodialysis patients in Libya: prevalence, incidence and risk factors. *BMC Infect Dis* 2012; **12**: 265 [PMID: 23082935 DOI: 10.1186/1471-2334-12-265]

10 **Daw MA**, El-Bouzedi A. Prevalence of hepatitis B and hepatitis C infection in Libya: results from a national population based survey. *BMC Infect Dis* 2014; **14**: 17 [PMID: 24405790 DOI: 10.1186/1471-2334-14-17]

11 **Daw MA**, Dau AA, Agnan MM. Influence of healthcare-associated factors on the efficacy of hepatitis C therapy. *ScientificWorldJournal* 2012; **2012**: 580216 [PMID: 23346018 DOI: 10.1100/2012/580216]

12 **Rong L**, Guedj J, Dahari H, Perelson AS. Treatment of hepatitis C with an interferon-based lead-in phase: a perspective from mathematical modelling. *Antivir Ther* 2014; **19**: 469-477 [PMID: 24434478 DOI: 10.3851/IMP2725]

13 **Chatterjee A**, Guedj J, Perelson AS. Mathematical modelling of HCV infection: what can it teach us in the era of direct-acting antiviral agents? *Antivir Ther* 2012; **17**: 1171-1182 [PMID: 23186606 DOI: 10.3851/IMP2428]

14 **Box GEP**, Jenkins GM. Time series analysis, control, and forecasting. San Francisco, CA: Holden Day, 1976: 10

15 **Helfenstein U**. Box-Jenkins modelling of some viral infectious diseases. *Stat Med* 1986; **5**: 37-47 [PMID: 3961314]

16 **Ren H**, Li J, Yuan ZA, Hu JY, Yu Y, Lu YH. The development of a combined mathematical model to forecast the incidence of hepatitis E in Shanghai, China. *BMC Infect Dis* 2013; **13**: 421 [PMID: 24010871 DOI: 10.1186/1471-2334-13-421]

17 **Sutton AJ**, Gay NJ, Edmunds WJ, Hope VD, Gill ON, Hickman M. Modelling the force of infection for hepatitis B and hepatitis C in injecting drug users in England and Wales. *BMC Infect Dis* 2006; **6**: 93 [PMID: 16762050]

18 **Akhtar S**, Carpenter TE. Stochastic modelling of intra-household transmission of hepatitis C virus: evidence for substantial non-sexual infection. *J Infect* 2013; **66**: 179-183 [PMID: 23103288 DOI: 10.1016/j.jinf.2012.10.020]

19 **Corson S**, Greenhalgh D, Taylor A, Palmateer N, Goldberg D, Hutchinson S. Modelling the prevalence of HCV amongst people who inject drugs: an investigation into the risks associated with injecting paraphernalia sharing. *Drug Alcohol Depend* 2013; **133**: 172-179 [PMID: 23791029 DOI: 10.1016/j.drugalcdep.2013.05.014]

20 **Khodabandehloo M**, Roshani D, Sayehmiri K. Prevalence and trend of hepatitis C virus infection among blood donors in Iran: A systematic review and meta-analysis. *J Res Med Sci* 2013; **18**: 674-682 [PMID: 24379843]

21 **Yu HK**, Kim NY, Kim SS, Chu C, Kee MK. Forecasting the number of human immunodeficiency virus infections in the korean population using the autoregressive integrated moving average model. *Osong Public Health Res Perspect* 2013; **4**: 358-362 [PMID: 24524025 DOI: 10.1016/j.phrp.2013.10.009]

22 **Firmino PR**, de Mattos Neto PS, Ferreira TA. Correcting and combining time series forecasters. *Neural Netw* 2014; **50**: 1-11 [PMID: 24239986 DOI: 10.1016/j.neunet.2013.10.008]

23 **Zhang X**, Zhang T, Young AA, Li X. Applications and comparisons of four time series models in epidemiological surveillance data. *PLoS One* 2014; **9**: e88075 [PMID: 24505382 DOI: 10.1371/journal.pone.0088075]

24 **Ezzikouri S**, Pineau P, Benjelloun S. Hepatitis B virus in the Maghreb region: from epidemiology to prospective research. *Liver Int* 2013; **33**: 811-819 [PMID: 23530901 DOI: 10.1111/liv.12135]

25 **Breban R**, Doss W, Esmat G, Elsayed M, Hellard M, Ayscue P, Albert M, Fontanet A, Mohamed MK. Towards realistic estimates of HCV incidence in Egypt. *J Viral Hepat* 2013; **20**: 294-296 [PMID: 23490375 DOI: 10.1111/j.1365-2893.2012.01650.x]

26 **Sheikh MY**, Atla PR, Ameer A, Sadiq H, Sadler PC. Seroprevalence of Hepatitis B and C Infections among Healthy Volunteer Blood Donors in the Central California Valley. *Gut Liver* 2013; **7**: 66-73 [PMID: 23423771]

27 **Offergeld R**, Ritter S, Hamouda O. [HIV, HCV, HBV and syphilis surveillance among blood donors in Germany 2008-2010]. *Bundesgesundheitsblatt Gesundheitsforschung Gesundheitsschutz* 2012; **55**: 907-913 [PMID: 22842883 DOI: 10.1007/s00103-012-1516-1]

28 **Liu Q**, Liu X, Jiang B, Yang W. Forecasting incidence of hemorrhagic fever with renal syndrome in China using ARIMA model. *BMC Infect Dis* 2011; **11**: 218 [PMID: 21838933 DOI: 10.1186/1471-2334-11-218]

29 **Ji ZH**, Li CY, Lv YG, Cao W, Chen YZ, Chen XP, Tian M, Li JH, An QX, Shao ZJ. The prevalence and trends of transfusion-transmissible infectious pathogens among first-time, voluntary blood donors in Xi'an, China between 1999 and 2009. *Int J Infect Dis* 2013; **17**: e259-e262 [PMID: 23195637]

30 **Kershenobich D**, Razavi HA, Sánchez-Avila JF, Bessone F, Coelho HS, Dagher L, Gonçales FL, Quiroz JF, Rodriguez-Perez F, Rosado B, Wallace C, Negro F, Silva M. Trends and projections of hepatitis C virus epidemiology in Latin America. *Liver Int* 2011; **31** Suppl 2: 18-29 [PMID: 21651701 DOI: 10.1111/j.1478-3231]

31 **Weinmann A**, Koch S, Niederle IM, Schulze-Bergkamen H, König J, Hoppe-Lotichius M, Hansen T, Pitton MB, Düber C, Otto G, Schuchmann M, Galle PR, Wörns MA. Trends in epidemiology, treatment, and survival of hepatocellular carcinoma patients between 1998 and 2009: an analysis of 1066 cases of a German HCC Registry. *J Clin Gastroenterol* 2014; **48**: 279-289 [PMID: 24045276 DOI: 10.1097/MCG.0b013e3182a8a793]

32 **Pinchoff J**, Drobnik A, Bornschlegel K, Braunstein S, Chan C, Varma JK, Fuld J. Deaths among people with hepatitis C in New York City, 2000-2011. *Clin Infect Dis* 2014; **58**: 1047-1054 [PMID: 24523215]

33 **Kershenobich D**, Razavi HA, Cooper CL, Alberti A, Dusheiko GM, Pol S, Zuckerman E, Koike K, Han KH, Wallace CM, Zeuzem S, Negro F. Applying a system approach to forecast the total hepatitis C virus-infected population size: model validation using US data. *Liver Int* 2011; **31** Suppl 2: 4-17 [PMID: 21651700 DOI: 10.1111/j.1478-3231.2011.02535.x]

34 **Edlin BR**, Eckhardt BJ, Shu MA, Holmberg SD, Swan T. Towards a more accurate estimate of the prevalence of hepatitis C in the United States. *Hepatology* 2015 Jul 14; Epub ahead of print [PMID: 26171595 DOI: 10.1002/hep.27978]

35 **Daw MA**, El-Bouzedi A, Dau AA. Libyan armed conflict 2011: Mortality, injury and population displacement. *Afr J Emerg Med* 2015; **14**:101-107 [DOI: 10.1016/j.afjem.2015.02.002]

36 **Daw MA**, El-Bouzedi A, Dau AA. The assessment of efficiency and coordination within Libyan Healthcare System during the Armed Conflict-2011. *Clinical Epidemiology & Global Health* 2015; In press [DOI: 10.1016/j.cegh.2015.07.004]

37 **Daw MA**, El-Bouzedi A, Dau AA. Geographic distribution of HCV genotypes in Libya and analysis of risk factors involved in their transmission. *BMC Res Notes* 2015; **8**: 367 [PMID: 26293137 DOI: 10.1186/s13104-015-1310-x]

38 **Daw MA**, El-Bouzedi A. Viral haemorrhagic fever in North Africa; an evolving emergency. *J Clin Exp Pathol* 2015; **5**: 215 [DOI: 10.4172/2161-0681.1000215]

39 **Watkins NA**, Dobra S, Bennett P, Cairns J, Turner ML. The

management of blood safety in the presence of uncertain risk: a United kingdom perspective. *Transfus Med Rev* 2012; **26**: 238-251 [PMID: 22126710 DOI: 10.1016/j.tmrv.2011.09.003]

40 **Kim MJ**, Park Q, Min HK, Kim HO. Residual risk of transfusion-transmitted infection with human immunodeficiency virus, hepatitis C virus, and hepatitis B virus in Korea from 2000 through 2010. *BMC Infect Dis* 2012; **12**: 160 [PMID: 22817275 DOI: 10.1186/1471-2334-12-160]

41 **Lucky TT**, Seed CR, Keller A, Lee J, McDonald A, Ismay S, Wand H, Wilson DP. Trends in transfusion-transmissible infections among Australian blood donors from 2005 to 2010. *Transfusion* 2013; **53**: 2751-2762 [PMID: 23461827 DOI: 10.1111/trf.12144]

42 **Zou S**, Dorsey KA, Notari EP, Foster GA, Krysztof DE, Musavi F, Dodd RY, Stramer SL. Prevalence, incidence, and residual risk of human immunodeficiency virus and hepatitis C virus infections among United States blood donors since the introduction of nucleic acid testing. *Transfusion* 2010; **50**: 1495-1504 [PMID: 20345570 DOI: 10.1111/j.1537-2995.2010.02622.x]

P- Reviewer: Borzio M, Smith MA
S- Editor: Gong XM **L- Editor**: Cant MR **E- Editor**: Li D

World Journal of Virology

Submit a Manuscript: http://www.wjgnet.com/esps/
Help Desk: http://www.wjgnet.com/esps/helpdesk.aspx
DOI: 10.5501/wjv.v5.i1.23

World J Virol 2016 February 12; 5(1): 23-30
ISSN 2220-3249 (online)

ORIGINAL ARTICLE

Basic Study

Pathogenicity of a currently circulating Chinese variant pseudorabies virus in pigs

Qing-Yuan Yang, Zhe Sun, Fei-Fei Tan, Ling-Hua Guo, Yu-Zhou Wang, Juan Wang, Zhi-Yan Wang, Li-Lin Wang, Xiang-Dong Li, Yan Xiao, Ke-Gong Tian

Qing-Yuan Yang, Zhe Sun, Fei-Fei Tan, Ling-Hua Guo, Yu-Zhou Wang, Juan Wang, Zhi-Yan Wang, Li-Lin Wang, Xiang-Dong Li, Yan Xiao, Ke-Gong Tian, National Research Center for Veterinary Medicine, Luoyang 471003, Henan Province, China

Ke-Gong Tian, College of Animal Science and Veterinary Medicine, Henan Agricultural University, Zhengzhou 450002, Henan Province, China

Author contributions: Yang QY, Sun Z, Tan FF, Guo LH, Wang YZ, Wang J, Wang ZY and Wang LL performed the experiments; Li XD performed the statistical analysis and wrote the paper; Li XD and Tian KG analyzed the data; Tian KG and Xiao Y conceived and designed the experiments; all authors read and approved the final manuscript.

Supported by Major Science and Technology Program in Henan Province, No. 131100110200.

Institutional review board statement: All procedures involving animals were reviewed and approved by the Institutional Animal Care and Use Committee of the National Research Center for Veterinary Medicine (IACUC protocol number: 2015010402). Conventional animal welfare regulations and standards were taken into account.

Institutional animal care and use committee statement: All procedures involving animals were reviewed and approved by the Institutional Animal Care and Use Committee of the National Research Center for Veterinary Medicine (IACUC protocol number: 2015010402).

Conflict-of-interest statement: The authors declare no conflict of interest.

Data sharing statement: Technical appendix, statistical code, and dataset are available from the corresponding author at tiankg@263.net.

Correspondence to: Dr. Ke-Gong Tian, National Research Center for Veterinary Medicine, Cuiwei Road, High-Tech District, Luoyang 471003, Henan Province, China. tiankg@263.net
Telephone: +86-379-60687971
Fax: +86-379-60687976

Received: May 8, 2015
Peer-review started: May 9, 2015
First decision: June 18, 2015
Revised: November 17, 2015
Accepted: December 1, 2015
Article in press: December 2, 2015
Published online: February 12, 2016

Abstract

AIM: To test the pathogenicity of pseudorabies virus (PRV) variant HN1201 and compare its pathogenicity with a classical PRV Fa strain.

METHODS: The pathogenicity of the newly-emerging PRV variant HN1201 was evaluated by different inoculating routes, virus loads, and ages of pigs. The classical PRV Fa strain was then used to compare with HN1201 to determine pathogenicity. Clinical symptoms after virus infection were recorded daily and average daily body weight was used to measure the growth performance of pigs. At necropsy, gross pathology and histopathology were used to evaluate the severity of tissue damage caused by virus infection.

RESULTS: The results showed that the efficient infection method of RPV HN1201 was *via* intranasal inoculation

at 10^7 $TCID_{50}$, and that the virus has high pathogenicity to 35- to 127-d old pigs. Compared with Fa strain, pigs infected with HN1201 showed more severe clinical symptoms and pathological lesions. Immunochemistry results revealed HN1201 had more abundant antigen distribution in extensive organs.

CONCLUSION: All of the above results suggest that PRV variant HN1201 was more pathogenic to pigs than the classical Fa strain.

Key words: Pseudorabies virus; Pathogenicity; Virus variant; Gross pathology; Histopathology

Core tip: Pseudorabies virus (PRV) variant HN1201 has pathogenicity in 35 to 127-d old pigs *via* intranasal inoculation at 10^7 $TCID_{50}$. Intranasal inoculation is more efficient than intramuscular inoculation for PRV challenge. PRV variant HN1201 showed higher pathogenic ability, as shown by the more severe clinical symptoms, pathological lesions, and abundant antigen distribution in extensive organs than the classical PRV Fa strain.

Yang QY, Sun Z, Tan FF, Guo LH, Wang YZ, Wang J, Wang ZY, Wang LL, Li XD, Xiao Y, Tian KG. Pathogenicity of a currently circulating Chinese variant pseudorabies virus in pigs. *World J Virol* 2016; 5(1): 23-30 Available from: URL: http://www.wjgnet.com/2220-3249/full/v5/i1/23.htm DOI: http://dx.doi.org/10.5501/wjv.v5.i1.23

INTRODUCTION

Pseudorabies virus (PRV), also known as Aujeszky's disease virus or Suid herpesvirus type 1 (SuHV-1), is the causative agent of pseudorabies (PR). Belonging to the family *Herpesviridae*, subfamily *Alphaherpesvirinae*, and genus *Varicellovirus*, the virus causes substantial economic losses in the pig industry worldwide[1-3]. The PRV genome is a double-stranded linear DNA which is about 143 kb in size and has about 70 ORFs[4,5]. This pathogen can infect numerous mammals, including carnivores, ruminants, and rodents, yet pigs are the only natural host for PRV as the reservoir of the virus[6,7]. PRV infection is characterized by neurologic symptoms and death in newborn piglets, respiratory disorders in elder pigs, and reproductive failure like stillbirths and abortions in sows. Like other alphaherpesviruses, PRV can establish a lifelong latent infection in the peripheral nervous system of infected pigs. Latently infected pigs can be recognized as a source of reinfection when the latent viral genome reactivates spontaneously and the infectious virus is developed[8].

Attenuated live or killed PRV vaccines have played a critical role in the control and eradication of PR. Bartha-K61, a vaccine imported from Hungary, have been widely used in China since the 1970s, and was reported to provide complete protection from field virus infection[2]. Nevertheless, since October 2011, severe PRV outbreaks have occurred on pig farms and spread rapidly to the northern parts of China[9,10]. Most of the infected farms had used Bartha-K61 vaccine according to the manufacturer's instructions, and the serum samples obtained from the infected pigs had a considerable positive rate of gE Ab detected by ELISA (IDEXX Laboratories, Westbrook, United States)[10,11]. The affected pigs presented with multiple clinical signs, including high fever (usually ≥ 40.5 ℃), depression, anorexia, respiratory distress, shivering, and systemic neurological symptoms[11,12]. Pathologic examination of viscera samples collected from dead pigs from different provinces displayed consolidation, edema, and hemorrhage in the lungs, as well as necrosis in the kidneys, indicating that newly-emerging PRV variants may have higher pathogenicity than the classical strains[13]. The PRV infection in vaccinated pig herds indicates that the traditional Bartha-K61 vaccine could not provide complete protection to the current prevalent PRV variants in China[11,14]. Accordingly, it is imperative to study the pathogenicity of the currently circulating PRV variant strains and develop newly effective vaccines to tackle the problem.

In this study, we first established a PRV variant HN1201 infection model in pigs according to different inoculation routes, virus loads, and pig ages. The characterized PRV variant HN1201 was then compared with the virulent classical PRV strain Fa to determine pathogenicity.

MATERIALS AND METHODS

Viruses and cells

The PRV variant HN1201 was previously isolated from the brain of infected pigs in Henan province[12]. Briefly, the infected pig brain sample was homogenized and the supernatant of homogenization was subjected to 0.22 μm filtration. The filtrated supernatant was inoculated on a PK-15 cell monolayer until the appearance of CPE after 3 d. The virus was harvested after two cycles of freeze-thaw and store at -80 ℃ until use. The classical PRV Fa was purchased from the Institute of China Veterinary Medicine Inspection[15]. Permissive PK-15 cells were cultured in Dulbecco's Modified Eagle's Medium supplemented with 5% fetal bovine sera.

Experiment design and animals

To establish a PRV HN1201 infection model in pigs, in the first animal experiment, twenty 60-d old pigs, five 35-d old pigs, and five 127-d old pigs were used to evaluate the pathogenicity of the virus by different inoculating routes, virus loads, and ages of pigs. Twenty 60-d old pigs were randomly allocated into the first four groups

Table 1 Outcome of infections with pseudorabies virus HN1201 strain in pigs

Group	Pig age (d)	Pig No.	Virus titer	Route	Euthanized
1	60	5	10^7	im	3/5
2	60	5	10^7	in	5/5
3	60	5	10^6	in	2/5
4	60	5	10^5	in	1/5
5	35	5	10^7	in	5/5
6	127	5	10^7	in	5/5

im: Intramuscular; in: Intranasal.

(Table 1). Pigs in group 1 and group 2 were inoculated with 10^7 $TCID_{50}$ PRV HN1201 strain *via* intramuscular (im) and intranasal (in) routes, respectively. Pigs in group 3 and 4 were inoculated *via* the intranasal route with 10^6 $TCID_{50}$ and 10^5 $TCID_{50}$ of PRV HN1201 strain, respectively. To test the susceptibility of pigs to the virus at different ages, five 35-d old pigs in group 5 and five 127-d old pigs in group 6 were inoculated *via* the intranasal route with 10^7 $TCID_{50}$ PRV HN1201 (Table 1).

In the second animal study, ten 56-d old pigs were randomly divided into two groups with five pigs in each group. Pigs in group Ⅰ were inoculated with 10^7 $TCID_{50}$ PRV HN1201 *via* the intranasal route and group Ⅱ were inoculated with classical PRV Fa strain with the same dose and route.

All pigs used in the above two animal trials were free of PRV and excluded by using gB- and gE-ELISA Kits (HerdChek PRV, IDEXX, United States) and PCR method. All pigs were also free of porcine reproductive and respiratory syndrome virus, classical swine fever virus, and porcine circovirus 2. Experimental pigs in different groups were insulated in separate rooms throughout the study. After virus inoculation, rectal temperature and clinical signs were recorded on a daily basis. At 14 d post-inoculation (dpi), all surviving pigs were humanely euthanized and necropsied, and different organ samples were collected. The collected samples were subjected to pathological examination and gently inflated with 10% neutral-buffered formalin for immunohistochemistry examination. All animal trials in this study were approved by the Animal Care and Ethics Committee of the China National Research Center for Veterinary Medicine.

Histopathology and immunohistochemistry

Representative samples were cut from the fixed tissues and processed into paraffin blocks. Sections approximately 3-4 μm thick were cut into slides. Duplicates of the same sections were used for hematoxylin and eosin (H and E) staining and immunohistochemistry staining separately, as previously described[16]. The H and E staining was operated automatically by Leica fully automatic dyeing machine according to standard procedures. Immunohistochemistry staining was performed as below. The prepared paraffin sections were mounted on APES-treated slides and incubated overnight at 37 ℃. The slides were de-waxed *via* routine method by Leica automatic dyeing machine. The samples were blocked with 3% peroxide-methanol for 20 min at room temperature for endogenous peroxidase ablation and rinsed by phosphate buffer solution (PBS) twice. The following steps were carried out in a moisture chamber: (1) Samples were incubated with blocking buffer containing normal horse serum (Beijing Zhongshan Jinqiao, China) with 1:20 dilution with PBS at 37 ℃ for 20 min; (2) The horse serum was discarded and samples were incubated in PRV monoclonal antibody 3B5 solution (Beijing Tian Tech Biotechnology, China) with 1:800 dilution in PBS (pH 7.3) at 37 ℃ for half an hour and then 4 ℃ overnight; (3) After rinsing with PBS three times, HRP goat anti-mouse IgG (BTI, United States) with 1:100 dilution in PBS (pH 7.3) was added, and the slides were incubated for 1 h at 37 ℃; (4) After rinsing with PBS three times, the slides were incubated with AEC and kept at room temperature without light for 5-10 min; (5) After rinsing with PBS three times, the slides were stained with hematoxylin (freshly prepared) 1:10 dilution for 10 s; (6) The unbound hematoxylin was washed away by running water, and the slides were placed into water for 2 min; and (7) The slides were allowed to dry naturally and then mounted with water-soluble tablet seal before visualization by 200 × microscope photographs. The results were determined by negative (-) and positive (+), with positive signals interpreted as low (+), moderate (++), and intense (+++), according to the intensity of staining.

Animal care and use

The animal protocol was designed to minimize pain or discomfort to the animals. The animals were acclimatized to laboratory conditions (23 ℃, 12 h light/12 h dark, 50% humidity, and *ad libitum* access to food and water) for two weeks prior to experimentation. All animals were euthanized by barbiturate overdose (intravenous injection, 150 mg/kg pentobarbital sodium) for tissue collection. All procedures involving animals were reviewed and approved by the Institutional Animal Care and Use Committee of the National Research Center for Veterinary Medicine (IACUC protocol number: 2015010402).

Statistical analysis

Differences of body temperature and body weight between two infected groups in the second animal trial were determined by using *t*-test in GraphPad Prism 5.0 Software (San Diego, CA). Differences were considered statistically significant when $P < 0.05$.

RESULTS

Experimental infection of PRV HN1201

For routes of infection, all pigs in group 1 and group 2 inoculated with 10^7 $TCID_{50}$ PRV HN1201 strain *via* intramuscular and intranasal routes, respectively, showed PRV-specific clinical symptoms such as fever (40.0 ℃-41.5 ℃), respiratory distress, excessive

Table 2 Clinical manifestations of pseudorabies virus HN1201 and Fa infection

Groups	Respiratory symptom					Neurological symptom			
	Vomit	Respiratory distress	Cough	Sneeze	Salivation	Circling	Posterior paralysis	Muscle tremors	Lay recumbent and paddle
	+	+	-	+	-	+	-	+	-
Ⅰ (HN1201)	-	+	+	+	-	+	-	+	-
	+	+	+	+	-	-	+	+	+
	-	+	+	+	+	+	+	+	+
	+	+	+	+	+	+	+	+	+
	-	-	-	+	-	-	-	-	-
Ⅱ (Fa strain)	-	-	-	+	-	-	-	-	-
	-	-	-	+	-	-	-	-	-
	-	-	-	+	-	-	-	-	-
	+	+	-	+	+	+	-	+	+

Each row represents one pig in the corresponding group.

salvation, and neurological signs including convulsion and ataxia. All pigs in group 2 were euthanized due to moribund conditions from 5 to 7 dpi. Compared with group 2, three pigs in group 1 were euthanized from 5 to 7 dpi and the other two pigs survived until the end of the study (terminated at 14 dpi, Table 1).

All pigs in group 3 ($10^{6.0}$ $TCID_{50}$) showed severe respiratory symptoms and neurological signs, as described above, with two being euthanized 6 dpi. Compared to pigs in group 3, respiratory symptoms such as coughing and shivering were more often observed in group 4 ($10^{5.0}$ $TCID_{50}$). There was one pig out of the five in group 4 that showed neurological signs, and was euthanized by the end of study (terminated at 14 dpi).

Young piglets are more susceptible to PRV infection than elder pigs[6]. To determine the pathogenicity of PRV HN1201 in pigs of different ages, 35, 60, and 127-d old pigs were inoculated with 10^7 $TCID_{50}$ of virus. After virus inoculation, pigs of different ages showed the clinical symptoms as described above. All pigs in group 5 (35-d old pigs) were euthanized from day 4 to day 6 and all pigs in group 6 (127-d old pigs) were euthanized from day 5 to day 8 due to the moribund conditions. Therefore, unlike the classical PRV strains, this PRV variant strain showed high pathogenicity in pigs of different ages.

Comparison of pathogenicity between PRV variant HN1201 and classical Fa strain

Since the above results showed PRV variant HN1201 has high pathogenicity in pigs of different ages, a classical PRV Fa strain was used to compare pathogenicity. To exclude the bias of pathogenicity of two PRV strains due to the age of experimental pigs, ten 56-d-old healthy pigs were randomly assigned to two groups, with five pigs in each group. Pigs in groups Ⅰ and Ⅱ were inoculated with PRV HN1201 and Fa strain, respectively, *via* intranasal method at 10^7 $TCID_{50}$.

As expected, all pigs in group Ⅰ displayed high fever, anorexia, depression, respiratory symptoms, and neurological signs as described in the first animal study. In contrast, four pigs in group Ⅱ had no respiratory or neurological symptoms, aside from sneezing (Table 2), while only one pig showed the same clinical signs as pigs in group Ⅰ. Gross pathology examination at necropsy showed that PRV HN1201 infection led to severe pulmonary consolidation and necrosis in the lung (Figure 1A), encephalic hemorrhage in the brain (Figure 1B), and hemorrhage and necrosis in the tonsil (Figure 1C). By contrast, pigs infected with PRV Fa showed only slight hemorrhage in the lung tissue (Figure 1D) and had no obvious changes in the brain or tonsil (Figure 1E and F). No other obvious pathologic change was found after two virus infection in heart, liver, spleen, and kidney tissues. There was no significant difference in rectal temperature between the two groups in the first 5 d of study (Figure 2A). Pigs in group Ⅰ had significant body weight losses compared to pigs in group Ⅱ at 6 dpi (Figure 2B). At 5 dpi, two pigs were euthanized in group Ⅰ and one pig was euthanized in group Ⅱ. At 6 dpi, another three pigs were euthanized in group Ⅰ and all remaining pigs in group Ⅱ survived to the end of the study.

Organ samples of pig tonsil, lung, cerebellum, lymph nodes, kidney, and liver were collected for histological examination and immunohistochemistry staining. Typical PRV infection is characterized by necrosis in multiple organs. As shown in Figure 3, necrosis, congestion, or hemorrhage in all above organs of PRV HN1201-infected pigs were observed after H&E staining (Figures 3A-G), with neuronal intra-nuclear inclusions also being observed in the brain. Compared to the HN1201 infection, PRV Fa-infected pigs only showed neuronal degeneration, necrosis in the brain, Purkinje cell degeneration, and necrosis in the cerebellum (Figure 3H and Ⅰ). In accordance with histopathology results, immunohistochemistry staining showed significant strong positive signals in all of the above organs obtained from pigs infected with HN1201 virus, whereas only brain and cerebellum samples of one RPV Fa-infected pig revealed positive results (Table 3).

DISCUSSION

Since late 2011, outbreaks of PR-like diseases have occurred on numerous Bartha-K61-vaccinated pig farms and gradually spread in China, causing huge economic

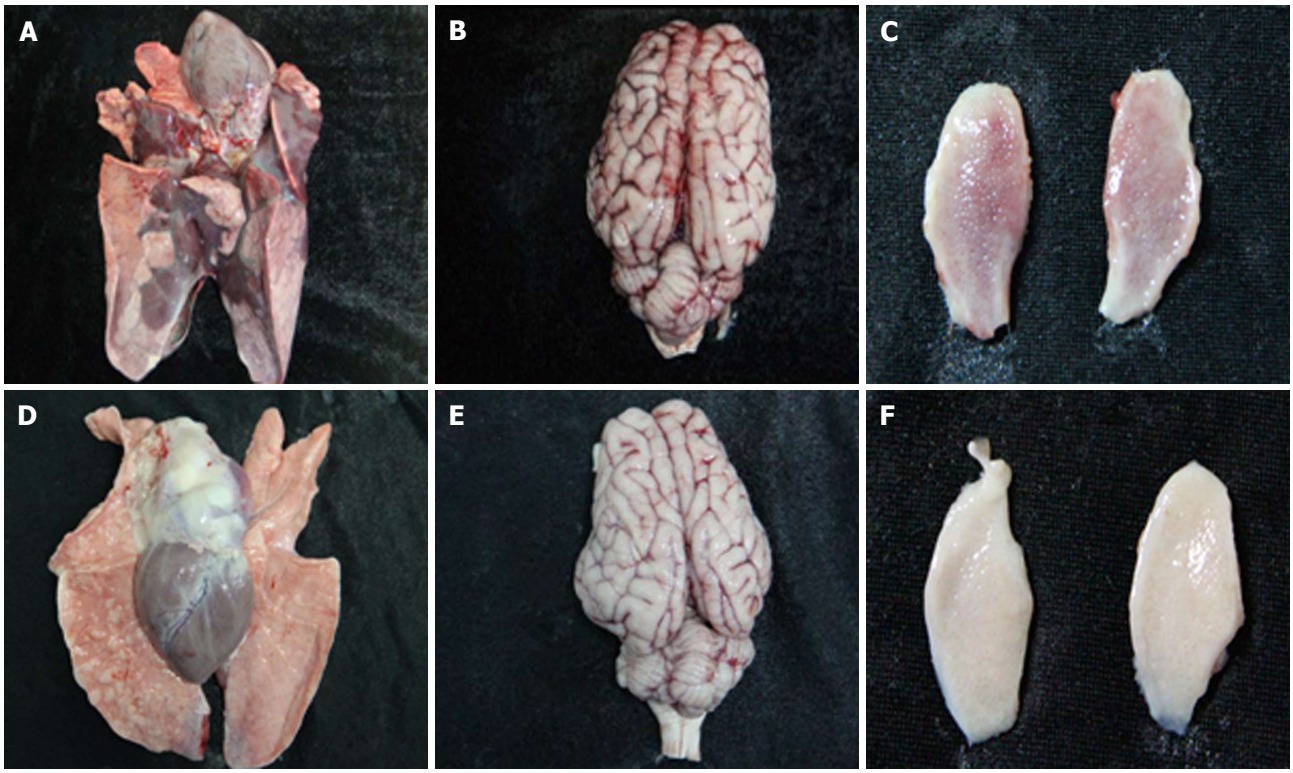

Figure 1 Gross pathology examination at necropsy. Lung, brain, and tonsil samples after PRV HN1201 (A-C) or Fa strain infection (D-F). PRV: Pseudorabies virus.

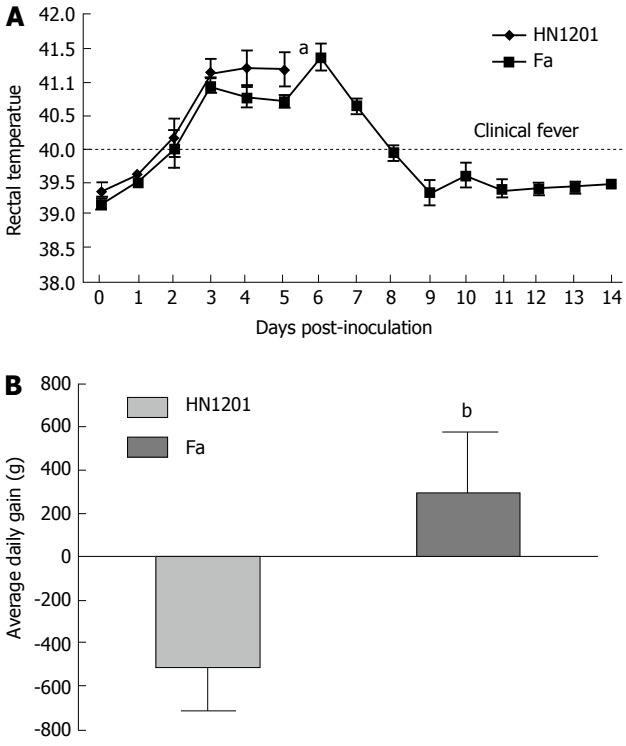

Figure 2 Rectal temperature (A) and average daily (B) body weight gain (6 d post-inoculation) of pigs after pseudorabies virus HN1201 or Fa infection. $^{a}P < 0.05$, $^{b}P < 0.001$.

losses to the Chinese swine industry[10,13]. Recent studies have shown that PRV variants contributed to the recent outbreaks of PR, and the traditional Bartha-K61 vaccine could not provide complete protection against the emerging PRV strains[11,14]. Similar to classical PR, the disease is characterized by the sudden death of new born piglets, respiratory and neurological symptoms in growing pigs, and stillbirth or the birth of weak piglets from sows. However, the pathogenicity of the new emerging PRV variant was never delineated and compared with classical PRV strains. Therefore, it is necessary to determine the pathogenicity of the current PRV variants before any control measures are implemented to control the disease.

PRV is tropic for both the respiratory and nervous systems of swine. Viral particles enter sensory nerve endings, thereby innervating the infected mucosal epithelium. Morbidity and mortality associated with PRV infection varies with host age, the animal's overall health status, and infectious dose[2]. In this study, we first tested the pathogenicity of PRV variant HN1201 by different routes of virus infection, virus loads for inoculation, and pig ages. Our results showed that intranasal infection is more effective than intramuscular infection when 10^7 $TCID_{50}$ viruses were used for inoculation. Pigs infected with PRV 1201 by the intranasal route showed more severe clinical symptoms and higher mortality rates than those with intramuscular routes, and virus loads were positively correlated with mortality rates. The pathogenicity of some other PRV variant strains have been studied recently[17]. In a study by Luo *et al*[17] (2014), pigs infected with the 10^6 $TCID_{50}$ PRV TJ strain by the intranasal route showed higher mortality than those with a lower dose or were infected by the

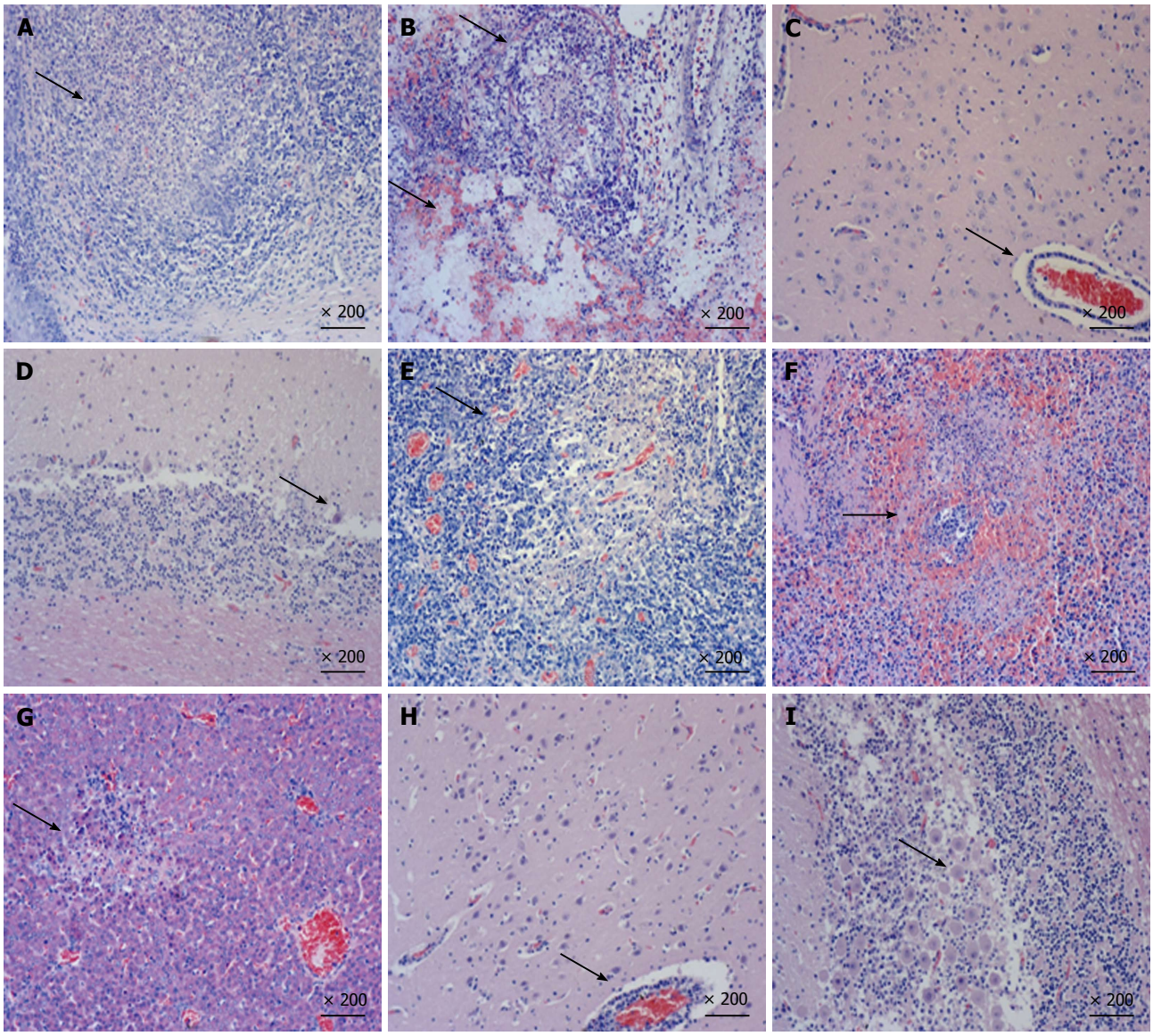

Figure 3 Hematoxylin and eosin staining of multiple tissues of pigs inoculated with HN1201 (A-G) and Fa strain (H and I). A: Tonsil - tonsillar lymphoid tissue necrosis and formation of large necrotic foci; B: Lung - vascular congestion and hemorrhage (lower arrow), with bronchial epithelial necrosis and necrotic cells within the lumen (upper arrow); C: Brain - lymphocyte infiltration around the small blood vessels in the brain cortex, non-suppurative encephalitis; D: Cerebellum - Purkinje cell degeneration and necrosis; E: Hilar lymph nodes - vascular dilatation and congestion, and lymphatic tissue necrosis; F: Spleen - white pulp structure disappeared and white necrotic marrow lymphocytes formed large necrotic foci; G: Liver - necrotic foci formation; H: Brain - coalescing non-suppurative encephalitis with neuronal degeneration and perivascular cuffing; I: Cerebellum - Purkinje cell degeneration and necrosis.

intramuscular route, which is consistent with our results. Bama miniature pigs injected intramuscularly with $10^{7.0}$ $TCID_{50}$ PRV strain HeN1, another virulent PRV variant, the animals exhibited only transient fever for 3-5 d, and no other clinical symptoms or postmortem changes were observed[10]. Differences in pathogenicity and mortality caused by different PRV viruses could be explained by the virus load for inoculation, viral strain, and breed of pigs, although these three viruses also share a more than 99.0% similarity in their whole genome sequences. Besides routes of inoculation and virus load, PRV HN1201 could infect pigs from 35 to 127 d old with PRV-specific clinical symptoms, indicating that the PRV HN1201 strain is highly pathogenic to pigs.

To compare the pathogenicity of newly-emerging PRV variants with the classical PRV strain, PRV HN1201 and Fa strains were used to infect pigs. Our results showed that HN1201-infected pigs showed more severe clinical signs and higher mortality rates than Fa-infected pigs (5/5 *vs* 1/5). Pigs in the PRV HN1201-infected group displayed high fever, anorexia, depression, respiratory symptoms, and neurological signs. In comparison, four pigs in the PRV Fa-infected group had no respiratory or neurological symptoms, aside from sneezing. Meanwhile, pigs infected with HN1201 had steady body weight loss as compared with pigs infected with the Fa strain (Figure 2B). Retarded growth was more often observed in young piglets after PRV infection. However, the loss of body weight of 56-d old pigs after PRV infection was seldom observed, which proves the high virulence of

Table 3 Virus antigen distribution and intensity in different organs of pseudorabies virus HN1201 or Fa strain by immunohistochemistry staining

Groups	Tonsil	Lung	Lymph nodes			Brain	Cerebellum	Spleen	Liver
			Mandibular	Superficial inguinal	Mesenteric				
HN1201	3+	3+	3+	2+	2+	2+	1+	2+	2+
	3+	2+	2+	2+	2+	2+	1+	3+	-
	3+	3+	3+	2+	2+	1+	2+	3+	+
	3+	3+	++	3+	2+	1+	2+	2+	2+
	3+	3+	3+	2+	3+	2+	2+	3+	3+
Fa strain	-	+	-	-	-	-	-	-	-
	-	-	-	-	-	2+	2+	-	-
	-	-	-	-	-	2+	2+	-	-
	-	-	-	-	-	2+	2+	-	-
	-	-	-	-	-	2+	2+	-	-

The positive staining signals were interpreted as negative (-), low (1+), moderate (2+), or intense (3+), according to the intensity of staining. Each row represents one pig in the corresponding group.

PRV HN1201.

Gross pathological examination at necropsy revealed more severe damage to the lung, tonsil, brain, cerebellum, and lymph nodes in pigs infected with HN1201 strain than in the Fa strain group. In line with pathological results, histopathology examination showed remarkably obvious necrosis in multiple tissues, such as the tonsil, lung, brain, spleen, and liver in HN1201-infected pigs; in contrast, necrosis caused by PRV Fa infection was only limited to the brain and cerebellum. Immunochemistry results also showed that PRV HN1201 infection lead to more extensive virus antigen distribution in different organs with more intense staining, while Fa infection only had one cerebellum sample from one pig that showed positive. Previous studies reported that inoculation of PRV through the nasal cavity resulted in virally-induced neuropathological lesions[2]. The kinetics and locations of lesion appearance were consistent with a transneuronal spread of PRV from the nasal epithelium to synaptically-connected higher-order structures in the nervous system. The intense PRV antigen location and severe lesions of the brain, tonsil, and lung coincided with the typical respiratory and neurological symptoms, and may be due to intranasal infection. Therefore, the above results further suggest the higher pathogenicity of PRV HN1201 when compared to the classical Fa strain.

In conclusion, PRV HN1201 infection is more effective through the intranasal route than the intramuscular inoculation route, and the virus is highly pathogenic to different ages of pig. Compared with classical PRV Fa strain, HN1201 causes more severe clinical symptoms and pathological lesions, with extensive antigen distribution in different organs.

COMMENTS

Background

Highly virulent pseudorabies virus (PRV) variants are circulating in most Chinese pig farms, causing huge economic losses. The pathogenicity of these PRV variants have not been previously compared with classical PRV strains.

Research frontiers

The authors aimed to test the pathogenicity of a newly-emerging PRV variant in pigs of different inoculation routes, virus loads, and ages. Differences in pathogenicity between the newly-emerging PRV variant and the classical PRV strain were also compared.

Innovations and breakthroughs

This study demonstrates that the currently-circulating PRV HN1201 variant has higher pathogenicity in pigs than the classical PRV Fa strain *via* the manifestation of more severe clinical symptoms and pathological lesions, with extensive antigen distribution in different organs.

Applications

The authors proved the PRV variant to be more pathogenic in pigs as compared to the classical Fa strain, which may partially explain the inefficacy of current commercial PRV vaccines. Thus, a better understanding of the differences of pathogenicity between variant and classical PRV may facilitate the development of more effective vaccines.

Terminology

Pathogenicity of pseudorabies virus is the potential capacity of PRV to cause PR-like syndrome in pigs. Pathogenicity of viruses may change due to virus mutation and/or recombination. Study into the pathogenesis of currently-circulating field viruses may provide first-hand data for disease control.

Peer-review

This manuscript reports the analysis of the pathogenicity of a new PRV variant that the commonly-used vaccine cannot protect against, and is therefore causing massive economic losses in China. The pathogenicity of this variant and the classical PRV Fa stain is also compared. The experiment design and results were clear and convincing. It will be interesting to see if the authors can further explore the mechanisms of the enhanced pathogenicity of the PRV variant behind these phenomena.

REFERENCES

1 **Mettenleiter TC**. Pseudorabies (Aujeszky's disease) virus: state of the art. August 1993. *Acta Vet Hung* 1994; **42**: 153-177 [PMID: 7810409]

2 **Pomeranz LE**, Reynolds AE, Hengartner CJ. Molecular biology of pseudorabies virus: impact on neurovirology and veterinary medicine. *Microbiol Mol Biol Rev* 2005; **69**: 462-500 [PMID: 16148307 DOI: 10.1128/MMBR.69.3.462-500.2005]

3 **Roizman B**, Baines J. The diversity and unity of Herpesviridae. *Comp Immunol Microbiol Infect Dis* 1991; **14**: 63-79 [PMID: 1935001 DOI: 10.1016/0147-9571(91)90122-T]

4 **Klupp BG**, Hengartner CJ, Mettenleiter TC, Enquist LW. Complete, annotated sequence of the pseudorabies virus genome. *J Virol* 2004; **78**: 424-440 [PMID: 14671123 DOI: 10.1128/JVI.78.1.424-440.2004]

5 **Szpara ML**, Tafuri YR, Parsons L, Shamim SR, Verstrepen KJ, Legendre M, Enquist LW. A wide extent of inter-strain diversity in virulent and vaccine strains of alphaherpesviruses. *PLoS Pathog* 2011; **7**: e1002282 [PMID: 22022263 DOI: 10.1371/journal.ppat.1002282]

6 **Mulder WA**, Pol JM, Gruys E, Jacobs L, De Jong MC, Peeters BP, Kimman TG. Pseudorabies virus infections in pigs. Role of viral proteins in virulence, pathogenesis and transmission. *Vet Res* 1997; **28**: 1-17 [PMID: 9172836]

7 **Müller T**, Hahn EC, Tottewitz F, Kramer M, Klupp BG, Mettenleiter TC, Freuling C. Pseudorabies virus in wild swine: a global perspective. *Arch Virol* 2011; **156**: 1691-1705 [PMID: 21837416 DOI: 10.1007/s00705-011-1080-2]

8 **Rziha HJ**, Mettenleiter TC, Ohlinger V, Wittmann G. Herpesvirus (pseudorabies virus) latency in swine: occurrence and physical state of viral DNA in neural tissues. *Virology* 1986; **155**: 600-613 [PMID: 3024403 DOI: 10.1016/0042-6822(86)90220-5]

9 **Wang TY,** Xiao Y, Yang QY, Wang YZ, Sun Z, Zhang CL, Yan SJ, Wang J, Guo LH, Yan H, Gao ZY, Wang LL, Li XD, Tan FF, Tian KG. Construction of a gE-deleted pseudorabies virus and its efficacy to the new-emerging variant PRV challenge in the form of killed vaccine. *Biomed Int Res* 2015; In press [DOI: 10.1155/2015/684945]

10 **An TQ**, Peng JM, Tian ZJ, Zhao HY, Li N, Liu YM, Chen JZ, Leng CL, Sun Y, Chang D, Tong GZ. Pseudorabies virus variant in Bartha-K61-vaccinated pigs, China, 2012. *Emerg Infect Dis* 2013; **19**: 1749-1755 [PMID: 24188614 DOI: 10.3201/eid1911.130177]

11 **Gu Z**, Dong J, Wang J, Hou C, Sun H, Yang W, Bai J, Jiang P. A novel inactivated gE/gI deleted pseudorabies virus (PRV) vaccine completely protects pigs from an emerged variant PRV challenge. *Virus Res* 2015; **195**: 57-63 [PMID: 25240533]

12 **Wu R**, Bai C, Sun J, Chang S, Zhang X. Emergence of virulent pseudorabies virus infection in northern China. *J Vet Sci* 2013; **14**: 363-365 [PMID: 23820207 DOI: 10.4142/jvs.2013.14.3.363]

13 **Yu X**, Zhou Z, Hu D, Zhang Q, Han T, Li X, Gu X, Yuan L, Zhang S, Wang B, Qu P, Liu J, Zhai X, Tian K. Pathogenic pseudorabies virus, China, 2012. *Emerg Infect Dis* 2014; **20**: 102-104 [PMID: 24377462 DOI: 10.3201/eid2001.130531]

14 **Wang CH**, Yuan J, Qin HY, Luo Y, Cong X, Li Y, Chen J, Li S, Sun Y, Qiu HJ. A novel gE-deleted pseudorabies virus (PRV) provides rapid and complete protection from lethal challenge with the PRV variant emerging in Bartha-K61-vaccinated swine population in China. *Vaccine* 2014; **32**: 3379-3385 [PMID: 24793946 DOI: 10.1016/j.vaccine.2014.04.035]

15 **Zhu L**, Yi Y, Xu Z, Cheng L, Tang S, Guo W. Growth, physicochemical properties, and morphogenesis of Chinese wild-type PRV Fa and its gene-deleted mutant strain PRV SA215. *Virol J* 2011; **8**: 272 [PMID: 21639925 DOI: 10.1186/1743-422X-8-272]

16 **Zhang C**, Guo L, Jia X, Wang T, Wang J, Sun Z, Wang L, Li X, Tan F, Tian K. Construction of a triple gene-deleted Chinese Pseudorabies virus variant and its efficacy study as a vaccine candidate on suckling piglets. *Vaccine* 2015; **33**: 2432-2437 [PMID: 25865469 DOI: 10.1016/j.vaccine.2015.03.094]

17 **Luo Y**, Li N, Cong X, Wang CH, Du M, Li L, Zhao B, Yuan J, Liu DD, Li S, Li Y, Sun Y, Qiu HJ. Pathogenicity and genomic characterization of a pseudorabies virus variant isolated from Bartha-K61-vaccinated swine population in China. *Vet Microbiol* 2014; **174**: 107-115 [PMID: 25293398 DOI: 10.1016/j.vetmic.2014.09.003]

P- Reviewer: Choi TG, Ghiringhelli PD, Hua XG, Shih L
S- Editor: Song XX **L- Editor**: Rutherford A **E- Editor**: Li D

World Journal of Virology

Submit a Manuscript: http://www.wjgnet.com/esps/
Help Desk: http://www.wjgnet.com/esps/helpdesk.aspx
DOI: 10.5501/wjv.v5.i1.31

World J Virol 2016 February 12; 5(1): 31-37
ISSN 2220-3249 (online)

ORIGINAL ARTICLE

Observational Study

Neuropathology of JC virus infection in progressive multifocal leukoencephalopathy in remission

Karen S SantaCruz, Gulmohor Roy, James Spigel, Elaine L Bearer

Karen S SantaCruz, Elaine L Bearer, Department of Pathology, University of New Mexico, University of New Mexico Health Sciences Center, Albuquerque, NM 87131, United States

Gulmohor Roy, Department of Neurology, University of California, Irvine, CA 92697, United States

James Spigel, Department of Pathology, Presbyterian Hospital, Albuquerque, NM 87110, United States

Author contributions: SantaCruz KS is a neuropathologist who reviewed all histopathology and determined the diagnosis, captured the histological images and helped to write the MS; Roy G was a resident in training who reviewed the medical chart and drafted and edited the MS; Spigel J performed the autopsy, contributed and edited clinical data and reviewed the MS; Bearer EL is an experimental neuropathologist who reviewed the pathology, edited the MS, added the references, selected the images, prepared the figures and replied to reviewers' comments.

Supported by The Harvey Family Endowment (ELB) and National Institutes of Health RO1 MH096093, RO1 NS062184, and RO1 NS046810.

Institutional review board statement: The Institutional review board of University of New Mexico finds IRB approval not applicable for post-mortem case reports.

Informed consent statement: Consent for post-mortem examination was obtained from the family.

Conflict-of-interest statement: The authors have no conflict of interest to report.

Data sharing statement: All blocks and slides from this report are available upon request to the corresponding author according to the policies of the pathology department at UNM.

Correspondence to: Elaine L Bearer, Professor, Department of Pathology, University of New Mexico, University of New Mexico Health Sciences Center, UNM Hospital (MSC08 4640), Albuquerque, NM 87131, United States. ebearer@salud.unm.edu
Telephone: +1-505-2722404
Fax: +1-505-2728084

Received: August 7, 2015
Peer-review started: August 11, 2015
First decision: September 22, 2015
Revised: October 14, 2015
Accepted: December 13, 2015
Article in press: December 15, 2015
Published online: February 12, 2016

Abstract

AIM: To investigate the neuropathology of the brain in a rare case of remission following diagnosis of progressive multifocal leukoencephalopathy (PML).

METHODS: Consent from the family for an autopsy was obtained, clinical records and radiograms were retrieved. A complete autopsy was performed, with brain examination after fixation and coronal sectioning at 1 cm intervals. Fourteen regions were collected for paraffin embedding and staining for microscopic analysis. Histologic sections were stained with Luxol blue, hematoxylin/eosin, and immunostained for myelin basic protein, neurofilament, SV40 T antigen and p53. The biopsy material was also retrieved and sections were stained with hematoxylin/eosin and immunostained for SV40 and p53. Sections were examined by American Board of Pathology certified pathologists and images captured digitally.

RESULTS: Review of the clinical records was notable for

a history of ulcerative colitis resulting in total colectomy in 1977 and a liver transplant in 1998 followed by immune-suppressive therapy. Neurological symptoms presented immediately, therefore a biopsy was obtained which was diagnosed as PML. Immunotherapy was adjusted and clinical improvement was noted. No subsequent progression was reported. Review of the biopsy demonstrated atypical astrocytes and enlarged hyperchromatic oligodendroglial cells consistent with JC virus infection. Strong SV40 and p53 staining was found in glial cells and regions of dense macrophage infiltration were present. On gross examination of the post-mortem brain, a lesion in the same site as the original biopsy in the cerebellum was identified but no other lesions in the brain were found. Microscopic analysis of this cerebellar lesion revealed a loss of myelin and axons, and evidence of axonal damage. This single burned-out lesion was equivocally positive for SV40 antigen with little p53 staining. Examination of thirteen other brain regions found no other occult sites.

CONCLUSION: Our study reveals residual damage, rare macrophages or other inflammation and minimal evidence of persistent virus. This case demonstrates the possibility of complete remission of PML.

Key words: Progressive multifocal leukoencephalopathy; Progressive multifocal leukoencephalopathy; JC virus; Remission; Demyelinating

Core tip: Progressive multifocal leukoencephalopathy after organ transplant is rapidly fatal in most cases, with an average time to death of 6.4 mo. We report a case with no clinical progression over 14 years despite ongoing immunosuppressive therapy. At initial diagnosis the biopsy demonstrated classic histopathological features of JC virus. At autopsy, microscopic analysis of the cerebellar lesion revealed a residual loss of myelin and evidence of axonal damage without evidence of viral activity. These results suggest that JC virus can be kept in check even in a setting of immunosuppression, and argue for more investigation into the microbiome of the brain.

SantaCruz KS, Roy G, Spigel J, Bearer EL. Neuropathology of JC virus infection in progressive multifocal leukoencephalopathy in remission. *World J Virol* 2016; 5(1): 31-37 Available from: URL: http://www.wjgnet.com/2220-3249/full/v5/i1/31.htm DOI: http://dx.doi.org/10.5501/wjv.v5.i1.31

INTRODUCTION

Progressive multifocal leukoencephalopathy (PML) is a demyelinating disease of the central nervous system caused by reactivation of latent JC virus in immunocompromised individuals. Oligodendroglial cells are preferentially infected with consequent loss of myelin and coalescing demyelination plaques, sometimes leading to mild-to-moderate axonal loss associated with axonal spheroids. Long-term survival in patients with PML is increasingly common in human immunodeficiency virus (HIV)-infected people treated with highly active antiretroviral therapy (HAART)[1-8]. In contrast, prolonged survival in patients with immunosuppression following solid organ transplant is unusual[9,10]. Here we present an unusual case in which there was a 14-year clinical remission after biopsy-proven PML, despite continued immuno-suppression after liver transplant.

PML had been universally fatal, usually within 6 mo, until the late 1990's. Although no specific treatment has proven particularly effective, enhancing natural immunity by reducing the effects of HIV virus or by altering immunosuppressant therapy has been shown to improve survival[11]. One explanation for prolonged survival is improved cellular immune responses against JC virus (JCV) in long term survivors *vs* those with poor outcomes[12]. Detectable cytotoxic T lymphocytes specific for JCV -T or VP-1 have been shown to be a prognostic indicator of long-term survival in HIV patients[12]. Although long-term survival in immunosuppressed transplant patients has been described[13,14] these cases are unusual[9] and detailed neuropathologic descriptions of residual demyelinating plaques in patients in complete remission are few, possibly because they are very rare or not frequently examined post-mortem[15]. This study therefore fills an important gap in our knowledge of pathological processes that appear in long-term survival.

MATERIALS AND METHODS

Consent for the autopsy from the family was obtained as approved by Presbyterian Hospital. According to Internal Review Board of University of New Mexico Health Sciences Center neither post-mortem material nor case reports require IRB approvals. Clinical records were retrieved, and the clinical history together with results of all brain imaging studies that had been performed at UNM (12/2006 and 4/2008) reviewed. The original imaging studies were not available, and, in the absence of neurological symptomatology, imaging and CSF sampling were not performed during the final hospitalization, nor was post-mortem brain imaging done.

A complete autopsy was performed with subsequent examination of the brain after fixation. Gross examination of the brain included coronal sectioning of the neocortex at 1 cm intervals, and sectioning of the cerebellum and brainstem at 0.5 cm intervals. The surface of each slice was examined. Thirteen brain regions were selected, slabs 1.5 cm × 1.5 cm × 0.1 cm dissected and these were submitted for paraffin embedding. Histologic sections were stained with Luxol blue, hematoxylin/eosin, and for myelin basic protein (Dako, polyclonal rabbit anti-human), neurofilament (Dako, Clone 2F11), SV40 T antigen (Calbiochem, Ab-2, PAb 416) or p53 (Dako,

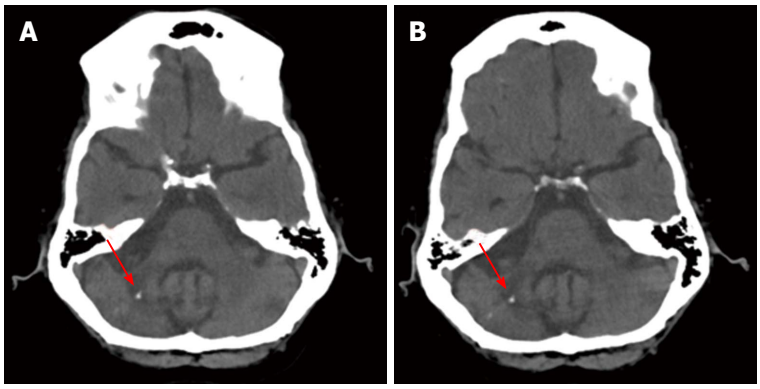

Figure 1 Computed tomography scans show no progression. A: Axial slice from the CT scan of 2006 showing the cerebellar lesion (red arrow), a small calcification, and atherosclerosis of cerebral vasculature; B: Axial slice of the same coordinates as in (A) from the CT scan of 2008 showing the cerebellar lesion (red arrow), as well as the calcification. Note the radiolucency of the cerebellar peduncle and the loss of tissue density in the cerebellum. This location corresponds to that of the 1999 biopsy and the histologic sections examined at autopsy. CT: Computed tomography.

Clone DO7) by immunohistochemistry at TriCore Reference Laboratories, Albuquerque, NM. The SV40 T-antigen (Ab-2) antibody is a mouse monoclonal antibody with specific determinants unique to the SV40 large T antigen and non-reactive with the small T antigen. The antigenic epitope is between Ile83 and Lys128 of the SV40 large T antigen, a region highly homologous to the JC virus large T antigen. For each immunostain, positive and negative controls were run in parallel. The paraffin block containing the biopsy was retrieved together with its slides from archives, new sections were made and also stained for SV40 and p53. Sections were examined on an Olympus BX40 microscope using 4 ×, 10 ×, 20 × and 40 × objectives, and digital images captured on an Olympus DP26 camera using cellSens Standard software. Images were prepared for figures using Adobe Photoshop to resize, create multi-image panels, adjust levels and add lettering.

RESULTS

Case history

A 76-year-old woman with a history of ulcerative colitis had a total colectomy in 1977 and subsequently developed sclerosing cholangitis. She received an orthotopic liver transplant in 1998. In 1999 neurological symptoms occurred, primarily consisting of ataxia in a setting of immunosuppressive therapy for the liver transplant. She was found to have a white matter lesion involving cerebellar white matter with no other sites of involvement. Brain biopsy performed in March 1999 showed classic changes of PML. The dosage of immunosuppressive therapy with Tacrolimus and Sirolimus was subsequently adjusted to minimize progression of further neurological disease and her mild cerebellar symptoms stabilized.

Her medical history was also significant for right hip fracture in 2003, status post hip replacement complicated by infection and requiring long term antibiotic therapy, chronic renal insufficiency, due to congenital hypoplastic kidney, end stage renal disease on dialysis since 2008, cardiovascular disease with episodes of atrial fibrillation and rapid ventricular response, hypothyroidism, gout and recurrent infections.

She had multiple hospital admissions from February 2012 to March 2013 due to gastroenteritis with subsequent workup for stool pathogens that was negative. She developed pancreatic insufficiency with findings on ultrasound examination that showed an atrophic right kidney, small liver and pancreatic cysts. Due to recurrence of the gastrointestinal illness, and to ultrasound findings, there was concern for an intraductal papillary mucinous neoplasm of the pancreas with associated pancreatic insufficiency. Computed tomography scan of the abdomen showed diffuse dilatation of the pancreatic duct, as well as a liver abscess. She died six days following abdominal imaging studies on March 25, 2013.

Mortality was due to complications related to remote liver transplantation for primary sclerosing cholangitis. An intraductal papillary mucinous neoplasm of the pancreatic duct was identified at autopsy with associated chronic atrophic pancreatitis. Post mortem examination determined the immediate cause of death to be due to infection from the liver abscess, cardiac arrhythmia and cardiomegaly.

Neurologic and Radiographic studies: The patient was seen by a neurologist at UNM on 3/2003, 2/2005, 12/2006, 6/2007, 4/2008, 7/2009, 4/2010 and 9/2011. During this period symptoms were stable on the reduced immunosuppressant protocol.

Imaging from 4/4/2008 was read as unchanged compared to the computed tomography (CT) done 12/12/2006 (Figure 1). Both images show diffuse cerebral as well as cerebellar atrophy. A region of greater volume loss and accompanying low attenuation appeared in the right cerebellar hemisphere and middle cerebellar peduncle. Small foci of calcification were noted. These were not significantly changed between the 2006 and 2008 images. No new areas of abnormal attenuation were identified within the brain. Vertebral and internal carotid artery calcifications were also noted.

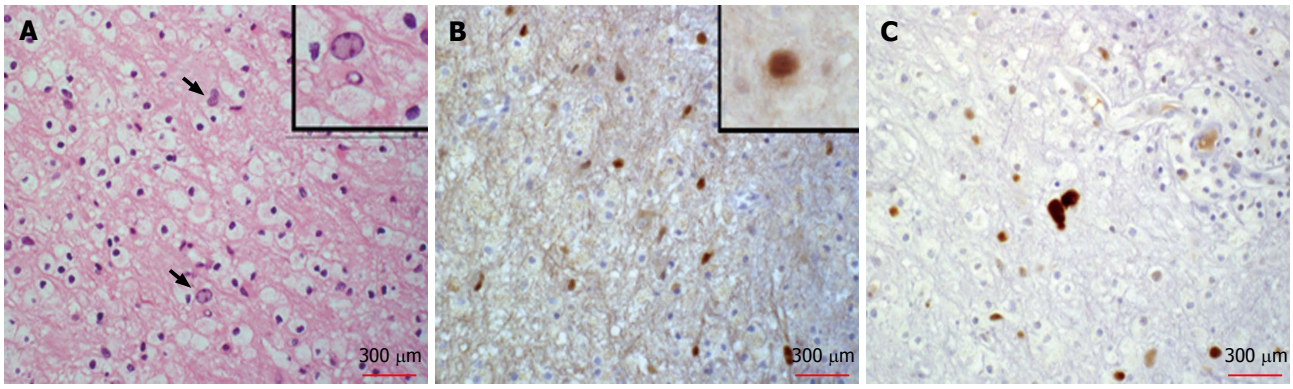

Figure 2 Histopathology of the original diagnostic biopsy. A: Histopathology of the cerebellar biopsy specimen from 1999 stained with hematoxilin and eosin. Atypical glia is indicated by arrows. Inset shows higher magnification of one example. Numerous macrophages surround the atypical cells and fill the parenchyma; B: Immunohistochemical staining for SV40 T antigen of another section from the biopsy shows numerous scattered strongly positive brown stain in nuclei of atypical glial cells, consistent with oligodendroglial infection by JC virus. Inset shows a higher magnification of another example of a positive glial cell; C: Immunohistochemistry for p53 detected strongly positive atypical glia and scattered weaker staining of macrophages consistent with inflammatory reaction to viral infection (A-C).

Pathological examination

Histopathologic review of the hematoxilin and eosin stained slides from the cerebellar stereotactic biopsy specimen of 1999 showed the classic features of PML, including demyelination with abundant macrophages, no lymphocytes or granulocytes and relative preservation of axons. Occasional enlarged oligodendroglial cells with dense chromatin and atypical astrocytes were also present (Figure 2). To detect virus, SV40 T antigen immunostaining was used. JC virus is a papovavirus in the polyoma family. SV40 monoclonal antibody was raised against a short peptide from the large T antigen of Simian Virus 40, another member of this virus family. This antibody also recognizes the large T antigen from both JC and BK viruses. It does not recognize small T antigens. SV40 immunostaining highlighted nuclei of infected oligodendroglial cells and occasional bland-appearing astrocytes, but did not highlight atypical astrocytes in the biopsy. Staining for p53 was performed to detect secondary viral effects on glia as support for the diagnosis[16]. The p53 antibody stained the nuclei of atypical glial cells. Thus these atypical astrocytes were likely reactive rather than infected. This review of the biopsy confirmed the previous diagnosis of PML.

At autopsy, gross examination of the brain surface and of coronal sections at 1 cm intervals revealed no ventricular enlargement, and no periventricular, or other white matter abnormalities. The brain was thoroughly examined by coronal sectioning from forebrain to brain stem and no areas of softening or discoloration were found. PML frequently extends initially to periventricular regions, yet no cerebral lesions were found in this case. Sagittal sectioning of the cerebellum revealed a 1.0 cm × 0.8 cm × 0.5 cm focus of tissue softening just lateral to the vermis on the left, in the region of the original biopsy. This is the area of the lesion identified in the 2006 and 2008 CT brain scans. This area of softening included cerebellar white matter and the dentate nucleus.

On histologic examination of the post-mortem brain sections from the original lesion in the cerebellar white matter were remarkable for white matter rarefaction, as evidenced by loss of myelin that was nearly proportional to axonal loss (Figure 3). Thus repair of the damage had not occurred. However, continuing damage was not detected. The heavy macrophage infiltration observed in the 1999 biopsy was absent, and macrophages were not apparent. Classical features of PML, such as enlarged oligodendroglial cells, were also mainly absent, atypical astrocytes were rare and only weak nuclear SV40 or p53 immunostaining was noted (Figure 3). We considered weak staining of the cytoplasm of glial cells to be non-specific since this low level of background staining was present in normal tissue within the section and also present in the negative control where no virus was present. A few rare cells displayed slightly more intense staining, which are shown in insets (Figure 3). Due to these rare cells, we cannot rule out residual viral antigens or continued low level of expression from latent virus in this burnt-out lesion.

There was minimal involvement of overlying cerebellar folia and minimal depletion of cerebellar granular cells, as determined by lack of detectable pathologic processes (Figure 3). Thirteen additional histologic sections from throughout the brain were dissected and processed according to the standard neuropathological brain examination procedure. Random sections of periventricular white matter, adjacent to the lateral ventricles and the aqueduct, where infection is most likely to spread, revealed no diagnostically significant abnormality. Sections from the pons were also stained for SV40 and p53 and no staining was detected.

Remarkably, fourteen years after diagnosis the lesion appeared confined to a single focus in the cerebellum, as in the original presentation. No additional foci throughout the brain, which are normally common in this multifocal disease, were found.

DISCUSSION

PML is a demyelinating disease of the brain caused by

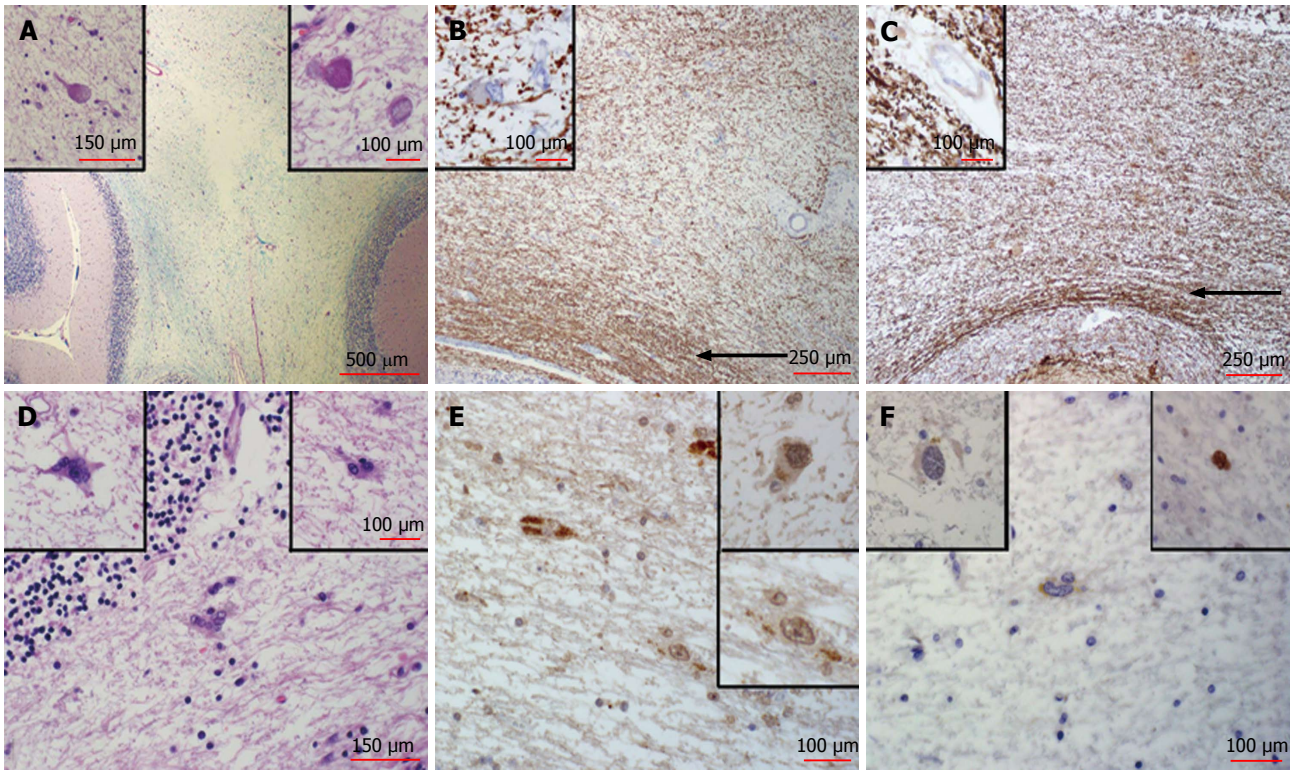

Figure 3 Post-mortem histologic analysis. A: The cerebellar lesion examined by histology shows a severe loss of myelinated fibers in the white matter, as stained by Luxol blue/Periodic Acid-Schiff. Note central pale area in the image. Also note that the surface folia, stained pink at the lower corners of the image, display no involvement. Inset (left) shows a higher magnification of an axonal spheroid from the region of the lesion, indicative of residual axonal damage, stained by H and E. Inset (right) shows another axonal spheroid from the same region at higher magnification also stained by H and E. Note that the pale lesion lacks evidence of active viral infection, with no macrophage infiltration or other inflammatory processes; B: Myelin basic protein immuno-staining reveals a severe loss of myelinated fibers stained brown in the cerebellar lesion. Note relative sparing of subcortical U-fibers (arrow). Inset (left) Higher magnification of a cell in the lesion stained for myelin basic protein that shows ragged myelin distribution. This demyelination appears to be quiescent; C: Section of the lesion in the cerebellum stained for neurofilament protein shows a loss of axons nearly proportional to the loss of myelin. Note relative sparing of subcortical U-fibers (arrow). Inset (left) shows higher magnification of neurofilament staining in the area of the lesion. Axons apparently lost in the acute phase in 1999 have not regenerated; D: Examples of rare atypical astrocytes found at the periphery of the lesion in H and E stained sections. Insets at higher magnification; E: SV40 immunostaining for T antigen shows some non-specific granular pattern within the cytoplasm of a few glial cells in the region of the lesion, some faint nuclear staining and scattered acellular granular deposits. This staining suggests latent infection with low levels of residual antigen. Insets show examples at higher magnification; F: The p53 immunostain shows that atypical astrocytes are mostly negative. Inset (left) another example of an atypical astrocyte that does not stain at the same magnification, and inset (right) a rare example of a p53 positive atypical glial cell. Macrophages were very rare and p53 staining was not observed. H and E: Hematoxilin and eosin.

the polyomavirus, JCV in immunosuppressed individuals. Although long-term survival has been reported in PML, the histological appearance of a demyelinating plaque in complete remission has not been well described. Here we show that demyelination in the original lesion was not repaired despite 14 years of remission, while evidence of continuing acute infection was absent.

The lack of defined viral particles, absence of progressive lesions, and inflammatory processes suggests that the virus had either been cleared or was latent. Since polyomaviruses persist in cells in a latent form, either episomally or when integrated into cellular DNA[17,18], surviving glia in the lesion could harbor latent virus and continue to express viral antigens at low levels without producing sufficient infective particles to spread the virus.

The risk of PML is present throughout the post transplantation period with a higher case fatality and incidence than reported in HIV patients on HAART or multiple sclerosis patients treated with natalizum[9]. There is no cure for PML, but prolonged survival rates are becoming increasingly common; although in one series, patients with cerebellar lesions tended to have a worse clinical outcome[6]. Magnetic resonance imaging brain findings typically show leukomalacia with ventricular enlargement secondary to destruction of the white matter at the site of previous PML lesions, and focal areas of subcortical atrophy with preservation of the cortical ribbon[6,8].

Although this case illustrates the classic histological features of PML at initial presentation together with neurological symptoms, imaging findings in the cerebellum and JCV confirmed biopsy, the patient's neurological symptoms were non-progressive despite continued immunosuppression. At autopsy, only residual damage in the location of the original lesion was observed, and histopathologic features of active infection in this region were absent, presumably indicating an effective cellular immune response against the virus. Serological workup of HIV cases has suggested a role for $CD8^+$ cytotoxic T-lymphocytes against JCV[12], although in this current

case no significant lymphocytic presence was detected in either the cerebellar biopsy or the post-mortem brain. Recent reports suggest findings of mutated JCV in CSF may correlate with slower or halted disease progression in HIV but no correlation was found in transplant recipients despite similarly mutated virus[2,19,20].

One of the earliest histopathological descriptions of patients with long term survival with PML revealed classical findings of progressive multifocal leukoencephalopathy, but with numerous eosinophils[21]. Viral particles were found in oligodendrocyte nuclei and cytoplasm with electron microscopy. Other cases of long term survival in non-HIV-infected patients are so rare as to be reportable, and include immunosuppressed patients for leukemia-lymphoma treatment[6,7,22] as well as solid organ transplant such as kidney[14] and liver[13]. The current case is unusual in that the neurological status was stable and at autopsy, gross evidence of multifocal pathology was absent, and histologic evidence of active viral infection was absent. Despite detection of low levels of viral antigen in the cerebellar region by immunostaining at autopsy this patient was clinically stable for fourteen years. No progression was detected symptomatically, neurologically, or radiographically. No evidence of progressive demyelination or spread of pathology beyond the original lesion was found in post-mortem evaluation of the brain.

A multicenter, retrospective cohort study of cases of PML was performed among transplant recipients at Mayo Clinic, Johns Hopkins University, Washington University, and Amsterdam Academic Medical Center[9]. The incidence of PML was calculated at 1.24 per 1000 post transplantation person-years. In this study of 69 cases of PML associated with solid organ and bone marrow transplantation, median survival following symptom onset was 6.4 mo for solid organ *vs* 19.5 mo for bone marrow recipients; with survival beyond one year of only 55.7%[9]. Anti-retroviral treatment for HIV improves the immune system and is beneficial for those with progressive multifocal leukoencephalopathy[1]; however the only effective treatment for iatrogenically immunosuppressed patients appears withdrawal or re-configuration of life-saving immunosuppressive therapy and consequent enhancement of their natural immunity.

The mechanisms for reactivation of latent JCV in brain are poorly understood but thought to be related to immune competence. Viral and/or host genotypes may also play a role, since variation in human leukocyte antigens correlates with antibody response[23]. Other viruses latent in brain include herpes simplex virus (HSV). While HSV DNA is found in a large percentage of normal brains, little evidence exists as to whether HSV reactivates in brain[24]. Attempts to correlate HSV reactivation in the brain with the risk of neurodegenerative diseases such as Alzheimer's are on-going[25,26]. How either HSV or JCV are kept in check in the immune-competent infected person remains a mystery.

Our study reveals residual damage, rare macrophages, a few reactive astrocytes and minimal evidence of persistent viral antigen expression with no evidence of viral replication and infective particle production. This case demonstrates the possibility of complete remission of PML with long-term survival in a patient after solid organ transplant who was maintained on immunosuppressive therapy.

ACKNOWLEDGMENTS

The authors would like to acknowledge the additional neuropathological guidance and editorial contributions of neuropathologist, Bette Kleinschmidt-DeMasters MD, technical assistance of Kevin Reagan at UNM, histotech Karen Buehler at TriCore Reference Labs, and digital image editing of the first draft by Mike Grady.

COMMENTS

Background

JC virus (JCV) causes progressive multifocal leukoencephalopathy (PML), especially in immun-compromised patients. After solid organ transplant is typically rapidly progressive and fatal.

Research frontiers

Here the authors present a case of PML in a patient who received a solid organ transplant that did not progress for over 14 years despite on-going immune-suppression. The diagnosis was validated by pathological analysis of brain biopsy.

Innovations and breakthroughs

Rare insight into the histopathology of quiescent JCV infection and residual damage, not repaired after 14 years, are presented. This is the first reported histopathology of a JCV-induced lesion in remission.

Applications

This report demonstrates that PML progression may be halted but the original lesion does not repair.

Terminology

JCV is a polyoma genetically similar to SV40. "JC" stands for John Cunningham, the first patient in which the virus was discovered. It is very common in the general population but only causes overt disease in immune compromised hosts. PML thought to be caused by JCV, is a rare and usually fatal disease of the white matter in the brain.

Peer-review

JCV is a human polyomavirus that infects greater than 60% of the human population during childhood, and establishes a latent infection in healthy individuals. Replication of the neurotropic strain of JCV in glial cells causes the fatal demyelinating disease of the central nervous system, PML, which is seen in patients with underlying immunocompromised conditions. PML has also been described in patients with autoimmune diseases treated with immunomodulatory therapies. PML is a mortal disease and there is no specific therapy. Long-term survivors have been reported with no sign of viral reactivation and replication. There is little known about neuropathologic description of long-term survivals. In this manuscript, authors provided an interesting case report of a long-term PML survivor with immunohistological evaluation. These observations are interesting for the readers of the Journal.

REFERENCES

1 **Engsig FN**, Hansen AB, Omland LH, Kronborg G, Gerstoft J, Laursen AL, Pedersen C, Mogensen CB, Nielsen L, Obel N. Incidence, clinical presentation, and outcome of progressive

multifocal leukoencephalopathy in HIV-infected patients during the highly active antiretroviral therapy era: a nationwide cohort study. *J Infect Dis* 2009; **199**: 77-83 [PMID: 19007313 DOI: 10.1086/595299]

2 **Ferenczy MW**, Marshall LJ, Nelson CD, Atwood WJ, Nath A, Khalili K, Major EO. Molecular biology, epidemiology, and pathogenesis of progressive multifocal leukoencephalopathy, the JC virus-induced demyelinating disease of the human brain. *Clin Microbiol Rev* 2012; **25**: 471-506 [PMID: 22763635 DOI: 10.1128/CMR.05031-11]

3 **Focosi D**. Does contrast enhancement predict survival in progressive multifocal leukoencephalopathy? *J Infect Dis* 2009; **199**: 1410-1411; author reply 1411-1412 [PMID: 19358677 DOI: 10.1086/597622]

4 **Gasnault J**, Costagliola D, Hendel-Chavez H, Dulioust A, Pakianather S, Mazet AA, de Goer de Herve MG, Lancar R, Lascaux AS, Porte L, Delfraissy JF, Taoufik Y. Improved survival of HIV-1-infected patients with progressive multifocal leukoencephalopathy receiving early 5-drug combination antiretroviral therapy. *PLoS One* 2011; **6**: e20967 [PMID: 21738597 DOI: 10.1371/journal.pone.0020967]

5 **Gheuens S**, Pierone G, Peeters P, Koralnik IJ. Progressive multifocal leukoencephalopathy in individuals with minimal or occult immunosuppression. *J Neurol Neurosurg Psychiatry* 2010; **81**: 247-254 [PMID: 19828476 DOI: 10.1136/jnnp.2009.187666]

6 **Lima MA**, Bernal-Cano F, Clifford DB, Gandhi RT, Koralnik IJ. Clinical outcome of long-term survivors of progressive multifocal leukoencephalopathy. *J Neurol Neurosurg Psychiatry* 2010; **81**: 1288-1291 [PMID: 20710013 DOI: 10.1136/jnnp.2009.179002]

7 **Stam FC**. Multifocal leuko-encephalopathy with slow progression and very long survival. *Psychiatr Neurol Neurochir* 1966; **69**: 453-459 [PMID: 5971458]

8 **Tavazzi E**, White MK, Khalili K. Progressive multifocal leukoencephalopathy: clinical and molecular aspects. *Rev Med Virol* 2012; **22**: 18-32 [PMID: 21936015 DOI: 10.1002/rmv.710]

9 **Mateen FJ**, Muralidharan R, Carone M, van de Beek D, Harrison DM, Aksamit AJ, Gould MS, Clifford DB, Nath A. Progressive multifocal leukoencephalopathy in transplant recipients. *Ann Neurol* 2011; **70**: 305-322 [PMID: 21823157 DOI: 10.1002/ana.22408]

10 **Shitrit D**, Lev N, Bar-Gil-Shitrit A, Kramer MR. Progressive multifocal leukoencephalopathy in transplant recipients. *Transpl Int* 2005; **17**: 658-665 [PMID: 15616809 DOI: 10.1007/s00147-004-0779-3]

11 **Antinori A**, Cingolani A, Lorenzini P, Giancola ML, Uccella I, Bossolasco S, Grisetti S, Moretti F, Vigo B, Bongiovanni M, Del Grosso B, Arcidiacono MI, Fibbia GC, Mena M, Finazzi MG, Guaraldi G, Ammassari A, d'Arminio Monforte A, Cinque P, De Luca A. Clinical epidemiology and survival of progressive multifocal leukoencephalopathy in the era of highly active antiretroviral therapy: data from the Italian Registry Investigative Neuro AIDS (IRINA). *J Neurovirol* 2003; **9** Suppl 1: 47-53 [PMID: 12709872 DOI: 10.1080/13550280390195388]

12 **Du Pasquier RA**. JCV-specific cellular immune response correlates with a favorable clinical outcome in HIV-infected individuals with progressive multifocal leukoencephalopathy. *J Neurovirol* 2001; **7**: 318-322

13 **Boulton-Jones JR**, Fraser-Moodie C, Ryder SD. Long term survival from progressive multifocal leucoencephalopathy after liver transplantation. *J Hepatol* 2001; **35**: 828-829 [PMID: 11738115 DOI: 10.1016/S0168-8278(01)00202-1]

14 **Crowder CD**, Gyure KA, Drachenberg CB, Werner J, Morales RE, Hirsch HH, Ramos E. Successful outcome of progressive multifocal leukoencephalopathy in a renal transplant patient. *Am J Transplant* 2005; **5**: 1151-1158 [PMID: 15816900 DOI: 10.1111/j.1600-6143.2005.00800.x]

15 **Gheuens S**, Wüthrich C, Koralnik IJ. Progressive multifocal leukoencephalopathy: why gray and white matter. *Annu Rev Pathol* 2013; **8**: 189-215 [PMID: 23092189 DOI: 10.1146/annurev-pathol-020712-164018]

16 **Yang B**, Prayson RA. Expression of Bax, Bcl-2, and P53 in progressive multifocal leukoencephalopathy. *Mod Pathol* 2000; **13**: 1115-1120 [PMID: 11048806 DOI: 10.1038/modpathol.3880206]

17 **Coelho TR**, Almeida L, Lazo PA. JC virus in the pathogenesis of colorectal cancer, an etiological agent or another component in a multistep process? *Virol J* 2010; **7**: 42 [PMID: 20167111 DOI: 10.1186/1743-422X-7-42]

18 **Wold WS**, Green M, Mackey JK, Martin JD, Padgett BL, Walker DL. Integration pattern of human JC virus sequences in two clones of a cell line established from a JC virus-induced hamster brain tumor. *J Virol* 1980; **33**: 1225-1228 [PMID: 6245274]

19 **Jensen PN**, Major EO. A classification scheme for human polyomavirus JCV variants based on the nucleotide sequence of the noncoding regulatory region. *J Neurovirol* 2001; **7**: 280-287 [PMID: 11517403 DOI: 10.1080/13550280152537102]

20 **Delbue S**, Elia F, Carloni C, Tavazzi E, Marchioni E, Carluccio S, Signorini L, Novati S, Maserati R, Ferrante P. JC virus load in cerebrospinal fluid and transcriptional control region rearrangements may predict the clinical course of progressive multifocal leukoencephalopathy. *J Cell Physiol* 2012; **227**: 3511-3517 [PMID: 22253012 DOI: 10.1002/jcp.24051]

21 **Kepes JJ**, Chou SM, Price LW. Progressive multifocal leukoencephalopathy with 10-year survival in a patient with nontropical sprue. Report of a case with unusual light and electron microscopic features. *Neurology* 1975; **25**: 1006-1012 [PMID: 1237816 DOI: 10.1212/WNL.25.11.1007]

22 **Demir E**, Liebert UG, Söylemezoglu F, Yalaz K, Köse G, Anlar B. Childhood case of progressive multifocal leukoencephalopathy with improved clinical outcome. *J Child Neurol* 2005; **20**: 241-244 [PMID: 15832618 DOI: 10.1177/08830738050200031301]

23 **Sundqvist E**, Buck D, Warnke C, Albrecht E, Gieger C, Khademi M, Lima Bomfim I, Fogdell-Hahn A, Link J, Alfredsson L, Søndergaard HB, Hillert J, Oturai AB, Hemmer B, Kockum I, Olsson T. JC polyomavirus infection is strongly controlled by human leucocyte antigen class II variants. *PLoS Pathog* 2014; **10**: e1004084 [PMID: 24763718 DOI: 10.1371/journal.ppat.1004084]

24 **Roizman B**, Whitley RJ. An inquiry into the molecular basis of HSV latency and reactivation. *Annu Rev Microbiol* 2013; **67**: 355-374 [PMID: 24024635 DOI: 10.1146/annurev-micro-092412-155654]

25 **Bearer EL**. HSV, axonal transport and Alzheimer's disease: in vitro and in vivo evidence for causal relationships. *Future Virol* 2012; **7**: 885-899 [PMID: 23335944 DOI: 10.2217/fvl.12.81]

26 **Itzhaki RF**. Herpes simplex virus type 1 and Alzheimer's disease: increasing evidence for a major role of the virus. *Front Aging Neurosci* 2014; **6**: 202 [PMID: 25157230 DOI: 10.3389/fnagi.2014.00202]

P- Reviewer: Sariyer IK, Williamson EM
S- Editor: Qiu S **L- Editor**: A **E- Editor**: Li D

Published by **Baishideng Publishing Group Inc**
8226 Regency Drive, Pleasanton, CA 94588, USA
Telephone: +1-925-223-8242
Fax: +1-925-223-8243
E-mail: bpgoffice@wjgnet.com
Help Desk: http://www.wjgnet.com/esps/helpdesk.aspx
http://www.wjgnet.com